An Investigation of Sources and Processes Impacting Mercury Dry Deposition

by

Naima L. Hall

A dissertation submitted in partial fulfillment
of the requirements for the degree of
Doctor of Philosophy
(Environmental Health Sciences)
in the University of Michigan
2018

Doctoral Committee:

Associate Professor J. Timothy Dvonch, Co-Chair
Professor Gerald J. Keeler, Co-Chair, Deceased
Professor Joel D. Blum
Associate Research Scientist Frank J. Marsik
Professor Marie S. O'Neill

Naima L. Hall

hallnai@umich.edu

ORCID iD: 0000-0001-6474-6547

Acknowledgements

Cross the river in a crowd and the crocodile won't eat you. ~ African proverb

This dissertation would not have been possible without my two advisors that helped me to this point. I'm grateful that a number of years ago during Public Health orientation I met with Dr. Gerald Keeler and was drawn in by his enthusiasm as well as being thrilled by the prospect of participating in exactly the kind of research that I entered the Department of Environmental Health hoping to participate in- work that was chemistry based but with a hopeful outcome of wanting to help "save the world." Jerry was always looking to test a new method or add an extra measurement to our field work- in general, pushing everyone around him to be the best scientist possible. This approach led to collecting some kind of crazy samples like pam-sprayed quartz filters or trips to art supply stores in Detroit, but it also led to true gems like when Jerry and Frank started sanding off the backing on an artificial turf doormat because it looked like grass and might be a make for a good surrogate surface. Later, while investigating the feasibility of scaling up what became the ATSS sampler, I learned that you could get a similar turf made by the same company that came with holes for drainage and without the backing. We had to sacrifice the green color because the turf that we used was for chicken coops and the grey was found to be most soothing for laying eggs.

Dr. Tim Dvonch stepped into the role of being my advisor and has always been unwaveringly supportive and always encouraging that completing this dissertation was absolutely possible even while it felt like I was floundering and buried under piles of data. Thank you, Tim, for making sure that I got to this point. Thanks as well to my committee who has been understanding about this less traditional course.

UMAQL has been an incredible lab to have belonged to. The long hours associated with prepping and participating in field work were bearable because of current and former members who were wonderful scientists, hard-working lab companions and wonderful friends. This

specifically includes Dr. Frank Marsik, Dr. Masako Morishita, Jim Barres, and Dr. Mary Lynam. Additionally, former students such as Dr. Bian Liu who allowed me to shadow her for the first couple of months in the lab as well as Dr. Emily White, Dr. Lynne Gratz, Dr. Ali Kamal, and Beth Oswald and Dr. Pearl Nathan many of whom were involved in collecting some of these samples. Over the years, I was also honored to work with Jane Clifford, Deborah Edelman, Summer Hitchens, Tiffany Jackson, Sonia Mathew, Tyler Osburn, Emily Thomas, Dave Torrone, Brandon Wills, Alex Costakis, Tim Finch, James Green, and Matt Salvadori, Dr. Jason Demers, Dr. Laura Sherman who were crucial to prepping supplies in lab, collecting samples in the field and processing and analyzing samples to provide the enormous amounts data that I've been fortunate enough to work with.

The support of my family has been crucial to allow me to reach this point. This includes my dad, Lewis J. Hall, and other family members who are not physically here to witness this occasion but I feel their presence surrounding me always. Dad understood that completing my dissertation would be a marathon not a sprint and was supportive of it looking more like an ultra-marathon if that was what I wanted to be doing. My mom and Dennis have been supportive providing everything from a room with a view when it seemed like a change of scenery would help me work to caring for my son Lewis so that I could work while knowing that he was being well loved and learning a lot from his grandparents. Lastly, I am appreciative to my husband, Perry, who has always cheered me on and been ready for whatever surprises have come along with this journey.

Table of Contents

List of Tables

List of Figures

Abstract

Atmospheric deposition of mercury (Hg) is a major process that contributes mercury loadings to ecosystems resulting in the bioaccumulation of mercury in fish and other wildlife. Methods for measuring Hg that is wet deposited have been well studied, but there are few established methods for directly measuring dry deposition of atmospheric Hg. We developed a new method of direct Hg dry deposition measurement using an artificial turf surrogate surface (ATSS) sampler. It was found that there was a collocated precision of 9%, low blanks (0.8 ng), high extraction efficiency (97%- 103%) and a quantitative matrix spike recovery of 100%.

Utilizing this method, ATSS samplers were deployed on a large-scale for the first time during measurement campaigns conducted as part of a Hg Total Maximum Daily Load (TMDL) project in Florida to investigate spatial patterns and temporal variability of wet and dry deposition of Hg as well as major ionic species and a suite of trace elements. As part of this project, wet and dry deposition of Hg and trace elements were measured concurrently at 15 monitoring sites in Florida in 2009 and 11 monitoring sites in 2010. The dry deposition of Hg measured during these month-long measurement campaigns ranged from 0.6 $\mu g/m^2$ to 2.1 $\mu g/m^2$. Wet deposition of Hg measured during the intensive periods ranged from 1.5 $\mu g/m^2$ to 6.9 $\mu g/m^2$. A north to south increasing spatial gradient was observed for wet deposition of Hg. Deposition from the trace elements and ionic species was integrated with the Hg deposition to investigate source impacts. Correlation coefficients and enrichment factors both suggested that at certain

sites much Hg deposition was primarily impacted by specific sources but also indicated that more work is needed to continue grow the understanding of Hg dry deposition.

This ATSS sampling method has allowed widespread and in-depth study of the dry deposition of Hg for this project in the state of Florida, enabling unique direct field measurement comparisons of wet versus dry Hg deposition contributions at a variety of site types (coastal, urban, rural) in Florida. Results demonstrate that the ratio of wet to dry deposition of mercury is highly variable spatially and temporally in Florida. Additionally, the ATSS method is widely applicable across site types as well as for various trace elements and ionic species. The method is especially advantageous in regions with frequent precipitation and for longer-term sampling.

Chapter 1 : Introduction

Mercury is one of only two liquid elements at room temperature. Its high volatility and persistence distinguish it from many other chemicals in the environment and contribute to its monitoring and analysis challenges. Mercury exists in several forms throughout the environment. In the atmosphere, mercury primarily exists in three major inorganic forms: elemental mercury (Hg^0), gaseous oxidized mercury (GOM) and particulate mercury (Hg_p). (ATSDR 1999a; WHO 2000). Elemental mercury comprises 90-95% of the mercury in the atmosphere. GOM is most likely to be influenced by the humidity of the air, the sources in the region and other atmospheric parameters. It has the shortest lifetime and its presence is the most variable of the three in the atmosphere. GOM is easily removed from air due to its high water solubility. It quickly deposits onto land and water surfaces as well as being washed out of air in precipitation processes (Landis et al. 2004). Elemental mercury has a comparatively long residence time in the atmosphere lasting 6 months to two years; Wangberg et al. 2003) allowing it to undergo global transport (UNEP 2002). All of these forms of mercury can further undergo chemical transformations in the atmosphere although more rapidly for GOM than for Hg_0. Mercury also exists in several organic forms, the primary concern being methylmercury (MeHg) which is formed when inorganic mercury in waterbodies is methylated by bacteria (USGS 2006) and bioaccumulates through the foodweb contaminating the ecosystem.

The high methylmercury concentrations in the environment have led to unhealthy levels of mercury in many fish and wildlife throughout waterbodies globally and the issuance of health

advisories limiting the consumption of fish in waterbodies. Methylmercury can also pose risks to wildlife (Beyer et al, 1997; Nilsen et al 1997; Barron et al 2004).

Hg deposition is a significant problem in many regions of the US; in particular, Florida consistently has some of the highest Hg wet deposition in the US (NADP 2017). Hg in the environment is from a mixture of natural sources including volcanoes, forest fires and volatilization from soils and oceans (Gustin et al 2008) and anthropogenic sources (UNEP 2015). The primary anthropogenic sources include coal-fired utility boilers, oil-fired utility boilers, municipal waste incineration, sewage sludge incineration, metal smelting, cement production and biomass combustion (U.S. EPA NEI 2017).

In the 1970s, with emergent concerns over air pollution, acid rain and the contamination of ecosystems; researchers began developing methods to measure wet and dry deposition of atmospheric species. Through these studies, standardized methods of measuring wet and dry deposition of pollutants like nitrates, sulfates, organic pollutants (including PCBs) and various metals were established (Lewis 1983; Balestrini, Consuma et al. 2000; Tasdemir and Holsen 2005); however, the measurement of mercury deposition was complicated by mercury's volatility and its presence in different forms. To accurately measure mercury, methods have developed which overcome such obstacles as evasion from samples before measurement, adsorption and loss to walls and other surfaces, and understand potential chemical reactions that could occur. Additionally challenging, mercury is present in small concentrations in the environment necessitating extensive and particular cleaning methods of the sampling equipment used and analytical methods applied to samples. As these challenges were understood and addressed, wet deposition measurement methods became standardized during the 1990s and networks of automated weekly, daily and event sampling were established (NADP 2017).

Measurement of Hg dry deposition has yielded additional complications. Many methods have been developed to determine mercury dry deposition flux including surrogate surface sampling with a variety of media, throughfall measurements, leaf washing, moss and lichen bags, flux chambers, modeling based on ambient mercury concentrations and other parameters, and micrometeorological towers. However, all of these methods have major limitations. Surrogate surface methods, which are used in this proposal work, are intended to physically or chemically imitate natural surfaces and dry deposition processes (Marsik et al. 2005); however, these surfaces only partially imitate the natural environment. In addition, most of the surrogate surface methods require on-site personnel monitoring to remove the samples prior to rainfall and in general they are only deployed for 12 or 24 hours resulting in studies with fairly short durations. There are very few recent automated dry deposition collectors but there is no widespread measurement network comparable to that for wet deposition.

Dissertation structure

This dissertation is structured with a main body consisting of three independent journal article-styled chapters that build towards improving the understanding of mercury dry deposition in Florida. Following this introduction, Chapter 2 presents the development of a new method to measure Hg dry deposition. The artificial turf surrogate surface method developed was an opportunity to conduct dry deposition measurements without some of the previously existing limitations. Much work was conducted to optimize this method and the validation of this method included in Chapter 2 enabled its deployment to explore Hg dry deposition across the state of Florida for the total maximum daily load (TMDL) study. Wet and dry Hg deposition was measured at 15 monitoring sites in Florida in 2009 and 11 monitoring sites in 2010. Chapter 3

investigates the spatial and temporal variability of Hg dry deposition using the ATSS method paired with Hg wet deposition to continue to build on knowledge of Hg dry deposition patterns in Florida. In Chapter four, we integrate the results of wet and dry deposition measurements of 29 trace elements and ionic species concurrently measured with the Hg deposition for the Florida study to investigate the sources that were contributing Hg to Florida.

Although much of the work presented in this dissertation is specific to Florida, much of the spatial and temporal patterns observed as well as the impact of the local and regional sources are broader issues that are valuable to increase the body of knowledge with respect to Hg dry deposition globally.

Chapter 2 : An Artificial Turf-Based Surrogate Surface Collector for the Direct Measurement of Atmospheric Mercury Dry Deposition

Introduction

In recent years, a growing number of intensive field campaigns and routine measurement networks have provided valuable information on the rates of total mercury (Hg) wet deposition in North America (Dvonch et al., 1999; Guentzel et al., 1995; Keeler and Dvonch, 2005; Landis and Keeler, 2002; Prestbo and Gay, 2009; Risch et al., 2012) . The ability to place bounds on the rates of total Hg dry deposition has been hampered by the relative lack of direct measurement approaches to quantify this critical process for the three most relevant forms of Hg: gaseous elemental Hg (Hg^0), gaseous oxidized Hg (GOM), and particulate bound Hg (Hg(p)). Initial mercury dry deposition measurement estimates focused on the use of micrometeorological (Fritsche et al., 2008; Kim et al., 1995; Lindberg et al., 1992; Meyers et al., 1996; Skov et al., 2006), dynamic flux chamber (Carpi and Lindberg, 1998; Fu et al., 2008; Graydon et al., 2006), vegetative throughfall (Iverfeldt, 1991; Rea et al., 2000, 1996; St. Louis et al., 2001) and inferential modeling approaches (Landis and Keeler, 2002; Marsik et al., 2007; Poissant et al., 2004; Zhang et al., 2003). The application of micrometeorological approaches, such as modified Bowen ratio and relaxed eddy accumulation, are typically focused on just the gaseous Hg species, can be challenging to use in remote areas as they require a stable source of electrical power, and stringent site selection criteria must be adhered to insure adequate uniform upwind

fetch (Businger, 1986). Dynamic flux chambers also require a stable source of electrical power, and can disrupt the natural temperature, humidity, and turbulent field responsible for the fluxes they are attempting quantify (Cobos et al., 2002; Fritsche et al., 2008). Vegetative throughfall approaches require an amenable canopy, sampling intervals are limited by the frequency of rain events, and spatial investigation is complicated by unique canopy structure and dry deposition collection characteristics of the canopy above each sampling location. Inferential modeling approaches rely on parameterizations of land surfaces, estimates of meteorological conditions and turbulence, ambient Hg measurements, and estimates of representative Hg(p) mass median aerodynamic diameter (MMAD).

Surrogate surface (e.g., water, filter, greased Mylar film) approaches have also been utilized for direct measurement of Hg dry deposition [(Caldwell et al., 2006; Fang et al., 2012; Huang et al., 2011; Lai et al., 2011; Lyman et al., 2009, 2007; Marsik et al., 2007; Peterson et al., 2012; Rea et al., 2000; Sakata and Marumoto, 2004; Shahin et al., 2002; Yi et al., 1997). While each of the aforementioned approaches were successfully utilized for the measurement of Hg dry deposition, each method has limitations with respect to widespread, long-term deployment, and application. Surrogate surface approaches often suffer from the need to be visually monitored and attended, such that the surfaces avoid potential contamination from precipitation (wet deposition). Additional complications include the impact of strong winds, which can cause a loss of sample solution in the case of water surrogate surfaces, and evaporation which disrupts the even surface across the surface and changes laminar flow. While some engineering approaches have been incorporated into automated water surrogate surface collectors to minimize evaporative water loss (Sakata and Marumoto, 2004) and loss of sample solution due to wind (Sakata et al.,

2006), the cost, power requirements, and region specific meteorological conditions may restrict the broad application of these solutions.

This manuscript describes the development and evaluation of an artificial turf surrogate surface (ATSS) methodology for the measurement of total Hg dry deposition. The ATSS has been developed to overcome many of the aforementioned limitations of other dry deposition measurement techniques. The ATSS is a passive surrogate surface approach that utilizes a three-dimensional deposition surface that more closely mimics the physical structure of many natural surfaces than traditional flat surrogate surface designs. The design of the ATSS allows for the surface to be deployed in the field for either short or extended periods of time (days to a weeks) without risk of contamination from rainfall because the system has been designed to measure total (wet and dry) Hg deposition. Mercury dry deposition to the ATSS is calculated by determining the difference between the total Hg deposition measured by the ATSS and a collocated measure of wet-only total Hg deposition.

Artificial Turf Surrogate Sampler Design

The ATSS (Figure 2.1) was modified from a static water surrogate surface (SWSS) configuration previously used by Marsik et al., (2007) and initially described by Keeler and Dvonch (2005). The ATSS consists of a high density polyethylene (HDPE) frisbee-shaped aerodynamic laminar flow airfoil designed to collect dry-depositing gases and particles without altering the existing turbulent air flow field (Wu et al., 2007). The ATSS airfoil contains a removable 19 cm outer diameter Teflon Perfluoroalkoxy alkane (PFA) sample plate insert that holds an 18 cm diameter circular piece of artificial turf that is mechanically punched from polyethylene AstroTurf® NXT (GrassWorx, St. Louis, MO, USA). The gridded turf backing consists of a

matrix of open spaces allowing precipitation to flow through the turf and into a “throughfall” collection bottle.

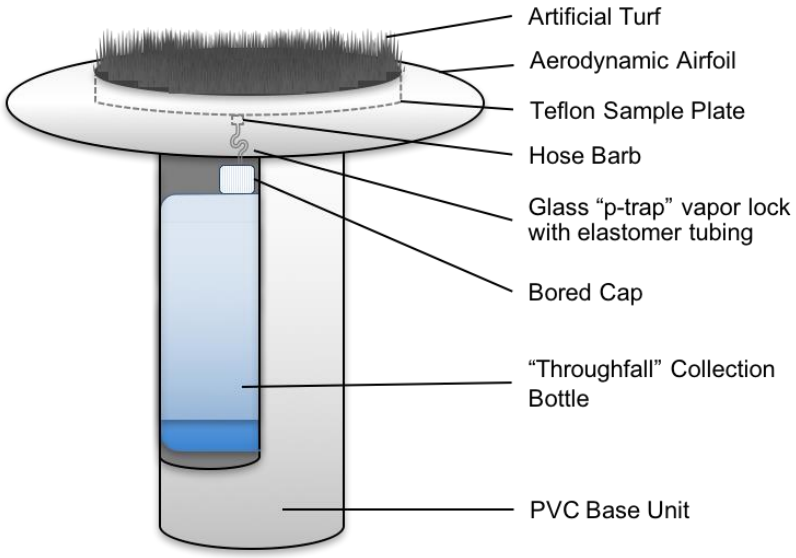

Figure 2.1: Schematic of artificial turf surrogate surface (ATSS) sampler.

The aerodynamic airfoil is attached to a 30 cm length of 10 cm diameter Polyvinyl Chloride (PVC) base unit using sheet metal screws via an attachment surface located under the bored well. The custom PVC base is bolted to a fabricated aluminum support bracket, and mounted vertically to an anchored tripod. Once the Teflon PFA plate is inserted into the airfoil well, a Teflon PFA hose barb attachment is threaded into the bottom. A 5 cm length of C-Flex thermoplastic elastomer tubing on either side of a glass “p-trap” vapor lock is attached to the Teflon PFA collection plate hose barb fitting. The other end of the tubing is fed through a bored cap into a 1 L fluorinated high density polyethylene (HDPE) throughfall collection bottle (Nalgene, Rochester, NY, USA, #2097-0032). The enclosed PVC support base has a small acrylic beam to support the weight of the bottle during sample collection, and a removable aluminum cover is installed to shield the sample from sunlight. The ATSS airfoil is deployed at a

height approximately 1–2 m above the ground in an area of clear fetch, depending upon the nature of the terrain and the average height of the surrounding vegetation, to insure uniformity of air flow and to insure that precipitation splash from any near-field objects did not enter the sampler.

Following deployment, the ATSS was left exposed to ambient air for a predetermined sampling period (typically three or four days for this study) after which the exposed turf, throughfall, and collocated wet deposition samples were collected and returned to the laboratory for analysis. The total Hg dry deposition collected by the ATSS was determined using Equation (1).

$$Total\ Dry\ Deposition\ (ng\ m^{-2}\ h^{-1}) = \frac{(Turf + Throughfall)\ \text{-}\ Wet\ Deposition\ Contribution}{Collection\ Surface\ Area \times Turf\ Exposure\ Time} \quad (1)$$

where

Turf = turf extract concentration × volume of extraction solution;

Throughfall = throughfall concentration × sample volume;

Wet Deposition Contribution = volume weighted average precipitation concentration × (throughfall sample volume—rinse solution volume); and

Collection Surface Area = 0.025687232 m^2.

Methods

Site Description

The ATSS method development and performance evaluations were conducted during three field measurement intensive studies in Michigan and Florida.

Michigan Studies

The initial ATSS field evaluation study was conducted at two urban sites in southeast Michigan, in Dearborn (42.3075° N, 83.1496° W) and in Detroit-Fort Street (42.3026° N, 83.1067° W). The Dearborn and Detroit sites were located at existing Michigan Department of Environmental Quality air monitoring sites. Sample collection was conducted during 18 July–8 August, 2007. A few of the ATSS samplers at Dearborn were deployed in duplicate to determine collocated precision.

Additional field evaluations were performed during 4 August–13 September 2008, as part of a multi-institutional Hg dry deposition measurement inter-comparison study. This study was performed at the University of Michigan Matthaei Botanical Gardens in Ann Arbor, MI (42.2987° N, 83.6647° W). The ATSS samplers at the Botanical Gardens were deployed in duplicate to determine collocated precision.

Florida Study

After cleaning method refinements, further evaluations of sampler blank performance were conducted at monitoring sites in Tampa and Davie, Florida (27.9134° N, 82.3752° W; 26.0854° N, 80.2407° W, respectively) from 4 July to 4 August 2010, and in Jacksonville, Florida (30.2475° N, 81.9510° W) from 25 July to 24 August 2010. While the ATSS Michigan studies were developed to measure Hg and trace element (see Chapter 4) dry deposition using a single surface, the Florida studies adopted expanded cleaning and sampling protocols to measure Hg dry deposition in one collector, and major ion and trace element dry deposition in a separate collocated ATSS sampler. The cleaning and sampling protocols below describe the finalized method used in the Florida studies.

Cleaning Procedure

Prior to use in the field, a multi-step acid cleaning procedure was performed on all supplies that were in contact with samples. The exact procedure followed varied by component of the sampling system. The turf surfaces were soaked in 3.5% *v*/*v* HNO_3 for five days, subsequently rinsed five times in ASTM type I (18.2 MΩ·cm) water, and then air-dried in a HEPA-filtered cabinet. The cleaning procedure applied for the turf surfaces punches used in Florida (Tampa, Davie and Jacksonville, FL, USA) added an additional 24-h soak in 1% BrCl solution after the HNO_3 soak, then were rinsed five times in ASTM type I water and dried in a HEPA-filtered air cabinet. The Teflon wells, Teflon hose barb adapters and glass vapor locks were soaked for six hours in a solution of 3.5% *v*/*v* HNO_3 at 70 °C, then were rinsed five times in ASTM type I water and dried in a HEPA-filtered cabinet. C-flex tubing was soaked in 3.5% *v*/*v* HNO_3 for 24 h before it was rinsed five times with ASTM type I water and dried in a HEPA-filtered air cabinet. All fluorinated HDPE sample and turf extraction bottles were acid-cleaned using the method described in Landis and Keeler [48]. Following drying, all sampling supplies were triple-bagged in sealable polyethylene bags to insure cleanliness during transportation to and from the field measurement sites.

Sample Deployment

Ultra-clean field handling techniques were employed to avoid contamination of samples. Site operators wore particle-free vinyl clean-room gloves for sample deployment, used acid-cleaned Teflon-coated forceps when handling turf, and always stood downwind from the sampling media. Before each ATSS and SWSS sample deployment, airfoils were wiped with particle-free polypropylene clean-room wipes and ASTM type I water, and all other acid-cleaned

sampling components were replaced after each sample collection. At the end of each sampling period, the site operator placed the turf surface into a 2 L wide-mouth fluorinated HDPE bottle, then rinsed the turf sample well with 30 mL 2.2% *v*/*v* HNO_3 solution to insure that residual dry deposition was washed off into the throughfall collection bottle. Field blanks were conducted by deploying clean sampling supplies, including a clean turf surface and throughfall bottle, and then pouring approximately 300 mL of ASTM type I water through the turf. The field blank turf and throughfall were then collected following the same protocols as described for sample collection. Collocated wet-only precipitation samples were collected using a modified MIC-B method described by Landis and Keeler (1997, 2002).

Sample Extraction and Analysis

Samples were stored in a dark cold room (4 °C) before and after processing prior to analysis. The ATSS throughfall and collocated modified MIC-B wet-only precipitation samples were oxidized to 1% (*v*/*v*) solution with concentrated BrCl in a class 100 clean room at least 24-h prior to analysis (Keeler et al., 2006). Turf surfaces were extracted in the 2 L bottles by adding 350 mL of ASTM type I water and immediately oxidizing with concentrated BrCl to a 4% solution (*v*/*v*). Bottles were then turned and followed by an ultra-sonic water bath for 2 h. All Hg sample analysis was conducted using a Tekran Instruments Corporation, (Knoxville, TN, USA) Model 2600 Cold Vapor Atomic Fluorescence Spectroscopy (CVAFS) analyzer following EPA Method 1631e.

Data Analysis

Data processing and descriptive statistics were performed using SAS v.9.4 (SAS Institute, Cary, NC, USA). The normality of the ATSS data distributions were examined using skewness

and kurtosis coefficients, and the Shapiro–Wilk test. Normality tests and the Brown–Forsythe test for equal variance were used to evaluate the assumptions of parametric procedures.

Results and Discussion

Performance Characteristics

Field Blanks

The addition of the 24-h BrCl soak to the turf cleaning method during the Florida studies (described above) resulted in a significant decrease in the mass of Hg in blank samples. Two different cleaning methods were used during the testing and deployment of this method. Consequently, the blank data from the Michigan monitoring sites was analyzed separately from blanks collected during the Florida studies. Six ATSS surface field blank samples were collected during the initial Michigan studies (Table 2.1) with a mean total Hg mass of 2.0 ± 1.1 ng, which was equivalent to a total mean Hg deposition of 76 ± 43 $ng \cdot m^{-2}$, and represented 18% of the measured Hg mass over a typical sample period. The total field blank mass was a sum of the Hg extracted from the ATSS surface plus the Hg from the throughfall blank and the acid solution. The average contribution of the throughfall blank toward the total blank was insignificant at 0.03 ng (<0.1%). After quantifying the relatively large field blank contribution of the ATSS surface during the early Michigan studies, the ATSS surface cleaning method was modified to include a 24-h soak in 1% BrCl, and the Michigan studies results were field-blank corrected using their site specific values.

After the new cleaning methodology was implemented, the average ATSS field blank mass of total Hg collected during the Florida studies ($n = 77$) was significantly reduced ($p < 0.05$) to

0.77 ± 0.44 ng (Table 2.2). Approximately 80% (61 out of the 77) of the ATSS field blanks were below the analytical detection limit. While improvements in the cleaning method led to a drastic reduction in the ATSS field blank mass, the blank turf mass still contributed on average 23% of the total Hg dry deposition measured over a typical three-day ATSS sample period at the Florida sites due to correspondingly lower deposition rates in Florida. As a result, the Florida ATSS results were also field blank corrected.

Extraction Efficiency

ATSS extraction tests were conducted to evaluate the efficiency of the extraction method. NIST SRM 1633b, (Constituent Elements in Coal Fly Ash) and 2704 (Buffalo River Sediment) were used to approximate Hg(p). The powders were weighed out and distributed onto an ATSS turf sampling surface. Extraction and analytical methods described above were followed. Analytical results were field-blank corrected with a control turf processed and analyzed concurrently. The field blank value was 1.78 ng which was comparable with the Hg mass from the Michigan study field blanks. The mean percent recovery using the SRM 1633b was 97% ± 10% (n = 3) and the mean percent recovery SRM 2704 samples was 103% ± 1% (n = 2). Matrix spikes were also conducted on the extracted turf samples throughout all study analyses using 250 μL addition of 2 mg/mL Hg solution. The percent recovery of matrix spikes (n = 28) was 100% ± 4% (mean ± standard deviation), with a minimum of 91% and a maximum of 110%.

ATSS Total Dry Deposition Partitioning

In the absence of precipitation during an ATSS collector sampling period, the total dry deposition is effectively calculated as the sum of the turf and the acid rinse of the turf well into the throughfall collection bottle Equation (1). During this study, we found in the absence of rain (n = 14) the percentage of the total Hg dry deposition collected onto the turf media was 98.3% ± 1.5% (mean ± standard deviation) suggesting a small amount of Hg(p) collected by the turf migrated down into the turf well (Table S1). For ATSS samples exposed to rain events (n = 15) the percentage of the total Hg dry deposition remaining on the turf media was 65.1% ± 11.9% demonstrating the translocation of dry deposition into the throughfall collection bottle. The variability in the amount of Hg mass collected on the ATSS turf media in rain exposed samples was a function of when during the sampling period the precipitation event occurred and the intensity of the event. The Hg mass collected into the throughfall collection bottle originating from the rain itself was subtracted (Equation 1) based on the volume of ATSS throughfall collected and the volume weighted average concentration of the associated collocated wet-only event precipitation sample(s).

ATSS Collocated Precision

The precision of the ATSS method was evaluated by deploying collocated samplers. The results from the collocated samplers were not significantly different for Hg dry deposition flux, evaluated by a dependent paired t-test modeling the primary collector against the collocated collector for any of the sites in Michigan (). The absolute percent difference (APD) for the individual sampling periods (n = 9) ranged from 3.3% to 26.7%. The mean APD between

collocated ATSS samplers was 8.7%, and the median APD was 5.4%. Based on the Figure 2a regression slope, the average difference between the primary and collocated samplers was ~5%.

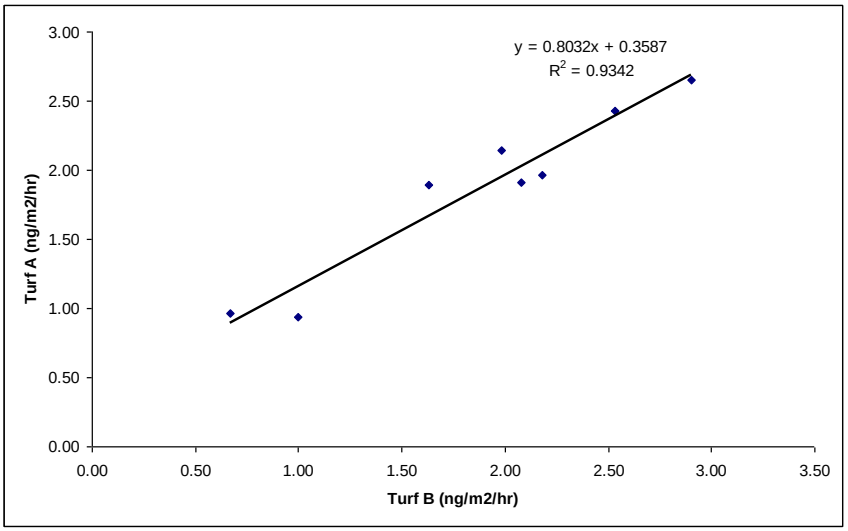

Figure 2.2: Collocated Artificial Turf Surrogate Surface (ATSS) results.

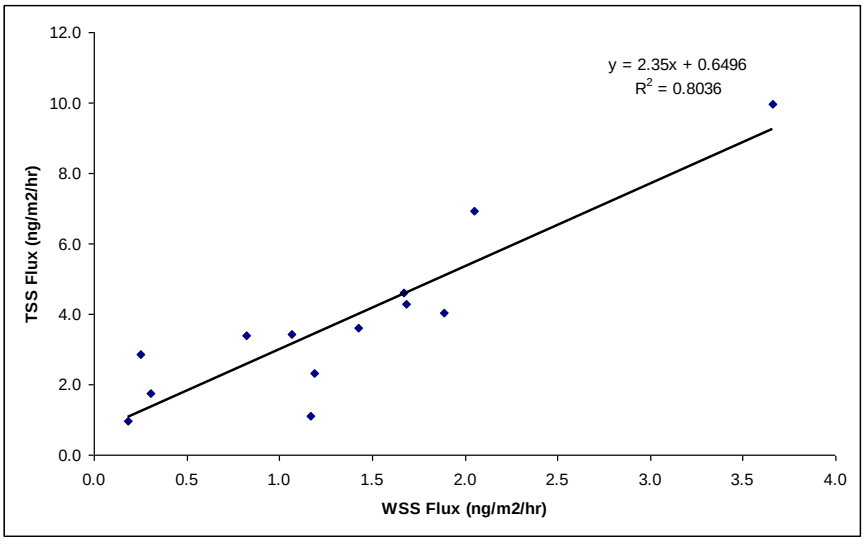

Figure 2.3: Artificial Turf Surrogate Surface (ATSS) versus the mean of collocated Static Water Surrogate Surface (SWSS) collector results for total Hg dry deposition results.

SWSS versus ATSS Comparison

Collocated SWSS collectors were deployed alongside the ATSS collector at the Dearborn site to compare the performance of the new ATSS collector design to the more routinely used

water collector configuration. The ATSS collector was found to measure systematically higher total Hg dry deposition flux than that from the SWSS sampler due to the greater bladed turf collection surface (Table 2.3), but the two methods were highly correlated (Figure 2.3) with a coefficient of determination of 0.879. On average, the ATSS collector provided results that were a factor of ~3 higher than the SWSS collector. Accounting for the average height, width, and density of the blades from turf surfaces we estimate an effective three-dimensional surface area of 0.131 m^2, approximately five times greater than the simple two-dimensional surface area calculations for the water surfaces (0.0257 m^2). The observation that the actual measured total Hg dry deposition flux enhancement (~3 times) was lower than the increased collection surface area (~5 times) is consistent with the published literature on real world vegetative edge effects and lower atmospheric deposition of in-stand atmospheric deposition (Beier, 1991; Beier and Gundersen, 1989; C. et al., 2002; Draaijers et al., 1994), and the observed importance of the physical structure and geometry of wild grasses as some species have higher deposition velocities despite lower leaf area indexes (Davidson et al., 1982).

The comparison between the ATSS and SWSS collector total Hg fluxes also need to be considered in light of SWSS samples that were invalidated due to contamination by wet deposition events. The ATSS method reflects deposition during a continuous exposure period (less the period of precipitation events), while the SWSS samplers were only deployed for 12- or 24 hour durations. Any precipitation during the SWSS sampling period invalidated the entire sample representing up to 24 hour of deposition, during which time the ATSS sampler was deployed and collecting. Consequently, during sampling periods with precipitation the valid collection time of the SWSS collectors were reduced to 50%–75% of the collocated ATSS collector. This comparison highlights several benefits of the ATSS sampler design: (i) the ATSS

collects a higher mass loading increasing Hg detectability; (ii) the ATSS method is more precise; (iii) the ATSS samplers can be deployed for longer unattended periods; and (iv) the ATSS method provides higher temporal coverage since periods of wet deposition do not invalidate the samples.

The ATSS and SWSS fluxes measured during these studies were similar to what has been measured in this region during other studies. Liu et al. (2007) measured an average dry deposition with the same SWSS method at a Detroit site of 3.3 $ng \cdot m^{-2} \cdot h^{-1}$ with a median of 1.2 $ng \cdot m^{-2} \cdot h^{-1}$ and Gildemeister (2001) measured Hg dry deposition fluxes at Detroit sites between 0.4 and 1.4·ng $m^{-2} \cdot h^{-1}$, using greased Mylar strips. Another difference between the suburban Botanical Gardens site and the urban/industrial Dearborn and Detroit-Fort Street sites was the mean concentration of GOM measured using the method described by Landis et al. (2002) was approximately five times higher at the Dearborn (23 $pg \cdot m^{-3}$) and Fort Street sites (27 $pg \cdot m^{-3}$). These GOM levels are similar to those previously reported at nearby Detroit sites by Liu et al. (2010, 2007).

Urban Gradients and the Relative Importance of Hg Dry Deposition

The ATSS data from the Dearborn study also provides insight into the potential impact of coarse particle Hg(p) dry deposition and the relative importance of wet and dry deposition in an urban/industrial area. The ATSS measurements were conducted at the Dearborn and Detroit-Fort Street sites concurrently. The distance between Dearborn and Detroit-Fort Street sampling sites is only 3.6 km, yet the total Hg dry deposition results for the ATSS samples starting on 22 July (1.16 $\mu g \cdot m^{-2}$ versus 0.69 $\mu g \cdot m^{-2}$) and 30 July (0.60 $\mu g \cdot m^{-2}$ versus 0.36 $\mu g\ m^{-2}$) were substantially different. The magnitude of the observed differences in total Hg dry deposition over such short

spatial scales suggests the influence of coarse fraction aerosols, which typically show more spatial heterogeneity in urban areas (Mukerjee et al., 2012; Sawvel et al., 2015) and have higher associated deposition velocities (Landis and Keeler, 2002; Lin et al., 1993). Total Hg wet deposition observed at the Dearborn (1.3 $\mu g \cdot m^{-2}$) and Detroit (1.4 $\mu g\ m^{-2}$) sites were virtually identical over the study period. The dry deposition of total Hg was found to be higher than total Hg wet deposition at the urban/industrial Dearborn and Detroit-Fort Street sites by a factor of 2.5 and 1.9, respectively.

Conclusions

The ATSS collector was found to be an effective new tool for the direct quantification of atmospheric total Hg dry deposition. The ATSS collector overcomes the major shortcomings identified with previous direct surrogate measurement approaches such as invalidation of samples impacted by precipitation or strong winds. The three-dimensional surface of the ATSS collector more realistically simulates natural vegetative surfaces, and results in the collection of additional Hg mass that decreases the analytical detection limit. Spike recoveries, collocated evaluations, and comparisons to SWSS collectors demonstrate that the ATSS collector is both accurate and precise.

The ATSS collector is ideally suited for investigating Hg dry deposition over both short collection times (day(s)) typically preferred during short-term intensive research studies, as well as longer collection times (week(s)) typical of long-term routine network monitoring when site operators may only be scheduled to visit a sampling site once a week. Longer deployment times would minimize the blank contribution, reduce method detection limits, and may increase the precision of the samples. Whereas frequent high volume rainfall events are common in Florida during the summer, in Michigan, the throughfall bottles could be deployed for up to seven days.

Samplers could also be modified to collect throughfall into 2 L bottles, thus eliminating a more frequent need to collect and change the sample bottles.

Acknowledgements: The U.S. Environmental Protection Agency (EPA) through its Office of Research and Development funded and participated in the research described here under an EPA Region 4 Regional Applied Research Effort (RARE) through cooperative agreement CR-83302001-0 with the Florida Department of Environmental Protection (FLDEP). The views expressed in this paper are those of the authors and do not necessarily reflect the views or policies of EPA. It has been subjected to EPA Agency review and approved for publication. Mention of trade names or commercial products does not constitute endorsement or recommendation for use. FLDEP administered the project through contract AQ198 with the University of Michigan Air Quality Laboratory (UMAQL). The authors would like to thank Thomas Atkeson and Robert K. Stevens from FDEP and the students and staff from UMAQL for their dedicated support of this work. The authors especially acknowledge the wisdom and guidance provided by the late Gerald J. Keeler. While Jerry passed prior to the completion of this work, he contributed immensely to its design and implementation.

Author Contributions: This work was a collaborative effort between all of the authors. Naima L. Hall, Frank J. Marsik, James A. Barres, Matthew S. Landis and Joseph Timothy Dvonch conceived and designed the field sampling campaigns. Naima L. Hall led field testing activities and laboratory analyses for the ATSS collector, and authored the first draft of the manuscript. Joseph Timothy Dvonch, Matthew S. Landis, Frank J. Marsik, and James A. Barres provided assistance with sampler design and fabrication, statistical analyses, and edited the manuscript.

References

Beier, C., 1991. Separation of Gaseous and Participate Dry Deposition of Sulfur at a Forest Edge in Denmark. J. Environ. Qual. 20, 460–466. https://doi.org/10.2134/jeq1991.00472425002000020020x

Beier, C., Gundersen, P., 1989. Atmospheric deposition to the edge of a spruce forest in Denmark. Environ. Pollut. 60, 257–271. https://doi.org/https://doi.org/10.1016/0269-7491(89)90108-5

Businger, J.A., 1986. Evaluation of the Accuracy with Which Dry Deposition Can Be Measured with Current Micrometeorological Techniques. J. Clim. Appl. Meteorol. 25, 1100–1124. https://doi.org/10.1175/1520-0450(1986)025<1100:EOTAWW>2.0.CO;2

C., W.K., L., C.M., A., P.S.T., 2002. Forest Edges as Nutrient and Pollutant Concentrators: Potential Synergisms between Fragmentation, Forest Canopies, and the Atmosphere. Conserv. Biol. 15, 1506–1514. https://doi.org/10.1046/j.1523-1739.2001.01090.x

Caldwell, C.A., Swartzendruber, P., Prestbo, E., 2006. Concentration and Dry Deposition of Mercury Species in Arid South Central New Mexico (2001−2002). Environ. Sci. Technol. 40, 7535–7540. https://doi.org/10.1021/es0609957

Carpi, A., Lindberg, S.E., 1998. Application of a teflon^{TM} dynamic flux chamber for quantifying soil mercury flux: Tests and results over background soil. Atmos. Environ. 32, 873–882. https://doi.org/https://doi.org/10.1016/S1352-2310(97)00133-7

Cobos, D.R., Baker, J.M., Nater, E.A., 2002. Conditional sampling for measuring mercury vapor fluxes 36, 4309–4321.

Davidson, C.I., Miller, J.M., Pleskow, M.A., 1982. The influence of surface structure on predicted particle dry deposition to natural grass canopies. Water. Air. Soil Pollut. 18, 25–43. https://doi.org/10.1007/BF02419401

Draaijers, G.P.J., Van Ek, R., Bleuten, W., 1994. Atmospheric deposition in complex forest landscapes. Boundary-Layer Meteorol. 69, 343–366. https://doi.org/10.1007/BF00718124

Dvonch, J.T., Graney, J.R., Keeler, G.J., Stevens, R.K., 1999. Use of Elemental Tracers to Source Apportion Mercury in South Florida Precipitation. Environ. Sci. Technol. 33, 4522–4527. https://doi.org/10.1021/es9903678

Fang, G.C., Zhang, L., Huang, C.S., 2012. Measurements of size-fractionated concentration and bulk dry deposition of atmospheric particulate bound mercury. Atmos. Environ. 61, 371–377. https://doi.org/https://doi.org/10.1016/j.atmosenv.2012.07.052

Fritsche, J., Wohlfahrt, G., Ammann, C., Zeeman, M., Hammerle, A., Obrist, D., Alewell, C.,

2008. and Physics Summertime elemental mercury exchange of temperate grasslands on an ecosystem-scale 7709–7722.

Fu, X., Feng, X., Wang, S., 2008. Exchange fluxes of Hg between surfaces and atmosphere in the eastern flank of Mount Gongga , Sichuan province , southwestern China 113, 1–12. https://doi.org/10.1029/2008JD009814

Gildemeister, A.E. (University of M.L.D.B., 2001. Urban atmospheric mercury: The impact of local sources on deposition and ambient concentration in Detroit, Michigan [electronic resource].

Graydon, J.A., St. Louis, V.L., Lindberg, S.E., Hintelmann, H., Krabbenhoft, D.P., 2006. Investigation of Mercury Exchange between Forest Canopy Vegetation and the Atmosphere Using a New Dynamic Chamber. Environ. Sci. Technol. 40, 4680–4688. https://doi.org/10.1021/es0604616

Guentzel, J.L., Landing, W.M., Gill, G.A., Pollman, C.D., 1995. Atmospheric deposition of mercury in Florida: The fams project (1992--1994). Water. Air. Soil Pollut. 80, 393–402. https://doi.org/10.1007/BF01189689

Huang, J., Liu, Y., Holsen, T.M., 2011. Comparison between knife-edge and frisbee-shaped surrogate surfaces for making dry deposition measurements : Wind tunnel experiments and computational fluid dynamics (CFD) modeling. Atmos. Environ. 45, 4213–4219. https://doi.org/10.1016/j.atmosenv.2011.05.013

Iverfeldt, Å., 1991. Mercury in forest canopy throughfall water and its relation to atmospheric deposition. Water Air Soil Pollut. 56, 553–564. https://doi.org/10.1007/BF00342299

Keeler, G.J., Dvonch, T.J., 2005. Atmospheric Hg: A Decade of Observations in the Great Lakes, in: Pirrone, N., Mahaffey, K.R. (Eds.), Dynamics of Mercury Pollution on Regional and Global Scales: Atmospheric Processes and Human Exposures Around the World. Springer US, Boston, MA, pp. 611–636. https://doi.org/10.1007/0-387-24494-8_25

Keeler, G.J., Landis, M.S., Norris, G.A., Christianson, E.M., Dvonch, J.T., 2006. Sources of Mercury Wet Deposition in Eastern Ohio, USA. Environ. Sci. Technol. 40, 5874–5881. https://doi.org/10.1021/es060377q

Kim, K.-H., Lindberg, S.E., Meyers, T.P., 1995. Micrometeorological measurements of mercury vapor fluxes over background forest soils in eastern Tennessee. Atmos. Environ. 29, 267–282. https://doi.org/https://doi.org/10.1016/1352-2310(94)00198-T

Lai, S., Huang, J., Hopke, P.K., Holsen, T.M., 2011. Science of the Total Environment An evaluation of direct measurement techniques for mercury dry deposition. Sci. Total Environ. 409, 1320–1327. https://doi.org/10.1016/j.scitotenv.2010.12.032

Landis, M.S., Keeler, G.J., 2002. Atmospheric mercury deposition to Lake Michigan during the Lake Michigan Mass Balance Study. Environ. Sci. Technol. 36, 4518–4524. https://doi.org/10.1021/es011217b

Landis, M.S., Keeler, G.J., 1997. Critical evaluation of a modified automatic wet-only precipitation collector for mercury and trace element determinations. Environ. Sci. Technol. 31, 2610–2615. https://doi.org/10.1021/es9700055

Landis, M.S., Stevens, R.K., Schaedlich, F., Prestbo, E.M., 2002. Development and Characterization of an Annular Denuder Methodology for the Measurement of Divalent Inorganic Reactive Gaseous Mercury in Ambient Air. Environ. Sci. Technol. 36, 3000–3009. https://doi.org/10.1021/es015887t

Lin, J.-M., Fang, G.-C., Holsen, T.M., Noll, K.E., 1993. A comparison of dry deposition modeled from size distribution data and measured with a smooth surface for total particle mass, lead and calcium in Chicago. Atmos. Environ. Part A. Gen. Top. 27, 1131–1138. https://doi.org/https://doi.org/10.1016/0960-1686(93)90148-R

Lindberg, S.E., Meyers, T.P., Taylor, G.E., Turner, R.R., Schroeder, W.H., 1992. Atmosphere-surface exchange of mercury in a forest: Results of modeling and gradient approaches. J. Geophys. Res. Atmos. 97, 2519–2528. https://doi.org/doi:10.1029/91JD02831

Liu, B., Keeler, G.J., Dvonch, J.T., Barres, J.A., Lynam, M.M., Marsik, F.J., Taylor, J., 2007. Temporal variability of mercury speciation in urban air 41, 1911–1923. https://doi.org/10.1016/j.atmosenv.2006.10.063

Liu, B., Keeler, G.J., Timothy Dvonch, J., Barres, J.A., Lynam, M.M., Marsik, F.J., Morgan, J.T., 2010. Urban–rural differences in atmospheric mercury speciation. Atmos. Environ. 44, 2013–2023. https://doi.org/https://doi.org/10.1016/j.atmosenv.2010.02.012

Lyman, S.N., Gustin, M.S., Prestbo, E.M., Kilner, P.I., Edgerton, E., Hartsell, B., 2009. Testing and application of surrogate surfaces for understanding potential gaseous oxidized mercury dry deposition. Environ. Sci. Technol. 43, 6235–6241. https://doi.org/10.1021/es901192e

Lyman, S.N., Gustin, M.S., Prestbo, E.M., Marsiks, F.J., 2007. Estimation of dry deposition of atmospheric mercury in Nevada by direct and indirect methods. Environ. Sci. Technol. 41, 1970–1976. https://doi.org/10.1021/es062323m

Marsik, F.J., Keeler, G.J., Landis, M.S., 2007. The dry-deposition of speciated mercury to the Florida Everglades: Measurements and modeling. Atmos. Environ. 41, 136–149. https://doi.org/10.1016/j.atmosenv.2006.07.032

Meyers, T.P., Hall, M.E., Lindberg, S.E., Kim, K., 1996. Use of the modified bowen-ratio technique to measure fluxes of trace gases. Atmos. Environ. 30, 3321–3329.

https://doi.org/https://doi.org/10.1016/1352-2310(96)00082-9

Mukerjee, S., Willis, R.D., Walker, J.T., Hammond, D., Norris, G.A., Smith, L.A., Welch, D.P., Peters, T.M., 2012. Seasonal effects in land use regression models for nitrogen dioxide, coarse particulate matter, and gaseous ammonia in Cleveland, Ohio. Atmos. Pollut. Res. 3, 352–361. https://doi.org/https://doi.org/10.5094/APR.2012.039

Peterson, C., Alishahi, M., Gustin, M.S., 2012. Testing the use of passive sampling systems for understanding air mercury concentrations and dry deposition across Florida, USA. Sci. Total Environ. 424, 297–307. https://doi.org/10.1016/j.scitotenv.2012.02.031

Poissant, L., Pilote, M., Beauvais, C., 2004. Atmospheric mercury speciation and deposition in the Bay St . Franc ¸ ois wetlands 109, 1–11. https://doi.org/10.1029/2003JD004364

Prestbo, E.M., Gay, D.A., 2009. Wet deposition of mercury in the U . S . and Canada , 1996 – 2005 : Results and analysis of the NADP mercury deposition network (MDN). Atmos. Environ. 43, 4223–4233. https://doi.org/10.1016/j.atmosenv.2009.05.028

Rea, A.W., Keeler, G.J., Scherbatskoy, T., 1996. The deposition of mercury in throughfall and litterfall in the lake champlain watershed: A short-term study. Atmos. Environ. 30, 3257–3263. https://doi.org/https://doi.org/10.1016/1352-2310(96)00087-8

Rea, A.W., Lindberg, S.E., Keeler, G.J., 2000. Assessment of dry deposition and foliar leaching of mercury and selected trace elements based on washed foliar and surrogate surfaces. Environ. Sci. Technol. 34, 2418–2425. https://doi.org/10.1021/es991305k

Risch, M.R., Gay, D.A., Fowler, K.K., Keeler, G.J., Backus, S.M., Blanchard, P., Barres, J.A., Dvonch, J.T., 2012. Spatial patterns and temporal trends in mercury concentrations , precipitation depths , and mercury wet deposition in the North American Great Lakes region. Environ. Pollut. 161, 261–271. https://doi.org/10.1016/j.envpol.2011.05.030

Sakata, M., Marumoto, K., 2004. Dry Deposition Fluxes and Deposition Velocities of Trace Metals in the Tokyo Metropolitan Area Measured with a Water Surface Sampler. Environ. Sci. Technol. 38, 2190–2197. https://doi.org/10.1021/es030467k

Sakata, M., Marumoto, K., Narukawa, M., Asakura, K., 2006. Mass balance and sources of mercury in Tokyo Bay. J. Oceanogr. 62, 767–775. https://doi.org/10.1007/s10872-006-0096-9

Sawvel, E.J., Willis, R., West, R.R., Casuccio, G.S., Norris, G., Kumar, N., Hammond, D., Peters, T.M., 2015. Passive sampling to capture the spatial variability of coarse particles by composition in Cleveland, OH. Atmos. Environ. 105, 61–69. https://doi.org/https://doi.org/10.1016/j.atmosenv.2015.01.030

Shahin, U.M., Holsen, T.M., Odabasi, M., 2002. Dry deposition measured with a water surface sampler : a comparison to modeled results 36, 3267–3276.

Skov, H., Brooks, S.B., Goodsite, M.E., Lindberg, S.E., Meyers, T.P., Landis, M.S., Larsen, M.R.B., Jensen, B., 2006. Fluxes of reactive gaseous mercury measured with a newly developed method using relaxed eddy accumulation 40, 5452–5463. https://doi.org/10.1016/j.atmosenv.2006.04.061

St. Louis, V.L., Rudd, J.W.M., Kelly, C.A., Hall, B.D., Rolfhus, K.R., Scott, K.J., Lindberg, S.E., Dong, W., 2001. Importance of the Forest Canopy to Fluxes of Methyl Mercury and Total Mercury to Boreal Ecosystems 35, 3089–3098. https://doi.org/10.1021/es001924p

Wu, Y., Davidson, C.I., Dolske, D.A., Sherwood, S.I., Davidson, C.I., Dolske, D.A., Sherwood, S.I., Wu, Y., Davidson, C.I., Sherwood, S.I., 2007. Dry Deposition of Atmospheric Contaminants : The Relative Importance of Aerodynamic , Boundary Layer , and Surface Resistances Dry Deposition of Atmospheric Contaminants : The Relative Importance of Aerodynamic , Boundary Layer , and Surface Resistances 6826. https://doi.org/10.1080/02786829208959538

Yi, S.M., Holsen, T.M., Noll, K.E., 1997. Comparison of dry deposition predicted from models and measured with a water surface sampler. Environ. Sci. Technol. 31, 272–278. https://doi.org/10.1021/es960410g

Zhang, L., Brook, J.R., Vet, R., 2003. A revised parameterization for gaseous dry deposition in air-quality models 2067–2082.

Table 2.1: Summary of total Hg ATSS field blanks at Michigan sites (ng).

Blank Metric	Throughfall	Turf	Total
n	6	6	6
Mean	0.03	1.96	1.99
Standard Deviation	0.02	1.12	1.12
Minimum	0.01	0.52	0.56
Maximum	0.05	3.07	3.09
Median	0.03	2.31	2.33

Table 2.2: Summary of total Hg ATSS field blanks at Florida sites (ng).

Blank Metric	Throughfall	Turf	Total
n	77	77	77
Mean	0.07	0.77	0.84
Standard Deviation	0.07	0.44	0.44
Minimum	0.01	0.12	0.19
Maximum	0.39	1.96	2.01
Median	0.05	0.71	0.75

Table 2.3: Comparison of Artificial Turf Surrogate Surface (ATSS) versus Static Water Surrogate Surface (SWSS) sampler at Michigan Sites.

Site	n	ATSS Flux ($ng \cdot m^{-2} \cdot h^{-1}$)	SWSS Flux ($ng \cdot m^{-2} \cdot h^{-1}$)
Botanical Gardens	3	1.56	0.26
Dearborn	5	6.42	2.22
Detroit-Fort Street	5	5.38	1.29

Chapter 3 : Spatial and Temporal Variability of Hg Wet and Dry Deposition in Florida

Abstract

Atmospheric deposition of mercury (Hg) is a major public health concern that contributes Hg loadings to ecosystems resulting in the bioaccumulation of this neurotoxic heavy metal in fish and other wildlife. A new method using an artificial turf surrogate surface (ATSS) was implemented during summertime field measurement intensives conducted as part of a Hg Total Maximum Daily Load (TMDL) project in the state of Florida. Wet and dry deposition of Hg was measured at 15 sites in 2009 and 11 sites in 2010. On average, across the sites, Hg dry deposition was determined to contribute 27% to the total Hg deposition during the one-month study periods and ranged in magnitude across sites from 0.6 $\mu g/m^2$ to 2.1 $\mu g/m^2$. In comparison, wet deposition of Hg measured during the month-long intensives ranged from 1.5 $\mu g/m^2$ to 6.9 $\mu g/m^2$. A North- South spatial gradient was observed for increased wet deposition of Hg. The ratio of wet deposition to dry deposition of Hg was also highly variable across the sites in the study ranging from 1.1 to 5.8. Findings of different spatial and temporal trends in wet and dry deposition suggest that different mechanisms and factors were influencing deposition.

Introduction

Elevated methylmercury concentration in fish is a public health concern impacting recreational fishers, subsistence fish-eaters, as well as susceptible populations like pregnant women and young children (Rothenberg et al., 2008). Florida, in particular, has been shown to have some of the highest total mercury (Hg) wet deposition fluxes in the United States (NADP, 2017). This had led the state to issue consumption advisories for fish in fresh and marine waterbodies (Florida Department of Health, 2017).

Atmospheric deposition is a process affecting concentrations of various pollutants in ecosystems and is a crucial part of mercury's biogeochemical cycle. Mercury is methylated in waterbodies and wetlands and bioaccumulates in the foodweb. Deposition to water and land surfaces through wet and dry processes results in high methylmercury levels in fish as well as other wildlife (Beyer et al, 1997; Nilsen et al 1997; Barron et al 2004).

To characterize and understand Hg deposition in Florida, many studies have been conducted across the state for several decades. The National Atmospheric Deposition Program (NADP) has had several monitoring stations throughout Florida since 1996 (NADP, 2017). Several other studies including the FAMS and SoFAMMS (Guentzel et al, 1995; Dvonch et al, 1995) were conducted to investigate atmospheric Hg including wet Hg deposition in Florida. There is a consensus that the highest Hg deposition rates are in southern Florida in the Everglades region of the US. However, while the amount of Hg being wet deposited has been well characterized, the amount of dry deposition is less known.

Measurement of dry deposition has presented a unique set of challenges and has limited research attempting to quantify Hg dry deposition loadings. Extensive work has been conducted estimating Hg dry deposition using inferential and deterministic models; however, these could be

enhanced with more directly measured dry deposition values for comparison and validation. In Florida, there have been few direct Hg dry deposition measurements, one was a study by Marsik et al (2007) where deposition velocity was measured using the water surrogate surface sampling method (WSS) in the Everglades. However, because samplers must be covered from precipitation events, the method was difficult to implement in Florida especially during seasons when rainfall events are frequent.

Recent methods have been developed that avoid some of the difficulties of traditional dry deposition measurements. Surrogate surface methods and passive measurements of gaseous oxidized mercury (GOM) have been used to calculate dry deposition of Hg (Lyman et al, 2009, Peterson et al, 2012). Still, a research gap remains for directly measuring RGM and $Hg_{(p)}$ dry deposition.

The artificial turf surrogate surface (ATSS) sampler method (Hall et al, 2017) was developed to address some limitations of the WSS sampling approach, including rainfall contamination and sample loss due to wind and evaporation. This was the first major field campaign where the ATSS samplers were deployed across a large network of sites for dry deposition measurements. ATSS sampling is particularly well suited for a climate like Florida where summertime precipitation events are frequent.

This study was conducted to improve the understanding of Hg deposition, specifically dry deposition loadings in Florida. Additionally, it seeks to determine if dry deposition significantly contributes to the total deposition particularly during the summer wet season when the state receives most of its wet deposition of Hg. The study also characterized the spatial variability of Hg dry deposition to investigate broader geographic trends across the state.

Methods

Site Descriptions

As a part of a Hg total maximum daily load (TMDL) study for the state of Florida, the University of Michigan Air Quality Laboratory (UMAQL) conducted several field intensive campaigns during the summers of 2009 and 2010. The intensives built on the existing TMDL framework consisting of multi-year supersites situated in four regions of Florida. Twenty-six sites were established over the two summer seasons in the regions around the supersites for one month of sampling. These intensives were conducted during summer months to take advantage of known seasonal high rainfall in Florida.

The Western, Eastern, Central and Southern regions and sites are shown in Figure 3.1 and described in Table 3.1. The Central region measurement intensive was conducted from July 4- August 4, 2009. Seven sites; CRS, UCF, HSB, PCT, SDK, DSO, and MKA were located around the Tampa supersite (TPA). The Southern region measurement intensive was also conducted during July 4- August 4, 2009 and included the sites of OKB, FKE, EHP, MIA, KYB, and ENP located around the Davie supersite (DVE) and included the Miami metropolitan area as well as portions of the Everglades. The Eastern region measurement intensive was conducted between July 24- August 23, 2010 and included the sites of OCS, LTI, NJK, CSF, and GBP around the Jacksonville supersite (JKS). The Western region measurement intensive was conducted between July 24- August 23, 2010 and included the sites of UWF, BLG, BWR, and MBI located around the Pensacola supersite (OLF) encompassing western Florida and the Mobile site in southern Alabama.

Point sources for Hg emissions were identified using the US EPA National Emissions Inventory, (U.S. EPA NEI, 2012) which estimates Hg emissions from sources including electrical generating utilities using coal as well as other fuels; area emissions from electric arc furnaces; municipal waste combustors; cement processing; and industrial, commercial or institutional boiler (ICI boilers). For these categorizations, point sources that had an estimated emission of Hg greater than 2 kg/ year were included for analysis. ArcGIS was used to determine the distance and direction between the sites and the emission sources. Sites that were within 10 km were considered "near-field" and those further than 50 km were considered "far-field."

Sites were further described by their relationship to the coastline and proximity to highly populated areas. Distance and direction to the coastline was calculated by ArcGIS, establishing the nearest point of the coastline to a site as defined by U.S. States GIS layer (ESRI, 2017). Sites were determined to be "coastal" if they were within 0.5 km of the coast. Population density was determined using the urban spatial layer from the 2010 census (ESRI, 2017). Sites were categorized as "urban" or "rural" depending on whether they were inside a census-defined urban area or further than 10 km away respectively.

ATSS and Precipitation Collection

Dry deposition of Hg was measured using the ATSS method (testing and evaluation is described in full in Hall et al. (2017)). Turf surfaces were deployed in aerodynamic airfoils that were set-up at approximately 8:00 am EDT and were collected after 72-hours, upon which time new samples were deployed. Throughfall bottles positioned below the turf to receive precipitation were collected and exchanged the morning following any measurable precipitation

event. After collection, turf surfaces were placed into 2 L wide-mouth FLPE bottles. Sample wells were rinsed with a 50 mL of 0.2% HNO_3 solution that was added to the bottle with the turf sample.

Daily precipitation events were also collected and analyzed. Samples were statistically integrated into three-day averages as part of the ATSS method in addition to use as measurement of wet deposition. Automated Sequential Precipitation Samplers (ASPS II) were used for wet deposition sample collection at the DVE and UCF sites, following the protocol described in Landis and Keeler (1997). Bulk precipitation was collected using methods previously described (Dvonch et al., 1998 and White et al., 2009) at the remaining sites. Bulk precipitation samples were collected the morning following precipitation events. Rain gauge tipping buckets (Young, USA) with data loggers (Onset HOBO®, Pocasset, MA) recording tips and temperature were deployed to confirm the amount of precipitation received at each site.

The frequency of field blank collection was 30% for the ATSS samples and correspondingly three times during the sampling months for the bulk precipitation samples, which represented 17-43% frequency. Field blanks with the ASPS samplers were conducted 10% of the time. The field blanks for precipitation samples were below the MDL. There was a measurable field blank for the ATSS method that was averaged on a regional basis and subtracted from measured values to achieve the Hg deposition results presented.

Sampling and analytical supplies that came into contact with samples were acid cleaned using the method described in Landis and Keeler (1997). Glass funnels, Teflon® adaptors and glass vapor locks used as part of the bulk precipitation sampling trains were cleaned in the field

using a modified version of this procedure that substituted a 72-hr soak in 5% HNO_3 solution for the 6-hour heated bath.

Laboratory analysis

Laboratory analysis for wet and dry Hg deposition samples was conducted at the UMAQL. Sample processing and analysis was described in Hall et al (2017). Quality control and analysis was conducted through duplicates, analytical blanks, matrix spikes and control standard recovery. The method detection limit was 0.33 ng/L. Analytical replicates were conducted after every six samples analyzed. There were 181 samples with replicate analysis that were above the method detection limit. These replicates had an average absolute percent difference of 1.9%, and ranged from 0.0 to 7.4%. There were 287 control standards that were analyzed during the study. The control standard recovery percentage was an average of 102.0%, and the range of the control standard recovery was from 92.8 to 110.3%.

Results and Discussion

There were 26 sites where a total of 260 dry deposition samples and 294 wet deposition samples were collected over the field intensives in summer 2009 and 2010. The mean dry deposition was 112.9 ng/m^2 per three-day sample period, while mean wet deposition at these sites was 263.8 ng/m^2. Hg dry deposition was, on average, 27% of the total Hg deposition during the study periods. The mass of Hg deposition varied considerably by site and region, as did the percentage of dry deposition. Both wet and dry deposition contributed substantially to the total Hg deposited at all of the sites.

Precipitation Events

Table 3.2 summarizes descriptive statistics for the precipitation events, wet and dry deposition of Hg by site and by region. The amount of precipitation received during the study ranged from 7.1 cm at OKB to 23.7 cm at DVE. Precipitation events (> 0.1 cm) occurred, on average, on 11.3 days across the sites (from a minimum of seven days at DSO and KYB to a maximum of 17 precipitation days at DVE). Because the 20 mL of HCl preservative in the sample bottle contributes to decreased precision in measuring the concentration of Hg in samples that had less than 0.1 cm, we followed other UMAQL study protocols and did not collect these events as separate samples. The sites in the Western region had the highest average monthly precipitation amount, 17.6 cm. The average precipitation frequency by region was very similar; 11.0 days at the Eastern, Western and Central regions and 12.1 days in the Southern region. Field intensive studies at the Central and Southern regions were 31 days in duration, while intensives in the Eastern and Western regions were 30 days in duration.

The average Hg volume-weighted mean (VWM) concentration across the study sites was 19.7 ng/L, with a range from 11.2 ng/L (UWF) to 36.8 ng/L (MIA) (standard deviation= 6.8). Figure 3 shows the magnitude of the Hg VWM concentrations and the spatial range. A strong regional spatial pattern was observed where the average Hg VWM concentration ranged from 13.4 ng/L in the Western region to more than twice that, at 27.5 ng/L in the Southern region. The least variation in VWM concentration by region was in the Eastern region where the standard deviation of Hg VWM concentration of sites was 1.2 ng/L. The highest standard deviation of the VWM concentration was in the Southern region at 7.3 ng/L.

Deposition

Total Hg deposition, the sum of wet plus dry Hg deposition varied widely by site ranging from 2.2-8.3 μg/m^2, with KYB having the least total deposition and DVE having the greatest. The statewide average total deposition was 4.1 μg/m^2 (standard deviation of 1.6 μg/m^2 and a median of 3.8 μg/m^2). The highest total mean deposition occurred in the southern region, which was 5.3 μg/m^2. The other regions had mean total deposition ranging from 3.3 to 3.9 μg/m^2.

The mean Hg dry deposition was 1.1 μg/m^2, median 1.1 μg/m^2 with a standard deviation of 0.3, across all study sites. Hg dry deposition ranged from 0.55 μg/m^2 at OLF (Western region) to 1.9 μg/m^2 at CRS (Central region). The mean Hg wet deposition was 3.0 ug/m^2, median 2.4 ug/m^2 with a standard deviation of 1.5, across all study sites. Hg wet deposition ranged from 1.5 μg/m^2 at LTI (Eastern region) to 6.9 μg/m^2 at DVE (Southern region).

There was more Hg wet deposition than Hg dry deposition at all of the sites. However, the dry deposition of Hg comprised a sizeable amount of total Hg deposition at all of the sites, even those that received very high amounts of precipitation. The ratio of wet deposition to dry deposition of Hg across the sites in the study ranged from 6.3 at EHP to 1.1 at CRS (this represents a percentage Hg dry deposition of 14% to 48% of total deposition). The mean ratio of wet to dry deposition was 2.8. The region with the greatest wet to dry deposition ratio was the Southern region that had five out of seven of the highest ratios (average ratio of 4.2). This was also the area with the highest average wet deposition and the lowest average dry deposition. Dry deposition contributed 29-33% to the total deposition at the West, East and Central regions and was 18% of total deposition for the Southern region.

Spatial trends

A moderate North-South increasing gradient was observed for the total deposition of Hg. This was largely driven by the higher amounts of Hg wet deposition (from both higher Hg concentration in precipitation and higher precipitation amounts, see figure 3) at the southern sites. The Hg dry deposition varied slightly between regions but did not demonstrate as clear of a trend. None of the regions were statistically significantly different from each other for wet or dry Hg deposition. There were also no East-West gradients observed for wet or dry Hg deposition.

There was some site-to-site variability within regions for Hg dry deposition. The Western region had the most intra-region variability and the Eastern region had the least (standard deviations were 41.3 ng/m^2 and 13.5 ng/m^2 respectively). There was more site-to-site variability for Hg wet deposition where three of the regions had similar standard deviations of their sites' Hg wet deposition of 57.2 ng/m^2, 58.4 ng/m^2, 58.7 ng/m^2 (Eastern, Western and Central) and the Southern site had the largest standard deviation of 147 ng/m^2.

There were geographic patterns to the magnitude of the minimum and maximum concentration of Hg in precipitation at each of the sites. Among the 26 sites, the average Hg concentration of a precipitation event was 23.0 ng/L. The site with the lowest concentration in precipitation was UCF with 4.1 ng/L (see figure 4) in 3.8 cm of precipitation. The site with the highest minimum concentration was MIA with 18.8 ng/L in 0.28 cm of precipitation event. The maximum precipitation concentration by site was lowest at DSO (21.4 ng/L; 0.14 cm) while the highest was at MBI (95.6 ng/L; 0.26 cm). Regionally, the lowest minimum concentrations were in the Western region (regional mean= 6.4 ng/L) while the mean minimum concentrations in the

Southern region was twice as high at 12.9 ng/L. This is a similar pattern to that seen for VWM concentration.

The lowest minimums in the southern region were OKB and FKE with 8.4 ng/L and 9 ng/L respectively and both of these sites were picked to represent non-source impacted sites and non-populous areas. In contrast, even these low values were higher than even the highest site minimum in the western region, 7.8 ng/L at UWF. Overall, five out of the six highest minimum concentrations were from the seven sites of the Southern region.

The higher background Hg levels in the southern region were not associated with higher Hg dry deposition loadings as the southern region had the lowest regional mass of Hg dry deposition. Factors such as the amount, duration and frequency of precipitation, particularly in southern Florida could have lowered the atmospheric Hg available for dry deposition.

Coastal sites

On average, the coastal sites had less Hg deposition compared to inland sites. This consisted of both receiving less precipitation, having lower Hg concentration in precipitation events and having lower wet and dry Hg deposition as shown in Table 3.3. Among the six coastal sites, SDK, DSO, LTI, MBI, KYB and OCS, the largest differences between the coastal and non-coastal locations was for Hg wet deposition and precipitation frequency, which were both significantly lower. Six out of the eight lowest total Hg deposition values were coastal sites. This was largely driven by having six out of eight of the lowest Hg wet deposition totals. The remaining sites with the lowest values were OKB, located off of Lake Okeechobee and BLG, which was 0.67 km from the Gulf Coast near Pensacola and the seventh closest site to the coast.

The lower wet deposition was partially driven by lower precipitation frequency as well as slightly lower precipitation totals during events.

Earlier studies (Malcolm and Keeler, 2003; Engle et al 2008; Malcolm et al, 2009; Holmes et al 2009) have suggested that the sea salt aerosols present in the marine environment may provide a substrate to encourage the formation of particulate Hg that could lead to enhanced Hg dry deposition. However, the coastal sites in this study did not have more dry deposition than other sites on average. There were several potentially confounding factors. These include that non-coastal sites tended to be closer to larger Hg emission sources, on-shore breezes and, that the inland sites received more precipitation leading to more moisture on the turf surface which could enhance the adsorption of hydrophilic gaseous oxidized mercury (GOM). Furthermore, this process could occur by scavenging GOM from the environment so while we could be measuring more $Hg_{(p)}$ there would be less GOM available for deposition. There was also a large variation in the ground cover between the sampling location and the coast, ranging from trees, brush and other flora to just a few meters of sandy beach.

Temporal trends

There was a range in the magnitude of temporal variability observed among the different sites. During the intensives, the lowest variability of Hg dry deposition was at NJK with 29.6% standard deviation while the highest was at PCT with a relative standard deviation (RSD) of 159%. For Hg wet deposition, the lowest site was MBI (57.7%) and the highest was MIA (144%). Regional RSDs showed that the sites in the Southern region had the highest Hg dry deposition RSDs, while the lowest was at the Eastern sites. For wet deposition, the region with the lowest average was Southern region; while the Northern region had the lowest variability

(measured as RSD). The variability of Hg concentration in precipitation events was highest in the Western region and lowest in the Southern region. Although generally there was greater temporal variability for wet deposition than dry deposition, the temporal variability of Hg precipitation concentration was lower than the dry deposition variability for most of the sites.

The variability observed in dry deposition and in wet deposition is reflected in the following case studies where we examine trends and factors influencing Hg loadings in several 3-day turf sampling periods and their concurrent precipitation events. While these periods generally follow the same monthly trends described above, they often highlight the advantages of investigating deposition on finer timescales in addition to month-long or seasonal averages.

Case Studies

Case study one

The seventh turf sampling period (T7), spanned the 72 hours from July 23-26, 2009. During this time, sampling was conducted at 15 sites in the Central and Southern regions. Generally, the average event frequency, precipitation amount, and Hg concentration in precipitation followed the monthly temporal trends above; however, there were some particularly influential deposition events at KYB and MKA which contributed more than half of each site's total precipitation and Hg dry deposition for the month study.

As noted above, the coastal sites had some of the lowest precipitation amounts as well as wet and dry loadings of their intensives; however, T7 represented a period during which KYB had the greatest precipitation and wet deposition of the Southern region. Located near Miami on the East shore of Key Biscayne, its coastal position meant that due to Florida meteorology, it

received fewer of the late afternoon thunderstorms that contributed much of the precipitation to the other more inland sites. However, early on 7/25/2009, there was a large precipitation system that spanned from the Florida Keys reaching northeast across the southern-most portion of the state and past the island of Grand Bahama in the northern Bahamas. This system, which led to intermittent rainfall over the course of the day, was responsible for 5.5 cm of rain, which contributed 73% of the precipitation that was collected at KYB during the 31-day study intensive. This was more than five times the daily mean precipitation amount at KYB (1.1 cm). This event was also responsible for the majority of the total Hg deposition received at the site for the entire study period contributing 72% of the total Hg wet deposition and 56% of the total Hg deposition during this sampling period. The Hg concentration during this event was 20.8 ng/L, which was very close to the average VWM concentration for KYB of 21.6 ng/L. Despite the large amount of wet deposition, this period also had a higher than average dry deposition loading during the three-day period.

KYB had almost twice as much dry deposition as the average (106.4 ng/m^2 for T7 versus the intensive average at that site of 55.5 ng/m^2). Aside from KYB and FKE, which was also much higher than average (162.1 ng/m^2 as opposed to 81.8 ng/m^2 intensive average), the dry deposition of the Southern sites during T7 was similar to the study average. EHP and ENP had unusually low masses of Hg dry deposited; particularly at EHP, where T7 had the lowest mass of Hg measured at that site. Temporal variability of the Hg dry deposition was less than that of Hg wet deposition, for T7 and in general.

MKA also experienced a very influential event during this time. On 7/25/2009, it had higher than average precipitation depth of 2.21 cm with higher than average precipitation concentration (52.7 ng/L) yielding 1164 ng/m^2 of Hg which was also the highest mass of Hg wet

deposited from a single precipitation event during the 2009 central intensive. SDK also had a higher than average concentration of Hg in its rainfall event on 7/25/2009 with 43.9 ng/L (compared to its site average of 20.7 ng/L). At SDK, this was the highest Hg concentration event. Other rainfall events in the Central region during these days were closer to the average.

Spatial variability in the Central and Southern regions was similar to that observed during the month-long intensive. The Central sites on average had higher Hg dry deposition than the Southern sites, while the Southern sites had more precipitation events and had higher concentration of Hg in the precipitation. Contrary to the usual trend, during T7 the average precipitation amount at the Central sites was higher than that for the Southern sites.

The T7 period exhibits how the month-long intensive means do not fully reflect the high variability observed in shorter timescales. Furthermore, single precipitation events can be highly influential on the month-long deposition results. MKA received almost a third of its Hg wet deposition during this period because of a moderately heavy rain event that had a high concentration of Hg. Additionally, KYB not only received most of the Hg wet deposition during this time period, it also received twice as much wet deposition as the next highest site, a different pattern than what was observed for any other time period.

Case study two

The spatial variability of Hg wet deposition during T10 (August 20-23, 2010) was much greater than average in the Eastern region. The ratio of the highest to lowest wet deposition of Hg during the T10 period was greater than 6 while the average ratio was 2.6 for the month-long time period. There was high Hg wet deposition at the CSF, LTI and NJK sites, while only moderate Hg wet deposition at OCS. GBP and JKS had the least wet deposition and received

much smaller amount of precipitation. The concentration of Hg also showed some spatial variability, ranging by a factor of 3.3.

During T10, there was also greater variability than the average for dry deposition. The highest dry deposition was measured at CSF at 199.8 ng/m^2 while the lowest was at NJK (41.6 ng/m^2). This was a factor of 4.8 times greater (the intensive average was a factor of 1.39 between highest and lowest) which represents a RSD of 10%. The LTI and NJK sites had lower than average dry deposition during T10, while the OCS, CSF, and GBP sites were higher than average. The JKS site was within 10% of the average Hg dry deposition during a turf period. The variation in the dry deposition at the LTI, OCS and NJK sites was larger than average. There was more wet deposition than dry deposition at all of the sites, even those with fairly low volumes of precipitation.

This spatial variability was particularly apparent for the Eastern sites of LTI, OCS, and NJK where despite their close proximity (located within 6 km of each other) the sites received differing amounts of Hg wet and dry deposition during the T10 time frame. A similar pattern was observed over the month for mean Hg wet and dry deposition. There were six periods where at least two of the sites had precipitation. During five of those times the highest wet deposition was at least twice the lowest wet deposition. This variability was driven by the sites receiving some unique isolated thunderstorms and the difference in the concentration of Hg in the precipitation events. This variability was reflected in Hg dry deposition. Six out of 10 sampling periods had more than a two-fold difference between the highest and the lowest dry deposition.

The highest wet deposition occurred at NJK (1054 ng/m^2) which was more than twice as much as the lowest at OCS (491.1 ng/m^2). There were variable amounts of precipitation received at the LTI, OCS and NJK sites. There was an event at a minimum of one site during 11

of the 30 sampling days. However, only during five of those occasions, less than half of the time, was precipitation received at all three sites. On one occasion, there were precipitation events only at the NJK and OCS. LTI received a smaller precipitation amount than OCS or NJK. During the times with precipitation at all three sites, there were two instances when the sites received precipitation amounts that had greater than a two-fold difference. Once when all of the sites were all different (LTI lowest and NJK highest) and once when LTI and NJK were similar and OCS was much higher.

Likewise, the concentration of Hg in the precipitation frequent varied greatly between the three sites during turf sampling periods. Although the monthly average concentrations at the sites had low variability (concentrations were 19.8 ng/L, 20.0 ng/L, and 20.1 ng/L; NJK, OCS and LTI respectively); in 3 out of the 8 days with precipitation events at all three sites the highest Hg concentration was more than twice the lowest.

Month-long averages do indicate spatial variability observed for wet and dry deposition at NJK, OCS, and LTI; however, these long–term averages mask the high variability observed during individual 72-hr turf periods. Even though the averages for these close-proximity sites were similar for this sampling period, they were influenced by different conditions which could be important in better understanding the processes impacting wet and dry deposition of Hg. There was frequently high variability even within a smaller geographic area with respect to precipitation frequency, precipitation amount, and Hg concentration.

Case study three

All of the Central sites had precipitation events during T8 (July 26-29, 2009). This situation allowed exploration of some meteorological conditions in the region to better

understand the processes driving wet and dry Hg deposition. July 26, 2009 was the only day when it rained at all of the sites on the same day in the Central region. This was also the first precipitation event after the longest antecedent dry period for several of the sites (CRS, HSB, TPA). Two sites (DSO and SDK) split this same precipitation event between T7 and T8 and had also been experiencing long antecedent dry periods.

Antecedent dry periods were assigned according to the number of days preceding a measurable precipitation event greater than 0.1 cm. During our sampling, these antecedent dry periods ranged from one to 13 days (UWF). Periods were categorized as having an antecedent dry period of at least six days or a dry period of less than six days. The first precipitation event for each site was not included in this analysis because of uncertainty of the date of the previous rain event, excluding 26 events. Out of 297 precipitation events measured, 30 had long antecedent dry periods.

The concentration of Hg in the precipitation after long antecedent dry periods was generally slightly higher than the average concentration for those sites suggesting enhanced concentration of Hg in precipitation from the extended antecedent dry periods. They also had higher concentrations of Hg (average of 30.8 ng/L) than the other sites during T8 with more recent antecedent events on the same date (average of 19.9 ng/L). This example also reflected a broader trend where the mean concentration in a precipitation event following a long antecedent dry period was 26.1 ng/L with a median of 25.2 ng/L compared to the shorter dry periods that had a mean of 23.1 ng/L and median of 19.9 ng/L.

During T8, most of the eight Central sites had Hg dry deposition that was slightly above the average with the exception of DSO and HSB. All of the sites experienced significant amounts of wet and dry deposition during the T8 intensive period. The ratio of wet to dry

deposition ranged from 0.13 (CRS) to 4.46 (SDK). Although, over the month, all sites had more Hg wet deposition than dry deposition; during this period CRS and UCF both had greater dry deposition. SDK and TPA both had their highest ratio of wet to dry deposition. Despite precipitation every day of the sampling period at MKA, there was still a significant amount of dry deposition. In this case, there was a higher than average amount of Hg being dry deposited at MKA.

The occurrence of significant dry deposition despite precipitation was another pattern that was observed across all of the sites. The precipitation duration or percentage of turf sampling time when there was rainfall was not significantly associated with a change of Hg dry deposition. Analysis was conducted for all of the precipitation events where there was rain guage data yielding 114 days of which 12 had more than 150 minutes of precipitation. The average high rainfall duration day was 204 minutes while the average of low rainfall duration day was 46 minutes. Different meteorological conditions than those typically occurring in Florida during summer may have presented a data set with longer precipitation events and could have had a greater effect on Hg dry deposition. However, in this data, the longest precipitation duration was 488 minutes followed by 232 minutes which still left time for dry deposition. MKA did not have rain guage data for T8; however, National Oceanic and Atmospheric Administration (NOAA) radar maps were used to estimate a precipitation duration that was similar to other sites- shorter events that lasted from around 30 minutes to one lasting a few hours.

Precipitation frequency did seem to be associated with greater Hg dry deposition. At MKA, precipitation events occurred each day and there was greater than average Hg dry deposition. Overall, there were 24 turf periods in the study when there was precipitation on three days. These high precipitation frequency days had significantly higher Hg dry deposition

(p=0.261) than periods where there was only one or two precipitation days. (Periods with any precipitation also had higher Hg dry deposition those without.)

Examination of T8 revealed some evidence of enhanced Hg concentration in precipitation associated with the long antecedent dry periods. Furthermore, there was still a significant amount of dry deposition even when there was precipitation each day at MKA.

Conclusion

The turf surrogate surface sampling method has allowed widespread and in-depth study of the dry deposition of mercury in the state of Florida. It has enabled a unique comparison of wet to dry deposition at sites in Florida while demonstrating that there were measurable amounts of wet and dry deposition of Hg measured at all of the sites in the study. These Hg loadings varied by site as did the ratio of wet to dry deposition. Although there was more total monthly wet deposition than dry deposition of Hg measured at every site, this relationship varied in magnitude and the ratio of wet deposition to dry deposition varied by more than a factor of five. The variability of this ratio emphasizes the importance of measuring both wet and dry deposition of Hg as opposed to using a static ratio to estimate dry deposition from wet deposition. The ratios that we measured in this study were representative of only the rainy season in Florida and it is anticipated that the ratios would vary seasonally as well.

In general, there was much spatial and temporal variability observed in both wet deposition and dry deposition. The temporal variability in wet deposition was an effect of the variation in the concentration of Hg in precipitation events and precipitation amounts throughout the intensives. Dry deposition of Hg did not have as much temporal variability but did

demonstrate a level of variance that could not be directly correlated to wet deposition or other single meteorological events or conditions.

There were also interesting trends observed in spatial variability for both wet and dry Hg deposition. Regionally, the Southern region had the highest wet deposition while the Western region had the lowest. Regional trends in background Hg concentrations showed that the southern sites generally had minimum Hg concentrations that were much higher than the average minimums in the other regions. There was also evidence that even during a shared meteorological event that there was high variability of Hg wet deposition and in the concentration of Hg in a precipitation event. The coastal sites had a unique pattern where they had less wet and dry deposition than statewide averages.

We have recommendations for future work that could build on the findings from this study. Lengthening the duration of the intensives past 30 days or sampling during another season would allow analysis of Hg dry deposition trends during lower rainfall periods in Florida and capture a greater variety of meteorological events which were shown to be very influential on the month-long averages. Furthermore, although collecting samples on a finer temporal scale was beyond the resources for this study; the ATSS collection method is well suited for this (particularly in areas with a high Hg signal). Finer scale temporal data could reduce the variability in cofactors and might increase the power in statistical models.

References

Barron, Mace G., et al. "Retrospective and Current Risks of Mercury to Panthers in the Florida Everglades." *Ecotoxicology*, vol. 13, no. 3, 2004, pp. 223–29, doi:10.1023/B:ECTX.0000023567.42698.38.

Beyer, W.Nelson, et al. "Mercury Concentrations in Feathers of Wading Birds from Florida." *Ambio*, vol. 26, no. 2, 1997, pp. 97–100.

Dvonch, J.Timothy, et al. "An Investigation of Source Receptor Relationships for Mercury in South Florida Using Event Precipitation Data." *The Science of the Total Environment*, vol. 213, 1998, pp. 95–108, doi:10.1016/S0048-9697(98)00144-2.

Engle, Mark A., et al. "Characterization and Cycling of Atmospheric Mercury along the Central US Gulf Coast." *Applied Geochemistry*, vol. 23, no. 3, 2008, pp. 419–37, doi:10.1016/j.apgeochem.2007.12.024.

Esri. "Census 2010" [basemap]. 2017.

Florida Department of Health. *Your Guide to Eating Fish Caught in Florida*. *Your Guide to Eating Fish Caught in Florida*, Florida Department of Health, 2017.

Guentzel, J. L., et al. "Atmospheric Deposition of Mercury in Florida: The Fams Project (1992--1994)." *Water, Air, and Soil Pollution*, vol. 80, no. 1, Feb. 1995, pp. 393–402, doi:10.1007/BF01189689.

Hall, Naima L., et al. "An Artificial Turf-Based Surrogate Surface Collector for the Direct Measurement of Atmospheric Mercury Dry Deposition." *International Journal of Environmental Research and Public Health*, vol. 14, no. 2, 2017, doi:10.3390/ijerph14020173.

Holmes, Christopher D., et al. "Sources and Deposition of Reactive Gaseous Mercury in the Marine Atmosphere." *Atmospheric Environment*, vol. 43, no. 14, Elsevier Ltd, 2009, pp. 2278–85, doi:10.1016/j.atmosenv.2009.01.051.

Landis, M. S., and G. J. Keeler. "Atmospheric Mercury Deposition to Lake Michigan during the Lake Michigan Mass Balance Study." *Environmental Science & Technology*, vol. 36, no. 21, 2002, pp. 4518–24, doi:10.1021/es011217b.

Landis, Matthew S., and Gerald J. Keeler. "Critical Evaluation of a Modified Automatic Wet-Only Precipitation Collector for Mercury and Trace Element Determinations." *Environmental Science and Technology*, vol. 31, no. 9, 1997, pp. 2610–15, doi:10.1021/es9700055.

Lyman, Seth N., et al. "Testing and Application of Surrogate Surfaces for Understanding Potential Gaseous Oxidized Mercury Dry Deposition." *Environmental Science and Technology*, vol. 43, no. 16, 2009, pp. 6235–41, doi:10.1021/es901192e.

Malcolm, Elizabeth G. "The Effects of the Coastal Environment on the Atmospheric Mercury Cycle." *Journal of Geophysical Research*, vol. 108, no. D12, 2003, p. 4357, doi:10.1029/2002JD003084.

Malcolm, Elizabeth G., et al. "Experimental Investigation of the Scavenging of Gaseous Mercury by Sea Salt Aerosol." *Journal of Atmospheric Chemistry*, vol. 63, no. 3, 2009, pp. 221–34, doi:10.1007/s10874-010-9165-y.

Marsik, Frank J., et al. "The Dry Deposition of Speciated Mercury to the Florida Everglades: Measurements and Modeling." *Atmospheric Environment*, vol. 41, no. 1, 2007, pp. 136–49, doi:10.1016/j.atmosenv.2006.07.032.

National Atmospheric Deposition Program (NRSP-3). 2017. NADP Program Office, Wisconsin State Laboratory of Hygiene, 465 Henry Mall, Madison, WI 53706.

Nilsen, Frances M., et al. "Evaluating Mercury Concentrations and Body Condition in American Alligators (Alligator Mississippiensis) at Merritt Island National Wildlife Refuge (MINWR), Florida." *Science of the Total Environment*, vol. 607–608, Elsevier B.V., 2017, pp. 1056–64, doi:10.1016/j.scitotenv.2017.07.073.

Peterson, Christianna, et al. "Testing the Use of Passive Sampling Systems for Understanding Air Mercury Concentrations and Dry Deposition across Florida, USA." *Science of the Total Environment*, vol. 424, Elsevier B.V., 2012, pp. 297–307, doi:10.1016/j.scitotenv.2012.02.031.

Rothenberg, Sarah E., et al. "Evaluating the Potential Efficacy of Mercury Total Maximum Daily Loads on Aqueous Methylmercury Levels in Four Coastal Watersheds Policy Analysis Evaluating the Potential Efficacy of Mercury Total Maximum Daily Loads on Aqueous Methylmercury Levels in Four Coastal Watersheds." *Environmental Science and Technology*, vol. 42, no. 15, 2008, doi:10.1021/es702819f.

Sexauer Gustin, M., et al. "Investigating Sources of Gaseous Oxidized Mercury in Dry Deposition at Three Sites across Florida, USA." *Atmospheric Chemistry and Physics*, vol. 12, no. 19, 2012, pp. 9201–19, doi:10.5194/acp-12-9201-2012.

U.S. Environmental Protection Agency (U.S. EPA). National Emissions Inventory (NEI) Data and Documentation. http://www.epa.gov/ttnchie1/net/2008inventory.html 2008. [Site visited: October-11-2012; Site updated: 28-August-2012].

White, Emily M., et al. "Spatial Variability of Mercury Wet Deposition in Eastern Ohio: Summertime Meteorological Case Study Analysis of Local Source Influences."

Environmental Science and Technology, vol. 43, no. 13, 2009, pp. 4946–53, doi:10.1021/es803214h.

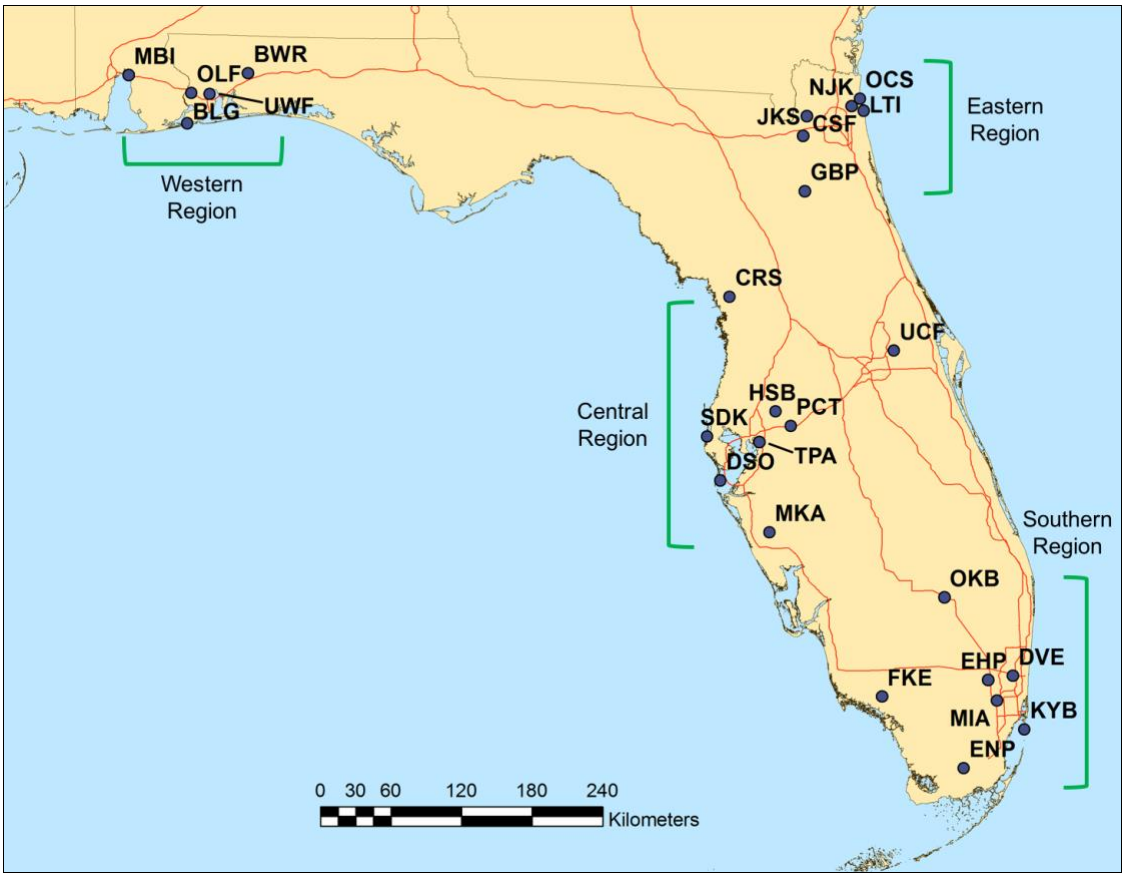

Figure 3.1: Measurement intensive site locations in Florida grouped by region. Eastern and Western region sampling tookplace during 2010. Central and Southern region sampling took place during 2009.

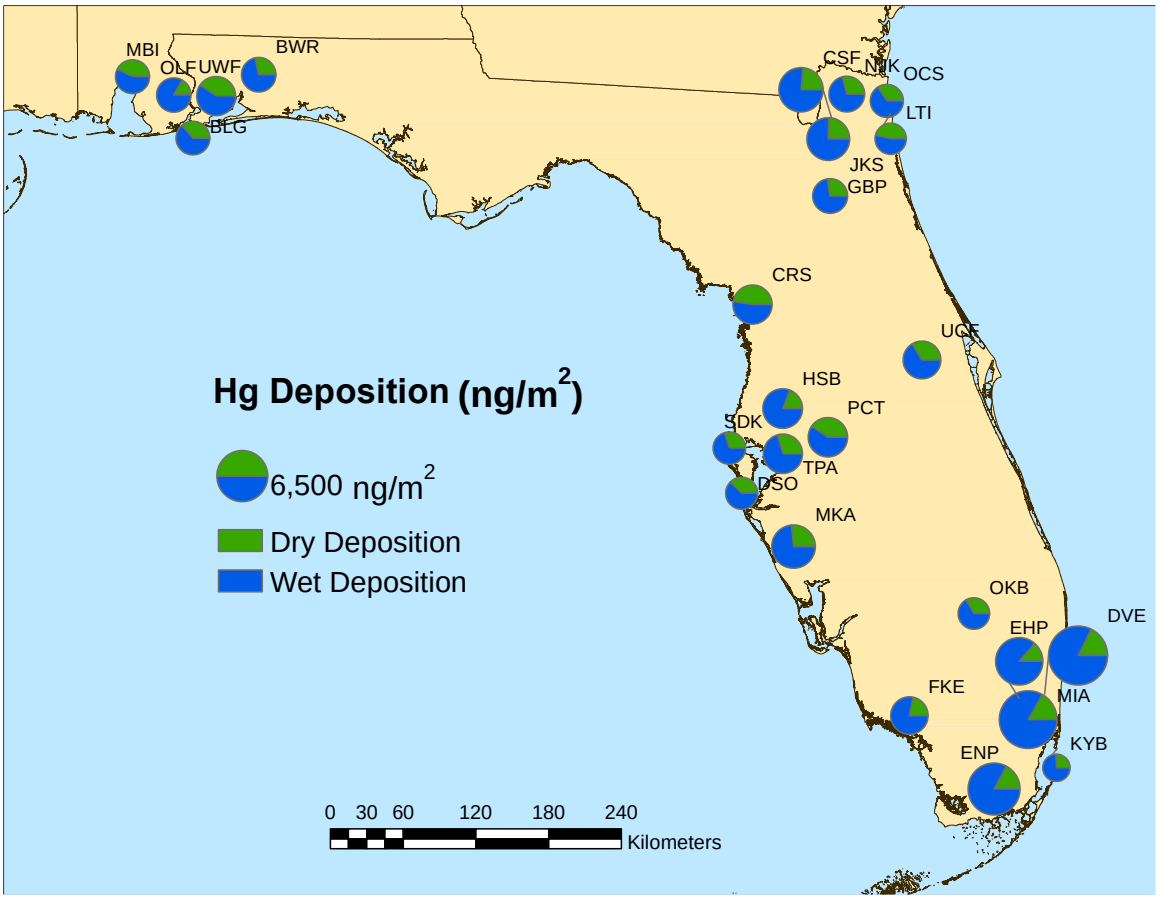

Figure 3.2: Total monthly wet and dry Hg deposition by site in ng/m^2.

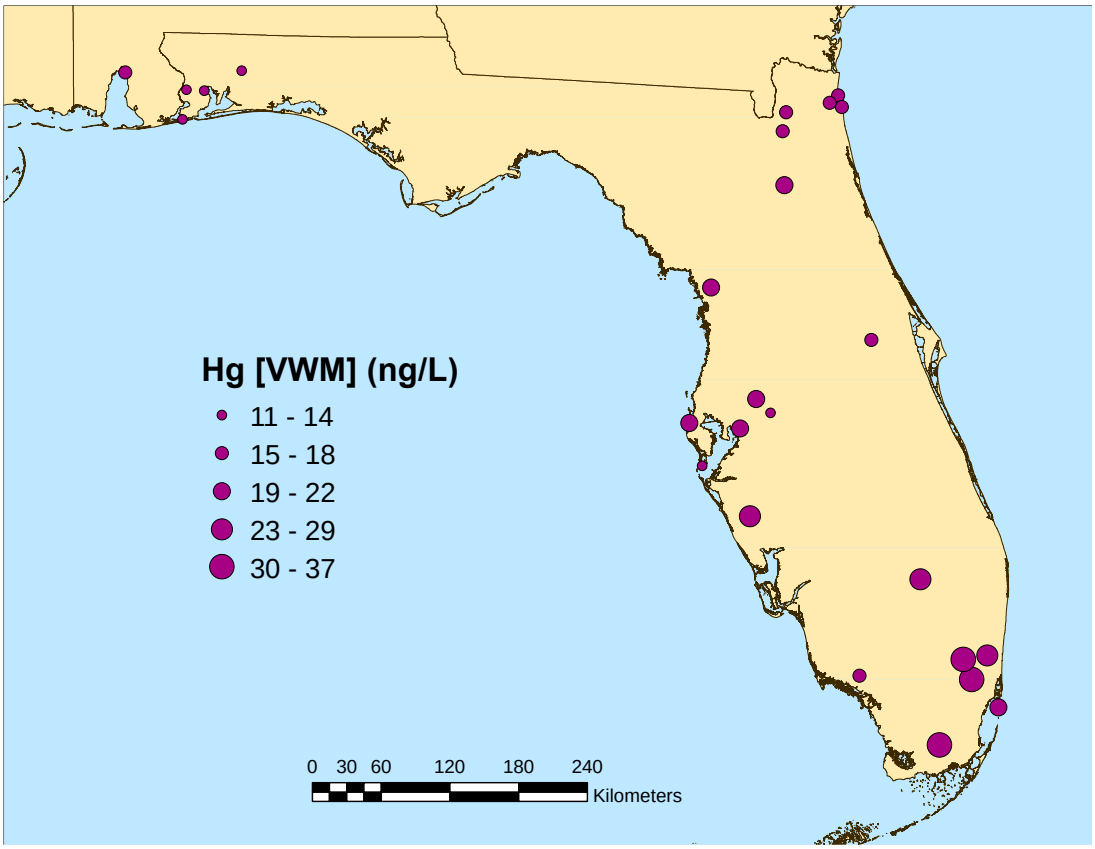

Figure 3.3: Hg VWM Concentrations in ng/L in precipitation by site.

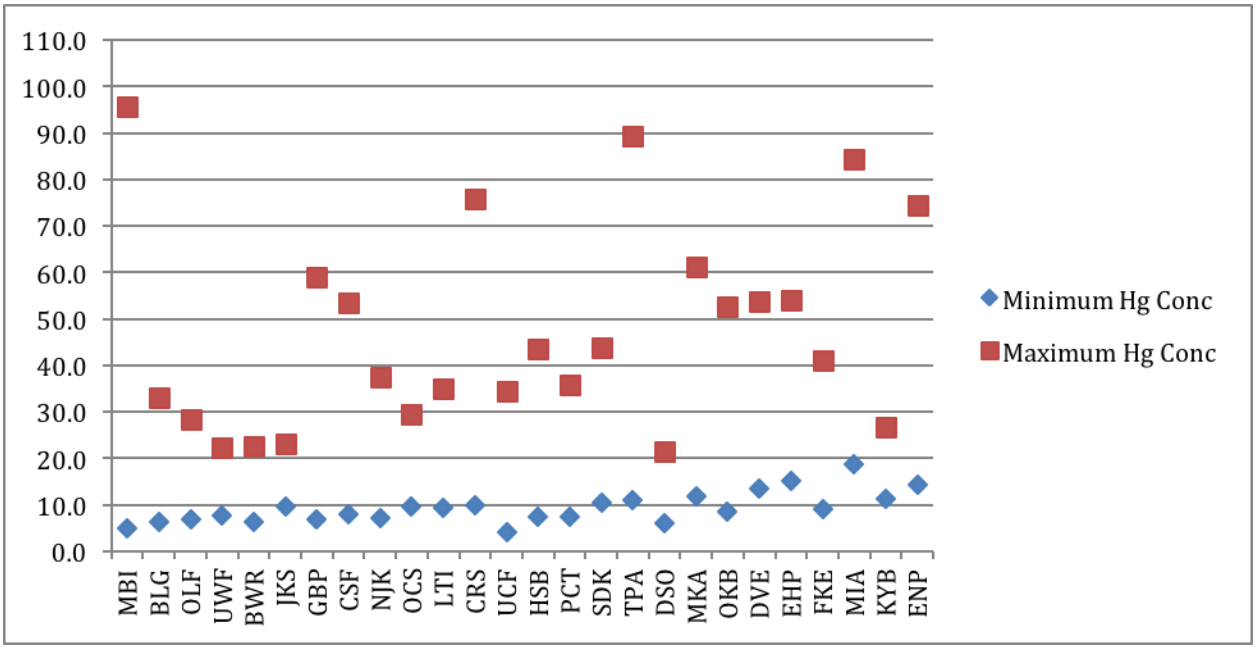

Figure 3.4: Maximum and minimum Hg precipitation concentrations (in ng/L) by site.

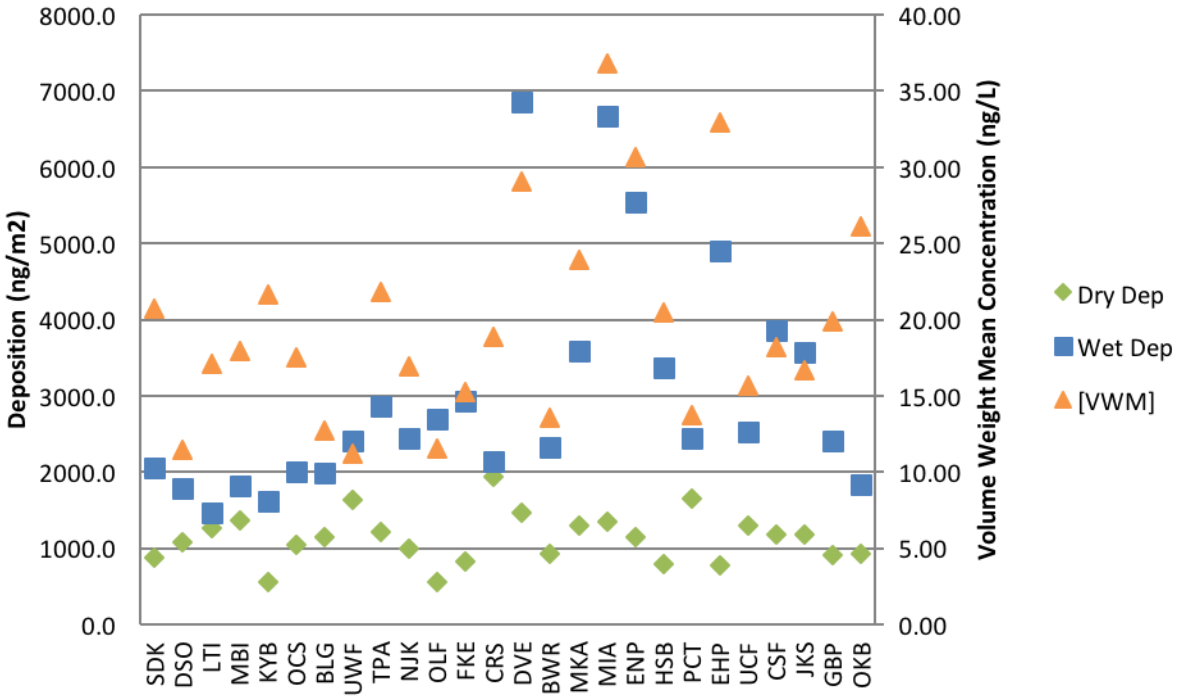

Figure 3.5: Hg dry and wet deposition and volume-weighted mean (VWM) concentration of sites ordered by distance to coast

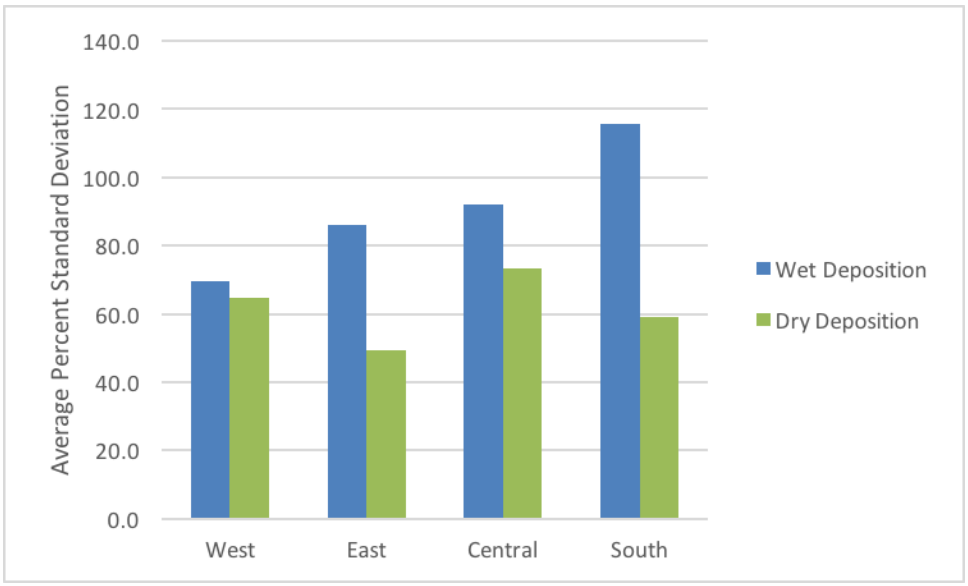

Figure 3.6: Average relative standard deviation (RSD) of wet and dry Hg deposition by intensive region.

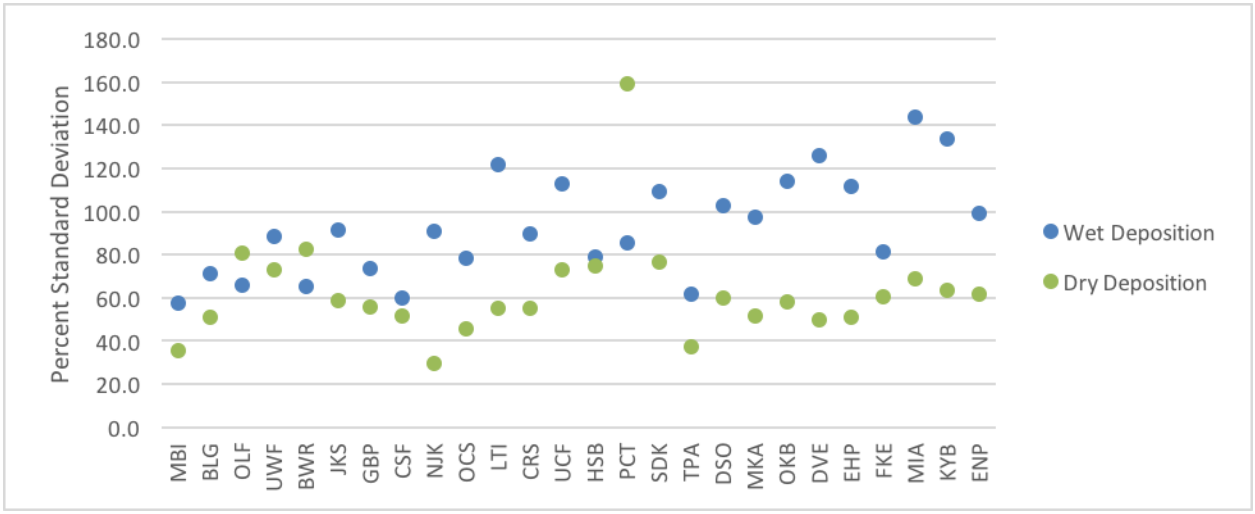

Figure 3.7: Temporal variability of Hg wet and dry deposition by site. Sites are ordered from Northwest to South.

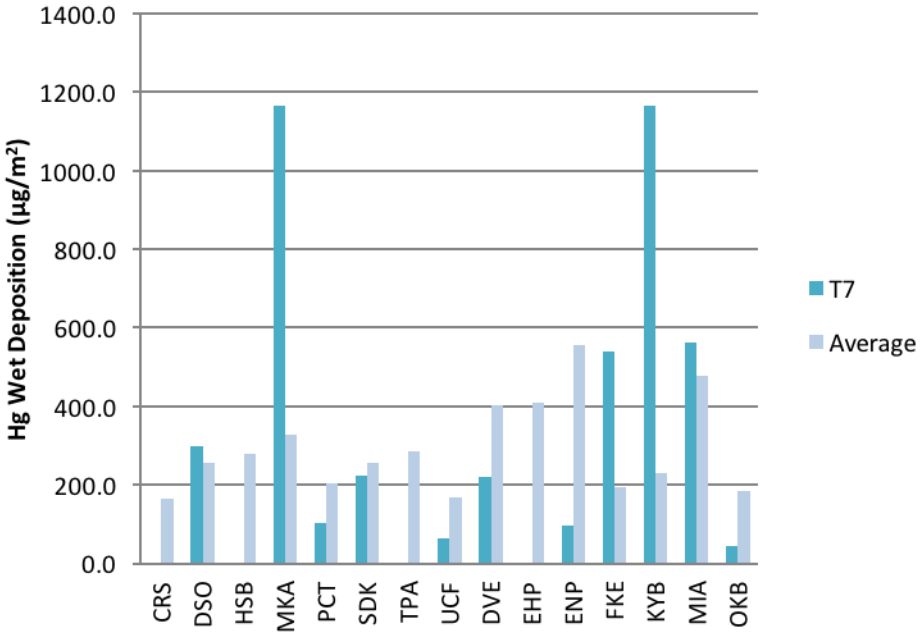

Figure 3.8: Comparison of turf period 7 (T7) Hg wet deposition to study average.

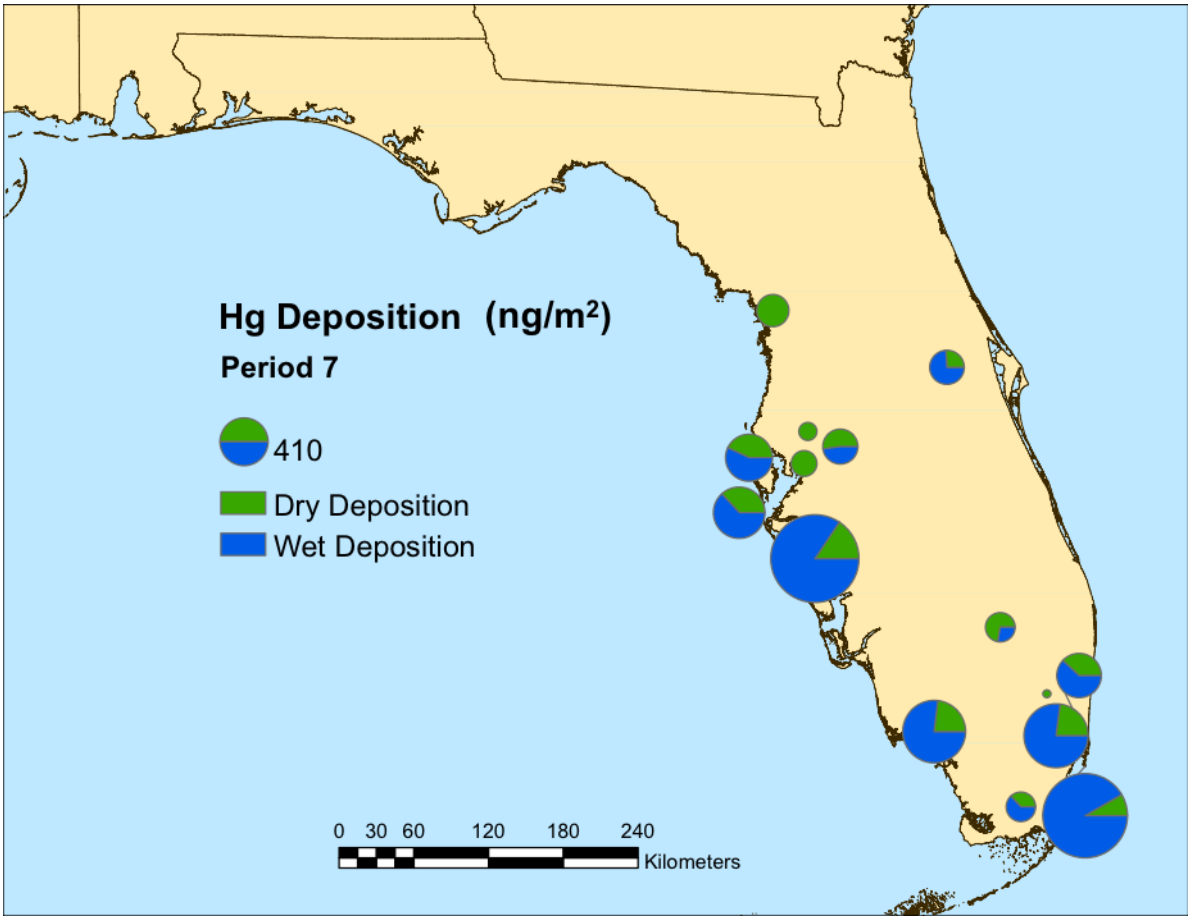

Figure 3.9: Wet and dry Hg deposition by site for turf period 7 (T7) from 2009 Central and Southern regions of Florida

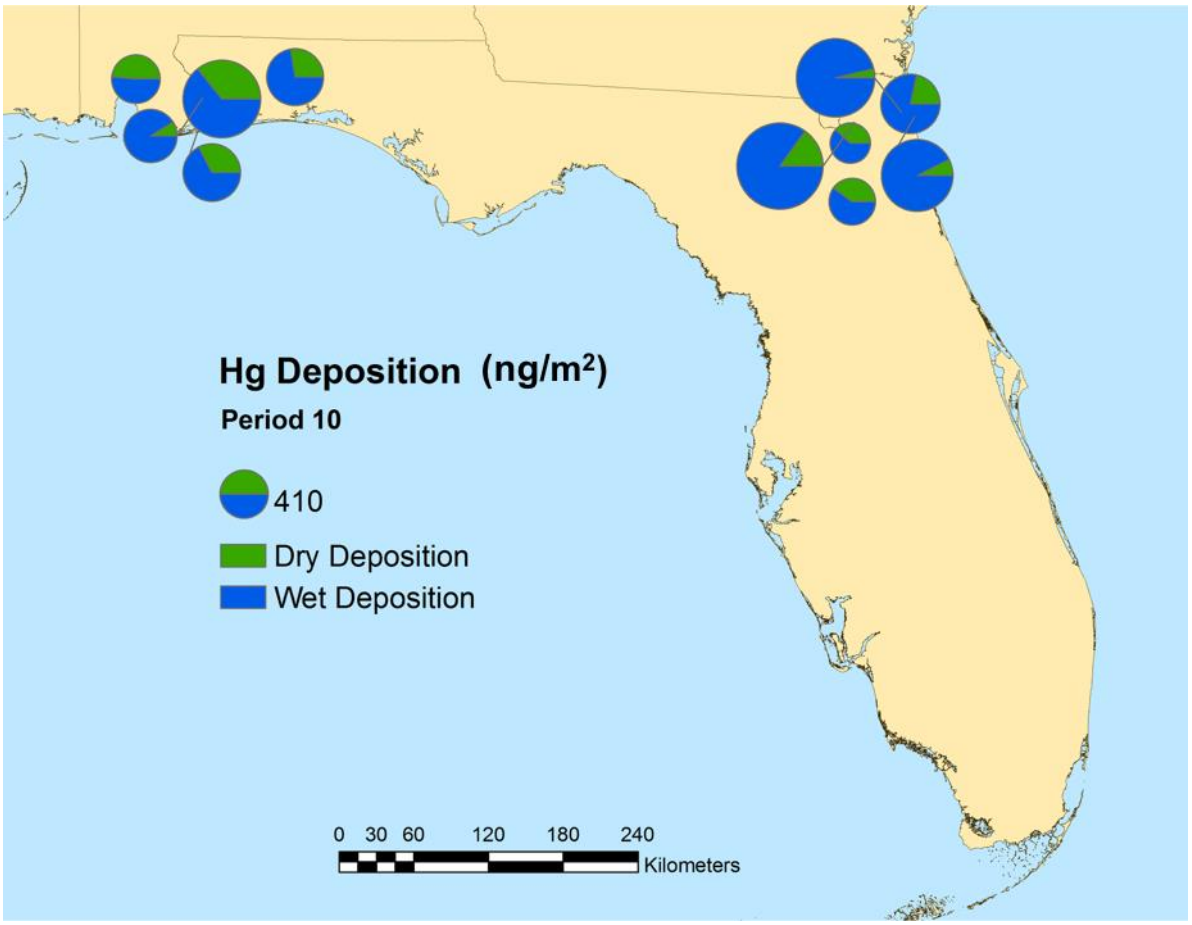

Figure 3.10: Wet and dry Hg deposition by site for turf period 10 (T10) for 2010 Eastern and Western regions of Florida.

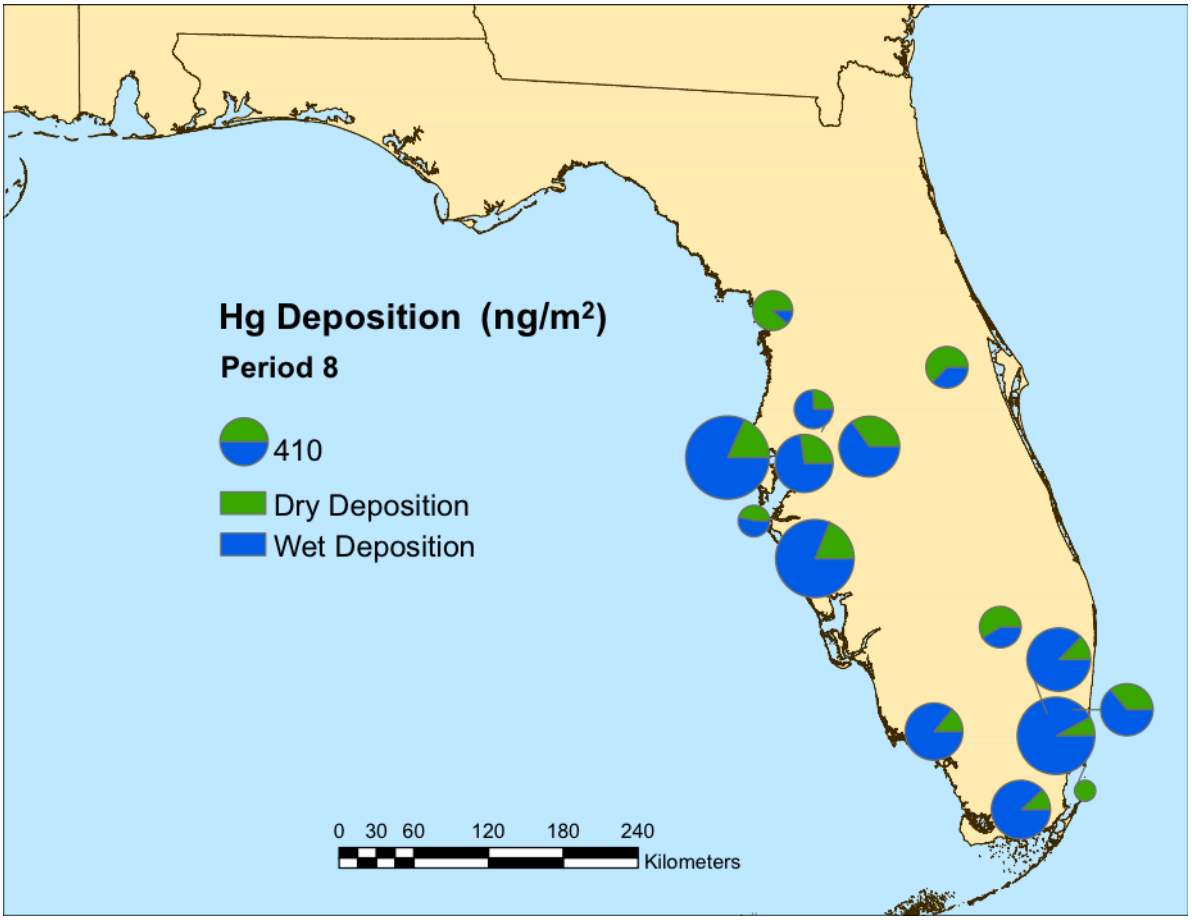

Figure 3.11: Wet and dry Hg deposition by site for turf period 8 (T8) for 2009 Central and Southern regions of Florida.

Table 3.1: Descriptions of sites from the 2009 and 2010 measurement campaigns.

Site Code	Site Name	Region	Latitude	Longitude	Coastal	Industrial	Population
MBI	Mobile Bay, AL	West	30.6715	-87.9360	Near		
BLG	Big Lagoon State Park	West	30.3166	-87.4038			Urban
OLF	Pensacola Supersite	West	30.5500	-87.3751			
UWF	University of West Florida	West	30.5455	-87.2114		Near	Urban
BWR	Blackwater River State Park	West	30.7111	-86.8764			Rural
JKS	Jacksonville Supersite	East	30.2475	-81.9512	Far	Near	
GBP	Goldhead Branch State Park	East	29.8235	-81.9434	Far		
CSF	Carey State Forest	East	30.3966	-81.9170			
NJK	Pumpkin Patch Site	East	30.4657	-81.5182			
OCS	Seahorse Ranch, Amelia Island	East	30.5227	-81.4415	Near		Urban
LTI	Little Talbot Island	East	30.4296	-81.4106	Near		
CRS	Crystal River	Central	29.0250	-82.6165			Rural
UCF	University of Central Florida	Central	28.5920	-81.1901			Urban
HSB	Hillsborough County Park	Central	28.1440	-82.2281			
PCT	Plant City	Central	28.0325	-82.1002			Urban
SDK	Sand Key State Park	Central	27.9599	-82.8245	Near		Urban
TPA	Tampa Supersite	Central	27.9134	-82.3751			Urban
DSO	Fort Desoto State Park	Central	27.6227	-82.7137	Near		
MKA	Myakka River State Park	Central	27.2224	-82.2971		Far	Rural
OKB	Okeechobee Lake	South	26.6981	-80.8076	Far		
DVE	Davie Supersite	South	26.0843	-80.2407		Near	Urban
EHP	Everglades Holiday Park	South	26.0580	-80.4517			
FKE	Fakahatchee Strand	South	25.9513	-81.3603		Far	Rural
MIA	Miami	South	25.8993	-80.3827		Near	
KYB	Bill Baggs Cape State Park	South	25.6719	-80.1574	Near		Urban
ENP	Everglades National Park	South	25.3896	-80.6800			Rural

Table 3.2: Summary of descriptive statistics of wet and dry Hg deposition and volume-weighted mean (VWM) concentration by site and measurement campaign region.

				Hg Dry Deposition (ng/m^2)					Hg Wet Deposition (ng/m^2)				
Site Code	**Region**	**N**	**Pcp Amt (cm)**	**Sum**	**Mean**	**Std**	**Min**	**Max**	**Sum**	**Mean**	**Std**	**Min**	**Max**
MBI	West	11	10.1	1356.8	135.7	47.8	60.4	203.1	1814.3	164.9	95.2	58.6	335.9
BLG	West	12	15.6	1137.2	113.7	57.9	36.2	192.5	1989.0	165.8	118.2	23.6	407.9
OLF	West	9	23.4	552.8	55.3	44.7	0.0	143.8	2691.6	299.1	196.2	40.5	609.9
UWF	West	13	21.5	1637.3	163.7	119.8	52.9	384.2	2407.3	185.2	164.0	26.2	485.0
BWR	West	10	17.2	931.7	93.2	76.9	5.8	265.7	2330.9	233.1	152.7	42.7	443.0
Average		**11.0**	**17.6**	**1123.2**	**112.3**	**69.4**	**31.0**	**237.9**	**2246.6**	**209.6**	**145.3**	**38.3**	**456.3**
JKS	East	12	21.4	1170.5	117.0	69.0	37.7	261.9	3576.2	298.0	271.7	12.4	821.4
GBP	East	13	12.1	908.3	90.8	50.4	10.0	165.3	2409.3	185.3	136.7	55.4	568.8
CSF	East	13	21.2	1187.2	118.7	61.3	32.7	229.2	3850.3	296.2	178.2	40.8	643.3
NJK	East	9	14.5	993.9	99.4	29.4	41.6	137.9	2448.8	272.1	246.5	27.6	695.0
OCS	East	11	11.5	1037.3	103.7	47.4	30.3	185.3	2010.3	182.8	142.7	17.6	435.4
LTI	East	8	8.5	1264.2	126.4	69.9	5.6	241.0	1457.8	182.2	221.9	71.6	717.6
Average		**11.0**	**14.9**	**1093.6**	**109.4**	**54.6**	**26.3**	**203.4**	**2625.5**	**236.1**	**199.6**	**37.6**	**646.9**
CRS	Central	13	11.3	1942.6	194.3	107.4	71.2	457.2	2133.3	164.1	147.3	17.1	470.6
UCF	Central	15	16.1	1288.3	128.8	93.8	44.4	342.7	2522.0	168.1	189.9	24.0	768.7
HSB	Central	12	16.4	794.3	79.4	59.2	0.0	168.9	3360.7	280.1	220.8	61.9	885.6
PCT	Central	12	17.7	1657.3	165.7	263.7	0.0	854.4	2436.1	203.0	173.0	44.5	630.6
SDK	Central	8	9.9	874.4	87.4	66.7	0.0	227.2	2053.6	256.7	280.3	59.4	897.8
TPA	Central	10	13.2	1208.2	120.8	45.1	56.1	201.3	2868.7	286.9	176.3	38.3	613.4
DSO	Central	7	15.6	1078.2	107.8	64.7	12.8	226.9	1784.4	254.9	261.8	30.0	625.9
MKA	Central	11	15.0	1299.7	130.0	67.3	0.0	216.0	3595.3	326.8	318.2	55.7	1164.7
Average		**11.0**	**14.4**	**1267.9**	**126.8**	**96.0**	**23.1**	**336.8**	**2594.3**	**242.6**	**220.9**	**41.3**	**757.1**
OKB	South	10	7.1	918.3	91.8	53.2	23.1	180.6	1843.1	184.3	210.6	42.7	766.1
DVE	South	17	23.7	1473.6	147.4	73.4	69.3	324.4	6863.9	403.8	509.1	31.1	2024.0
EHP	South	12	14.9	781.9	78.2	40.0	11.4	145.3	4900.1	408.3	456.3	33.5	1649.7
FKE	South	15	19.2	818.0	81.8	49.4	14.3	162.1	2930.5	195.4	159.0	17.9	520.6
MIA	South	14	18.1	1355.0	135.5	92.9	33.4	356.4	6676.9	476.9	687.0	41.5	2690.4
KYB	South	7	7.5	555.0	55.5	35.3	0.1	106.4	1616.4	230.9	308.7	31.4	913.6
ENP	South	10	18.1	1143.2	114.3	70.2	25.6	268.1	5544.4	554.4	549.6	28.2	1590.4
Average		**12.1**	**15.5**	**1006.4**	**100.6**	**59.2**	**25.3**	**220.5**	**4339.3**	**350.6**	**411.5**	**32.3**	**1450.7**

Site Code	Precipitation Concentration (ng/L) [VWM]	Std	Min	Max	Total Dep (ng/m^2)	Wet: Dry Ratio	% Dry Deposition
MBI	18.0	25.0	4.9	95.6	3171.1	1.3	
BLG	12.8	8.8	6.2	33.1	3126.2	1.7	
OLF	11.5	6.5	6.9	28.4	3244.4	4.9	
UWF	11.2	3.7	7.8	22.2	4044.7	1.5	
BWR	13.5	5.7	6.4	22.6	3262.6	2.5	
Average	**13.4**	**9.9**	**6.4**	**40.4**	**3369.8**		**33%**
JKS	16.7	4.3	9.6	23.1	4746.7	3.1	
GBP	19.9	15.3	6.9	59	3317.5	2.7	
CSF	18.2	14.1	8	53.4	5037.5	3.2	
NJK	16.9	9.1	7.2	37.4	3442.7	2.5	
OCS	17.5	8.2	9.7	29.5	3047.7	1.9	
LTI	17.1	9.8	9.3	35.1	2722.0	1.2	
Average	**17.7**	**10.1**	**8.5**	**39.6**	**3719.0**		**29%**
CRS	18.9	20.1	9.9	75.8	4075.9	1.1	
UCF	15.7	8.0	4.1	34.5	3810.3	2.0	
HSB	20.5	9.2	7.4	43.6	4155.0	4.2	
PCT	13.8	8.1	7.5	35.7	4093.4	1.5	
SDK	20.7	11.3	10.3	43.9	2928.1	2.3	
TPA	21.8	22.6	10.9	89.2	4077.0	2.4	
DSO	11.5	4.9	5.9	21.4	2862.6	1.7	
MKA	23.9	15.6	11.9	61.1	4895.0	2.8	
Average	**18.3**	**12.4**	**8.5**	**50.7**	**3862.1**		**33%**
OKB	26.1	12.9	8.4	52.5	2761.3	2.0	
DVE	29.0	12.6	13.5	53.7	8337.5	4.7	
EHP	33.0	10.0	15	54.1	5682.0	6.3	
FKE	15.2	10.5	9	41.1	3748.5	3.6	
MIA	36.8	18.2	18.8	84.5	8031.8	4.9	
KYB	21.6	5.1	11.2	26.8	2171.5	2.9	
ENP	30.6	19.0	14.2	74.4	6687.6	4.8	
Average	**27.5**	**12.6**	**12.9**	**55.3**	**5345.8**	4.2	**19%**

Table 3.3: Summary table of coastal averages.

	Average Coastal Site	Average Non-Coastal Site	Significantly different?
Precipitation Amount (cm)	1.05 (n=60)	1.69 (n=200)	Yes
Precipitation Frequency	8.7 (n=6)	12.1 (n=20)	Yes
Hg Concentration (ng/L)	20.8 (n=52)	23.6 (n=243)	No
Hg Wet Deposition (ng/m^2)	178.9 (n=60)	336.9 (n=200)	Yes
Hg Dry Deposition (ng/m^2)	102.8 (n=60)	116.0 (n=200)	No

Chapter 4 : Chemical Factors Influencing Mercury Dry Deposition in Florida

Abstract

Sources of mercury (Hg) are of public health interest because of the impact of Hg emissions on the ecosystems impairing waterbodies and bioaccumulating in fish and other wildlife. Florida has particularly high concentrations of Hg in precipitation (NADP 2017); however, there is little known about what sources are most responsible for Hg dry deposition and how these compare to sources impacting Hg wet deposition. During one-month measurement campaigns spread between July 2009 and July-August 2010, Hg wet and dry deposition was measured at a total of 26 sites in Florida using events-based bulk wet deposition collectors and the artificial turf surrogate surface (ATSS) samplers for Rb, Sr, Cd, La, Ce, Sm, Pb, Mg, Al, P, S, Ti, V, Cr, Mn, Fe, Co, Ni, Cu, Zn, As, Se, SO_4^{2-}, NO_3^-, Cl^-, NH_4^+, Na^+, Ca, and Ba. There were several distinct geographic trends observed for wet and dry deposition of the various trace elements and ionic species. Additionally, correlation coefficients and enrichment factors suggested that there were multiple sites that were likely be highly impacted by local emission sources.

Introduction

Mercury (Hg) in the ecosystem is a public health problem. It's presence in the food web has led to advisories limiting the type and amount of fish that people should consume, particularly susceptible populations like pregnant women and children. Although it is known

that some Hg in the environment is from anthropogenic sources (UNEP 2015), the impact of specific Hg emission sources is not as well understood, but can be investigated by examining co-depositing trace elements and ionic species. Several studies have assessed sources of Hg wet deposition using various receptor modeling techniques (Dvonch et al., 1998, Graney et al., 2004, Gratz et al., 2013, Michael et al., 2016); however, aside from Lynam et al. (2014a) there have been fewer studies investigating the sources of Hg in dry deposition.

Field measurement campaigns were conducted throughout four regions of Florida in 2009 and 2010 where dry and wet deposition of Hg was measured as well as wet and dry deposition of 30 other trace elements and ionic species. We assessed the spatial and temporal relationships between tracer species that are known to be associated with certain emission sources with the Hg in both wet and dry deposition. Examining the deposition patterns of trace elements and ionic species may help to better contextualize Hg deposition patterns and improve the understanding of processes and emission sources contributing to Hg dry deposition.

Methods

The University of Michigan Air Quality Laboratory (UMAQL), as part of a Total Maximum Daily Load (TMDL) study for Hg in Florida, conducted, four field intensives in 2009 and 2010 across the state measuring the wet and dry deposition of Hg as well as other species including Rb, Sr, Cd, La, Ce, Sm, Pb, Mg, Al, P, S, Ti, V, Cr, Mn, Fe, Co, Ni, Cu, Zn, As, Se, SO_4^{2-}, NO_3^-, Cl^-, NH_4^+, Na^+, Ca, and Ba. Field measurement campaigns covering the central and southern regions of the state were conducted during the summer of 2009 (July 4- August 4, 2009) around the Tampa area and the Miami area, while intensives covering the western and eastern parts of north Florida were conducted during the summer of 2010 (July 24- August 23,

2010) around the Pensacola area and the Jacksonville area. These measurement campaign sites covered a large geographic area and intentionally encompassing areas both near and far from known point emission sources as well as population centers. Sites are briefly described in Table 4.1 and Figure 4.1. Further descriptions of these 26 monitoring sites can be found in the previous chapter which specifically discusses the spatial and temporal trends of Hg deposition around Florida.

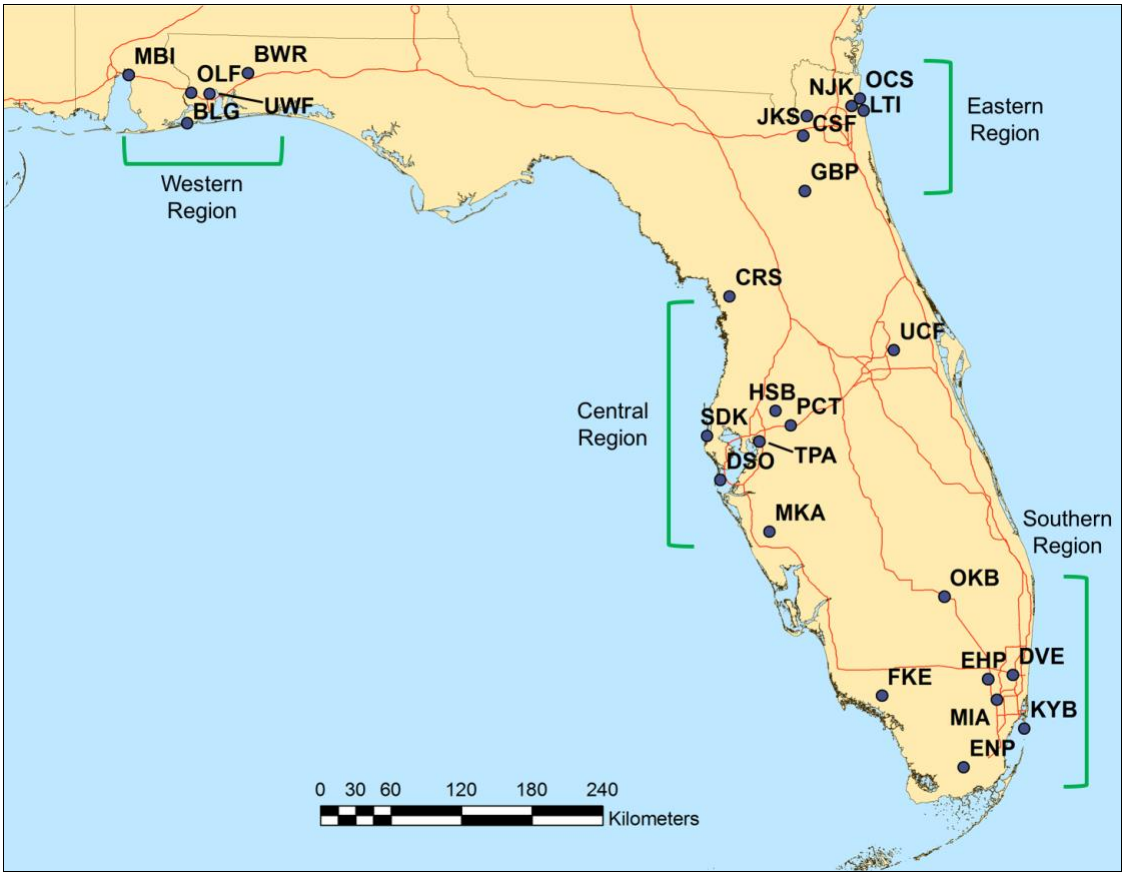

Figure 4.1: Measurement site locations for summer 2009 (Central and Southern regions) and summer 2010 (Western and Eastern regions).

Methods for Hg dry and wet deposition sampling were detailed in the previous chapters as well as Hall et al (2017). Parallel sampling chains were deployed with slight modifications to measure the deposition of other trace elements and ionic species. Fluorinated high-density

polyethylene (FLPE) funnels prepared at UMAQL were used instead of the glass funnels washed in the field. Funnel and turf plate adapters were made of polypropylene. All of the pieces were cleaned using the UMAQL acid-cleaning protocol for trace element and ion analysis (Hoyer et al 1995) which included a HCl cook, a HNO_3 soak and a final ASTM type I (18.2 Ω) water heated soak. Precipitation and ATSS (artificial turf surrogate surface) throughfall samples were collected in similarly prepared FLPE bottles. Fifty milliliters of ASTM type I water were used as a rinse for the trace element/ion turf collection plates instead of the HCl rinse used for the Hg turf samples.

Samples were sent to UMAQL for processing where ion samples were aliquoted from the full precipitation and throughfall samples for individual processing and analysis. Samples were prepared for analysis by acidifying trace element samples with concentrated Optima Grade HNO_3 (Fisher Chemical) to a 1% solution (v/v) allowing at least 14 days prior to analysis. The turf extraction process proceeded in two parts-- an initial sonication and rolling extraction step, pouring off a sample for ionic species' analysis and then the addition of HNO_3 to 1% v/v for a second sonication and rolling period. Trace element analysis was conducted using a Thermo Finnigan Element2 high-resolution magnetic sector field inductively coupled plasma mass spectrometer (HR-ICPMS). Major ion analysis was conducted using a Dionex (Sunnyvale, CA) ion chromatography system.

Field blanks were collected to represent a minimum of 10% of field samples collected. There were 3 wet deposition field blanks and 3 dry deposition field blanks that consisted of separate turf and throughfall components that collected at each site. Table 4.2 shows the method detection limit (MDL), average field blank value as well as the number of blanks below the MDL for each trace element and ionic species. Sampler precision (Table 4.3) was assessed

through collection of collocated ATSS at the TPA, ENP and JKS sites. Sample concentrations that were below the detection limit were assigned one-half of MDL as a working concentration for data analyses.

Results and Discussion

Descriptive statistics for trace elements and ionic species

The monthly totals for wet deposition and dry deposition of 30 trace elements and ionic species were calculated by site and shown on Table 4.4 and Table 4.5, respectively. Sites were also ranked according to the deposition of each trace element and ionic species and by the volume-weighted mean (VWM) concentration. Assessing which sites or regions trended towards higher or lower deposition or VWM concentration was useful in looking for site specific trends and understanding if high Hg deposition at sites was correlated with high deposition of other tracer species. Table 4.6 summarizes the sites most often ranked among the highest three and lowest three for mean wet deposition, mean dry deposition and VWM concentration.

A general spatial overview of the wet and dry deposition of V, Se, and Na^+ is presented in Figure 4.2. The wet and dry deposition of Hg is also included for comparison. As discussed in chapter 3, Hg wet and dry deposition generally increased from North to South. However, different geographic trends were often observed for other trace elements and ionic species. Se had a decreasing gradient from North to South while Na^+ showed particularly high wet and dry deposition at the coastal sites where we expected impact from sea salt aerosols. V deposition did not follow any specific pattern but appeared greater at sites near emission sources.

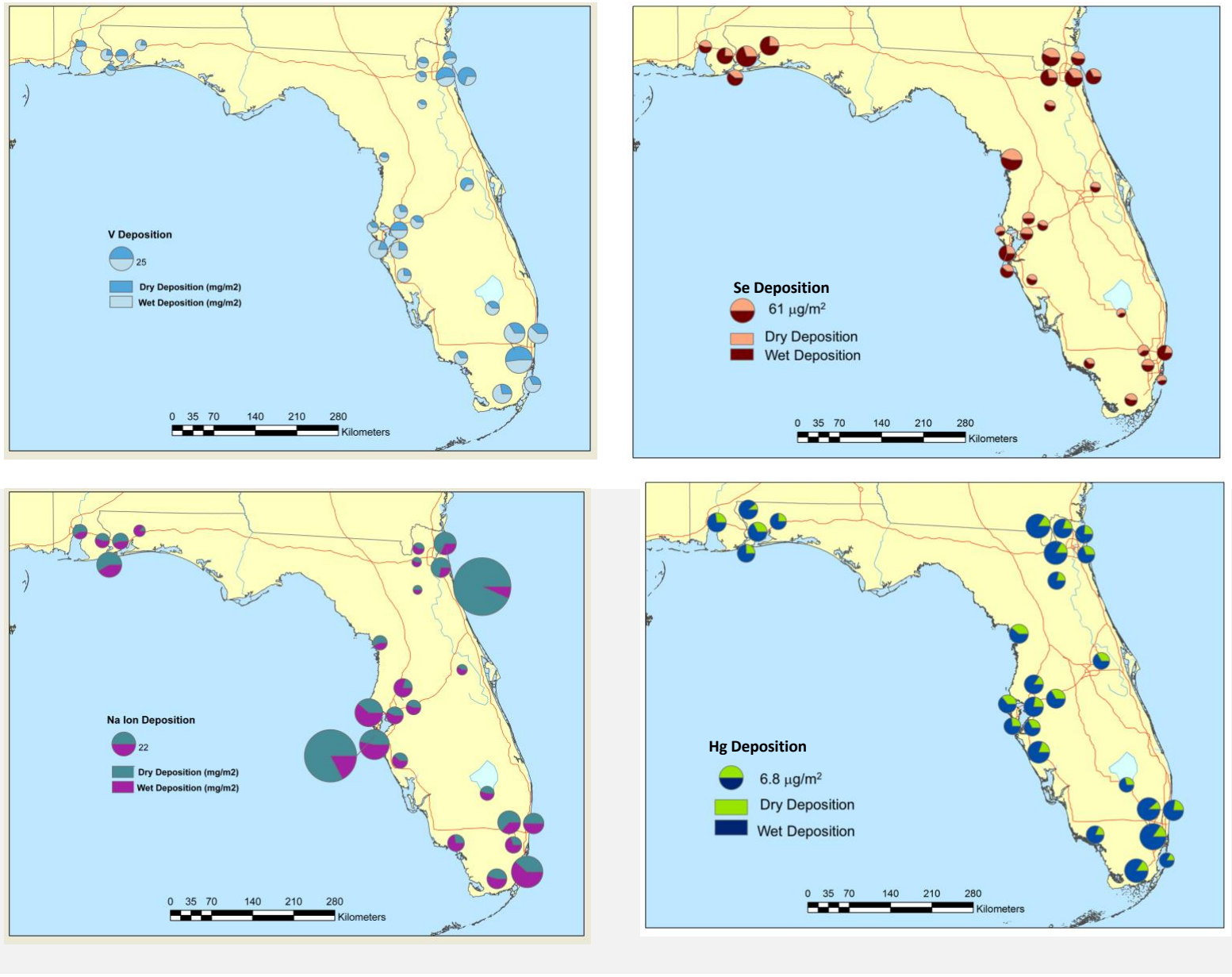

Figure 4.2: Wet and dry deposition of V, Se, Na^+, and Hg at the 2009 and 2010 measurement intensives.

The MIA site most often had the highest mean dry deposition of any given species (12 of the 30 species- Sr, La, Ce, Sm, Pb, Al, V, Cr, Fe, Co, Ca, Ba). The UWF site had the greatest dry deposition for seven species (Rb, Cd, P, Mn, Cu, Zn, As); followed by LTI, which had the highest of five trace elements and ionic species (S, SO_4, NO_3, Cl^-, Na^+). The MIA site was distinguished from the other sites even more when the trace elements were considered separately from the ionic species (MIA was not the highest among any of the ionic species analyzed for this study). For 12 of the 26 trace elements, the MIA site had the highest dry deposition. The EHP site ranked as either the second or third highest site for numerous trace elements and ionic species, frequently for the trace elements of which the MIA site had the highest deposition but also for the ionic species SO_4, Cl^-, NH_4. The BWR, GBP and OCS sites were most frequently ranked as one of the lowest three sites for mean dry deposition.

The MIA site and the EHP site were frequently ranked as one of the top three sites for mean wet deposition of multiple species which was similar to the results of sum dry deposition (Table 4.6). The MIA site was ranked as a top three site 19 times (five times as the highest, three times as second highest and 11 times as third highest), EHP was in the top three 17 times (2, 10, and 5). The ENP site was in the top three, 12 times (9, 2, and 1). For the total wet deposition, the ENP site is the highest for Hg, La, Ce, Sm, Al, Mn, Fe, Co, Ba. The lowest mean wet depositions were also examined. The GBP site was ranked in the bottom three for 15 of the species, the CRS site for 13 and OCS for 12. The ionic species seemed to follow a different pattern of rank order particularly for the ions associated with sea salt aerosols.

Minimum concentrations

The minimum concentrations of the trace elements and ionic species were compared by site to investigate when they were least impacted by emission sources or enhanced deposition processes. Table 4.7 shows the sites that had the highest minimum values by site—effectively, a list of maximum minimums. In general, high Hg minimum depositions did not predict high minimums for the tracer species. Of the three sites with the highest Hg minimum wet deposition, LTI, HSB, and SDK, these were also top three ranked 3, 8 and 16 times (among the 29 other tracer species). For dry deposition, the greatest Hg minimum deposition was for CRS, DVE, and MBI; however, when other tracer species were investigated those sites were in the top three four times for DVE and three times for MBI. CRS didn't have a high minimum for any of the other tracer species. The sites with the highest minimum depositions for dry deposition from the tracer species were the MIA, TPA and LTI sites which had 24 (out of 30 species), 18, and 10 times in the top three. For wet deposition, the total highest minimums were the MIA, SDK and PCT sites (17, 16, 11 times as a top three site for highest minimums).

Several of the sites noted above with high deposition or high minimums were sites that were near a large variety of Hg emission sources with large anthropogenic emissions like MIA, TPA, DVE and EHP. An additional group were coastal sites like LTI, MBI and SDK which were impacted by sea salt aerosols. These same sites that are noted in the more specific analysis of specific tracer element and ionic species below.

Spatial variability

Overall, the dry deposition variability across all of the sites (as measured by relative standard deviation (RSD) of each trace element or ionic species by site) was lowest for Se, NO_3^-,

and V. However, Hg had the lowest variability of any of the metals measured (29% compared with 50%, 59%, 77%, Table 4.8). The low variability was consistent for all regions.

The highest variability for mean trace element dry deposition (RSD) was Rb (296%), Ca (250%) and P (228%). Regionally, these follow a different pattern with low Rb variability in the eastern region and moderate variability in the southern region, while there was high variability for western and central regions. Ca also had different variability patterns when stratified for region. There was low variability for the eastern and central regions with moderate variability in the western region and high variability in the South. Much of this variability was driven by two sites with very high Ca dry deposition in the southern region (MIA and EHP) and two sites with moderately high Ca dry deposition in the western region (MBI and UWF). Most of the Ca dry deposition at the other sites was quite low although with an increasing north to south gradient. P had high variability in all of the regions although driven by a few sites with high P dry deposition.

For wet deposition, there were tracer elements that had lower RSD than Hg. NO_3^- and S were all below the RSD of Hg (38). Arsenic also had among the lowest RSD with 39%. The highest RSD was for Ca which was 151%. Ca was followed by Zn and P (130% and 123% respectively). There was less variation of the metals in the wet deposition over the different sites. When stratified by region, Hg still had low variability as did NO_3^- and As. S had lower variability in the southern region than the other regions. Ca had low variability in the western region (26%) and the highest in the southern region (101%) leading to its overall high statewide variability. This was also reflected in its increasing Southerly deposition gradient throughout the state similarly to that of dry deposition. The other high variability metals and ionic species, Zn

and P had consistently moderate or higher variability in all of the regions (lowest 52% for Zn in the western region and highest 130% in the central region also for Zn).

Wet to dry deposition ratio

Hg was the only element or ion where wet deposition was greater than dry deposition at every site (ratios that ranged from 1.1 (CRS) to 6.3 (EHP)). Table 4.9 shows the ratio of wet to dry deposition for the metals and ionic species. Of the other species, there were some that tended to have higher dry or wet deposition but it varied from site to site. Overall, the wet deposition was greater than the dry deposition more frequently. The ratio of wet to dry also varied with the amount of rainfall at a site; so that the southern sites, which had more rainfall, were more likely to have greater wet than dry deposition. NO_3^-, Fe and V, SO_4^{2-} had greater wet than dry deposition for the greatest number of sites (all but LTI for NO_3^- and 21 out of 26 sites for the others). However, there were also several trace elements for which dry deposition was frequently higher than wet deposition. Cu and Sr had higher dry deposition at 22 out of 26 sites; while there were at least 19 out of the 26 sites where Ca, Cd and Pb had more dry deposition than wet deposition.

This relationship between wet and dry deposition also reflects what was reported in Lynam et al (2014b). Findings there showed several sites with higher dry than wet deposition of Pb and Zn. In contrast, none of the sites in Illinois had greater dry than wet deposition for S, Se or Cu. In this study, S and Se had higher dry than wet deposition for some of the lowest frequencies compared to other trace elements or ionic species; however, it did occur almost 25% of the time. Cu was one of the highest elements for having greater dry deposition than wet deposition.

It is speculated that the dry deposition would be higher than the wet deposition for sites that were being highly impacted by local sources. It was also expected that the wet to dry relationship would be dependent on the physical and chemical nature of the element or species in question. However, there does not appear to be a particularly strong relationship between tracer species overall and the number or size of nearby estimated emission sources. Sites where there was less impact from estimated emission sources like the KYB site had fairly similar ratios of dry to wet deposition for many tracers as sites that were often shown to be highly impacted like the MIA site. Additionally, despite there being higher wet and dry deposition of Se in the northern part of the state where there are coal-burning utility boilers dry deposition of Se tended to be higher than wet deposition more frequently in the southern region. The chemical or physical state of an ionic species also did not broadly increase the frequency when the dry deposition was greater than wet deposition for ionic species despite their higher reactivity. Overall, across the trace elements and ionic species, sites tended towards having more wet deposition of any given metal than dry deposition. There were trends between the sites and species with greater wet dep; however, these did not follow the same patterns as those of Hg.

Correlations of trace elements and ionic species

To understand some of the chemical factors influencing Hg deposition, the correlations between Hg and the trace element and ionic species were investigated. Correlations between Hg and other tracer species has been shown to be suggestive of local source impacts both using simple correlation coefficients and factor analysis (Graney et al 2004, Gratz and Keeler 2011; Lynam et al 2014a). For this data, a more qualitative comparison using correlation coefficients was conducted because the limited samples at individual sites were not suited to doing an

analysis like positive matrix factorization (PMF). Overall correlations were calculated for the wet and dry deposition total masses. Additionally, correlation coefficients were calculated while the data was stratified by location and turf period in order to better understand associations that were obscured by the more general analysis that. In particular, stronger associations were observed when the data was stratified by region (as shown in Table 4.10 and

Table 4.11), site as well as certain time periods. Stratification by site indicated that sites were being influenced by different trace elements and ionic species but there were some groups of sites that tended to have similar deposition patterns. The correlation coefficients for wet deposition in contrast to dry deposition were also investigated.

For wet deposition by site, there were 12 species that were frequently highly correlated with other species (correlation coefficients with other species greater than 0.8 for at least 10 other species). These species were Sr, La, Ce, Sm, Al, Ti, V, Cr, Mn, Fe, Co, and Ba. The highest correlations across the state were between the rare earth elements La, Ce and Sm and Al and Fe for both wet deposition and dry deposition. All of these trace elements are associated with crustal or soil components (Mason and Moore 1982, Ma et al 1997).

For dry deposition, there were several species that were highly correlated with other trace elements including La, Ce, Sm, Al, and Fe (three and four times that they were correlated with another trace element above 0.9). For trace elements and ionic species with correlation coefficients above 0.8, there was La, Ce, Sm, Al, Ti, Mn, Fe, Co, and Cu.

The trace elements and ionic species, that appeared to be most strongly correlated with other trace elements and ionic species for dry deposition were not the same ones for wet deposition. There were more highly correlated trace elements for wet deposition than dry deposition. For wet deposition, the southern region had the most strongly correlated trace elements followed by the eastern region, and the northern region while the western region had the least. This is in contrast to the correlations for dry deposition where the western region had the most trace elements that were strongly correlated to each other ($r>0.8$); followed by southern, eastern and northern regions.

Correlations between Hg and other species

Hg is not highly correlated with any of the other trace elements or ionic species for dry deposition when examined across the state (the greatest correlation coefficient was 0.244 for Se). In the southern region, there were several trace elements associated with crustal sources that were moderately correlated with Hg. V, Mn, Ti, Cr, La, Sm, Nd, Ce, Fe, Co, Al all had correlation coefficients with Hg that were between 0.468 and 0.615, respectively. The correlations between Hg and the other species were weak in the remaining regions where the greatest correlation coefficient was with Se, r=0.335 in the central region.

When stratified by site, the correlations between Hg and other tracer species in dry deposition was stronger. EHP, HSB, ENP and MIA had moderate correlations between Hg and several tracer species. The Southern sites were particularly correlated with the above identified crustal sourced elements whereas HSB correlations also included Ca, As, S, Sr, Mg, Na and Cu suggesting different source impacts. Hg correlations to Se were specifically investigated because of its association with coal burning. Hg and Se were moderately correlated at the PCT and BWR sites (r=0.83, r=0.79).

The correlations between Hg and the trace elements and ionic species seemed to follow similar trends for wet deposition as that of dry deposition; however, with stronger correlations for the entire data set as well as at the regional and site level. The greatest correlation was between Hg and V (r=0.815) which was followed by 14 tracers that had correlation coefficients greater than 0.7. These included tracers beyond the crustal associated trace elements to include S, V, Cr, Pb, and Ba.

On a regional level, the southern region again had the strongest correlations between Hg and other trace elements followed by east, west and central regions. Stratified by site, there were

several sites that had several tracers that were strongly correlated with Hg. DSO, EHP and MIA were all correlated with at least 29 trace elements over 0.9. Unlike for dry deposition, there were not trace elements that had a strong negative correlation with Hg. The greatest negative correlation was with Rb, r=-0.129.

Enrichment factors

Enrichment factors can be used to compare trace elements and determine how much a certain element's deposition may be enhanced due to local sources or other factors (Mason and Moore, 1982). Calculated by choosing a crustal reference element, the ratio of the concentration of an element of interest to the reference element is compared to ratio of the concentrations of these elements in soil.

$EF = (C_x/C_R)_{sample} / (C_x/C_R)_{crust}$

Al is often used as a reference element because it is generally not emitted from any major anthropogenic sources. If the resulting enrichment factor of a specific element is below 10 then it is assumed that it is naturally occurring, between 10 and 500 is interpreted as moderately enriched and >500 is considered to be highly enriched, suggesting that there is an anthropogenic source strongly impacting the site. Enrichment factor analysis was able to provide some more quantitative analysis to investigate source impacts at the sites.

Median enrichment factors of the precipitation concentration and of dry deposition were calculated for 22 elements using Al as a reference element for each of the sites in Table 4.12 and

Table 4.13. There were only a few elements, Hg, S, Se and Zn that were indicated to be highly enriched at any of the sites. Hg was highly enriched for at least eight of the 26 sites for the precipitation samples and 11 sites for the dry deposition. S and Se were highly enriched for most of the sites with the exception of the southern sites that showed moderate enrichment. Zn showed evidence of moderate enrichment at all of the sites but was highly enriched only at the UCF site. There was also a strong north to south decreasing gradient for many of the elements, particularly those that were moderately or greatly enriched. The only site where Hg was highly enriched of the central or southern regions was CRS in precipitation. For S and Se, the sites that were not highly enriched were the furthest south of the Central sites or in the southern region.

The decreasing gradient for S and Se followed earlier observations that S and Se were present in lower concentrations among the southern region where there were not coal-fired utility boilers which were their primary emission sources; however, it was unexpected that any of the Southern sites would still indicate high enrichment of S or Se. These results also compared similarly to the results reported in Lynam et al (2014a) where only S and Se were highly enriched, although within a narrower range both with a higher minimum and a lower maximum value. This also indicates that the southern regional sites may have been impacted by regional coal-fired utility boilers' emissions, although not to the extent of the sites in northern Florida and the Illinois sites in the Lynam et al (2014a) study. Cd, Pb, Cu, Zn, As and V had enrichment factors showing evidence of moderate enrichment suggesting some anthropogenic impact. The coal-fired utility boilers have been associated with As, as well as S and Se (Gratz et al, 2013), while non-ferrous smelting was associated with Zn, As, Cd, and Pb. V has been associated with oil combustion as well as being in the some of the source factor profiles for coal-fired utility boilers (Dvonch et al, 1999; Gratz et al, 2013). Waste incineration factors were highly

associated with Pb. Cu which was moderately enriched is sometimes associated with non-ferrous metal smelting or municipal waste incineration (Lynam et al 2014a, Michael et al 2016); however, it has also been part of unidentified factors (Dvonch et al 1999, Graney et al 2004).

One concern in the use of Al as a reference element for this data set was that Al concentration in precipitation and dry deposition reflected a strong north to south increasing gradient with the average of Al precipitation concentration in the southern region being seven times greater than the average in the western region. The southern sites were also shown to be impacted by transported Sahara dust which could have functioned as a source of Al and depressed the enrichment factors of anthropogenic associated species (Prospero et al 2001). This may partially explain why Hg generally did not appear to be highly enriched in the southern and central regions despite precipitation concentrations and dry deposition values that suggested otherwise.

Analysis was conducted with Ti as a potential reference element to investigate the potential complications of Al (Table 4.14 and

Table 4.15). Like Al, Ti is primarily associated with crustal components and few anthropogenic sources. Ti also appeared favorable because it had a slightly less variability across the sites. When Ti was used as a reference element, median Hg enrichment factors indicated that Hg was highly enriched at all of the sites with an exception of the DVE site for precipitation concentration. For dry deposition, the enrichment factors indicated enrichment at many of the eastern and western sites, but only at CRS and DSO for the central and southern sites. S and Se were highly enriched at all sites for wet and dry deposition. There were other elements that were highly enhanced when Ti was a reference element as well including Cd at the HSB site, P at the OKB site, Zn at the OLF, UWF, OCS, LTI and KYB sites and As at the OLF, UWF, and LTI sites. These were elements that indicated moderate enrichment with Al as the reference element; however, Ti may have helped to better distinguish some patterns.

For dry deposition, median enrichment factors using Ti as a reference element also indicated some additional elements with strong anthropogenic contributions. Cd, P, Cu, Zn and As were all strongly enriched at the UWF site, while Ni and Zn were highly enriched at MBI and at MIA, Zn was also highly enriched.

Ti as a reference element does not seem to provide significant advantages over the benefits of using Al allowing stronger comparisons with other data sets. The usage of almost any crustal element, including Ti, could be complicated by the Sahara sand transport. Additionally, Ti as a reference element rarely changed the relationship of sites to each other. The relationship between Al and Ti is quite close, Al= 74.64(Ti) -3.0297; where 94.2 % of the Al concentration was explained by the concentration of Ti in precipitation. Enrichment factor analysis with known Sahara sand deposition episodes removed could be another potential solution.

Site-based investigations: CRS

According to the National Emissions Inventory estimates (U.S. EPA NEI, 2012), the CRS site was located less than 11 km from one of the largest power plants in Florida and had the second highest mass of Hg emissions within a 25 km radius of the sites after TPA. Unlike the TPA site, where the high Hg emissions was the total of four emission sources of three different source types, this coal-fired electric utility was the only local point Hg emission source resulting in a less mixed signal of species that could be impacting the site. Additionally, its rural location eliminates many urban non-point Hg emission sources that could also mix signals.

This unique situation is reflected in the wet and dry deposition of Hg and the other tracer species. The CRS site had the highest Hg dry deposition during these measurement campaigns. It also had the greatest dry deposition of Ni and Se. The CRS site had the second highest dry deposition of S (after the PCT site). Notably, it was also frequently ranked as one of the lowest sites for the dry deposition of many other species. For 19 out of 30 of the tracer species, the CRS site was ranked as one of the bottom three sites of the central region. These species included those that are crustal associated, those with anthropogenic sources and ionic species which suggests little impact from other major point or non-point sources outside of the coal-fired utilities discussed above.

Hg dry deposition at the CRS site was not strongly correlated with any of the tracer species measured. The greatest correlations were between Hg and Ca ($r= 0.727$) and Se ($r= 0.611$). These were stronger correlations than those of the broader central region where the highest correlation was $r=0.26$ for Se. For other specific sites, BWR and PCT had higher correlations between Se and Hg ($r=0.83$, $r=0.79$).

CRS had fewer than the regional average of other tracer elements and ions that were highly correlated with each other for dry deposition. Se was strongly or moderately correlated with S, SO_4, V and to a lesser extent As and NO_3. These correlated tracer species are largely associated with coal-fired power utilities and provide further evidence of the impact of the coal-fired electrical utility on the CRS site. The impact of the near-field coal-fired power utility to the CRS site was also suggested in Sherman et. al. (2011) using Hg isotopic analysis of precipitation combined with meteorology and Hg concentrations.

The medium to low dry deposition of metals like Ca, Mn, and Al, which are associated with Florida soils suggests that the high Hg dry deposition at CRS was largely due to greater concentrations of Hg in the area and instead of other conditions at the site. Enrichment factors also suggest that the Hg at CRS was enriched over the other sites in the central and southern regions.

The mass of Hg wet deposition at CRS was lower than average for the central region. It had the third lowest total Hg wet deposition for the region although the concentration of Hg in precipitation was the third highest. Similarly, to that of dry deposition, the greatest Se wet deposition in the central region was also at CRS (after UWF and BWR study-wide). CRS ranked among the top three in the region for trace element wet deposition for P and S. Of the other species, CRS tended to be ranked in the bottom three if not the lowest (for everything except NH_4 and SO_4). The concentration of these species in precipitation mostly followed the same trends, CRS was higher ranked among the central sites for the concentration of Hg, was ranked first and second for S and P respectively and ranked highest for Se. Other species where CRS ranked in the top three by precipitation concentration included As, SO_4 and NH_4. Again, the Hg and tracer species' wet deposition patterns at the CRS site suggest that the site was being

impacted by emissions from a coal-fired utility with an absence of much impact from other emission source types.

For precipitation deposition, there were more trace elements and ionic species that were moderately and highly correlated with each other. Ca was most correlated to the Hg deposition (r= 0.96). There were 22 trace elements and ionic species that were strongly correlated to Hg (r > 0.8). The correlation coefficient for Se was 0.89. This varied from other sites in the Central region where the correlation between Hg and Se and Ca were not as strong and the highest correlated species was NO_3^-.

Site-based investigation: MIA

Within a 25-km radius of the MIA site were five Hg emissions sources (U.S. EPA NEI, 2012) making MIA the site impacted by the most near-field Hg emission sources. This included a variety of source types including cement manufacturing, municipal waste combustors, iron foundries, and general medical and surgical hospitals. The MIA site was 3 km from the nearest point source of Hg emissions which was the closest distance of a site in the study. The MIA site was in the upper quartile of sites for the mass of Hg emitted within a 25-km radius at 82 kg Hg (U.S. EPA NEI, 2012). Because the surrounding area was highly industrial, included several large highways and was less than 1 km from the boundaries of large urban area; the MIA site was also likely impacted by additional non-point emission sources.

As described above, the MIA site had high wet and dry deposition of many elements compared to the other sites. Hg dry deposition was comparatively low for the MIA site where the Hg dry deposition was slightly above the study mean. However, MIA had the highest VWM concentration and had the second highest average wet deposition of Hg in the study after the ENP site. As noted earlier, the MIA site was frequently ranked as the site with the highest wet

and dry deposition of many of the tracer species investigated although this pattern largely only held for metals and not the ionic species. Additionally, as expected based on geography, the MIA site did not rank highly for tracer species that were associated with coal-fired electrical generating utilities such as S and Se. This continues to be true even when compared to other sites in the southern region.

The species that were highly correlated with each other at the MIA site suggested crustal element deposition. La, Ce, Sm, Al, Mn, Fe, and Co concentrations were highly correlated with each other in precipitation events. Additionally, Sr was highly correlated ($r>0.9$) with Zn, As, and Ca and Na and Cl ions were associated with each other.

There were no particularly strong correlations between Hg and other species. Hg was moderately correlated ($r>0.7$) with crustal associated metals-- Sm, Ce, Al, Co, Ti, Mn, Cs and Fe in dry deposition. For precipitation, the Hg concentration in precipitation was moderately correlated with Cr, Fe, Ba and Ti (>0.7). The MIA site did rank in the top three for the moderate correlations that existed between Hg and other species; however, the mixture of sources and the small size of the data set meant that it was difficult to identify a specific source that might be influential beyond a correlation between Hg deposition and crustal deposition.

Enrichment factors of Zn (159, 347 for concentration and wet deposition respectively), Pb (55, 97), and Cd (40, 127) were moderately enriched and generally higher than the other southern sites (the Zn enrichment factor at the MIA site was second highest in the state for dry deposition). These enrichment factors suggest that the MIA site may be impacted by the local cement manufacturing facilities which were responsible for 85% of the Hg emissions within the 25 km radius including the closest source. However, the enrichment factors of other elements

that we would expect to also be emitted from cement manufacturing like Cu, As and Ni (Dong et al 2015) indicated minimal anthropogenic contribution.

The CRS site had the highest Hg dry deposition of the sites in the study as well as a Hg VWM concentration that was greater than the study-wide average. The CRS site also had high dry deposition of S, Se, and Ni and high wet deposition of Se, S and P. Additionally, Hg was correlated with several of these tracer species as well as S, Se and SO_4 all being moderately correlated to each other. Combined with the enrichment factors of S, Se and Hg at the CRS site (particularly when combined with the other 2009 central and southern sites) there is strong evidence to support that CRS was almost solely impacted by the local coal-fired utility.

In contrast, MIA tended to frequently be a site where there was particularly high deposition of Hg as well as many of the tracer species. It also had higher minimum concentrations and dry depositions for more tracer species than the other sites although this did not include Hg. The southern sites dominated the highest wet deposition masses for the most tracer species from a combination of being present in high concentrations and having more precipitation than most of the other regions. Of note, both CRS and MIA did have higher enrichment factors for dry deposition than wet deposition for elements depositing from near-field sources providing evidence to support the hypothesis that dry deposition was more likely to reflect near-field emissions.

Sahara sand deposition

During the 2009 measurement campaign, there were two periods when global atmospheric conditions led to high amounts of sands from the Sahara being carried over the

Atlantic and reaching southern to central Florida. Imaging [citation] shows that many of the southern region sites were impacted by the event that occurred between July 17- July 19, 2009. This event also coincided with the fifth turf sampling period (T5) that was July 17- July 20, 2009 allowing an opportunity to compare the dry deposition to non-impacted time frames.

Sahara sand events have been shown to influence the type and amount of trace elements and ionic species being deposited from the Caribbean through the Southeastern United States (Prospero 1999, Prospero et al 2010, Lenes et al 2012). We investigated if the Sahara sands could be a direct source of Hg deposition in Southern Florida, or if the presence of increased particulates in the environment could provide a substrate to enhance increased Hg deposition (Seinfeld and Pandis, 2016, Malcolm et al 2009). The Sahara dust deposition can be partially quantified by the enhanced deposition of a variety of trace elements including Al, Fe, and Mn (Prospero et al 2001, Trapp et al, 2010). Other studies have associated Sahara sands with Al, Fe (Landing et al 1995) and Al, Fe, Ca, Si, and Ti (Perry et al 1997).

The precipitation events during this period ranged from zero precipitation days to three precipitation days in both the Southern and Central regions. There was rain at five of the southern sites during T5, with none at FKE and KYB. Most of the highest Hg concentrations in precipitation occurred during T5. Five out of six of the highest Hg concentrations in precipitation in the Southern region were during this turf period with events at MIA, ENP, MIA a second day during a different event, EHP, and DVE. Hg concentrations during these events ranged from 53.7 ng/L to 84.5 ng/L. These events spanned all three days of the turf period. There were also large amounts of precipitation at MIA, DVE, and EHP leading to the top three events of Hg deposition over the entire study. The sites DVE, EHP, MIA, and OKB received

greater than 40% of the Hg wet deposition from the study during this turf period. The highest percentage was at 54.1% (EHP).

The sites also received a substantial proportion of other trace element and ionic species wet deposition during this sampling period. Because there was higher wet deposition during this turf period in general, this analysis was conducted by comparing percentage of T5 deposition of the study total to see if this was greater than 1.5 times the percentage of precipitation based on amount. Using this metric, there were at least four sites, EHP, ENP, MIA, and OKB with greater than expected percentage of wet deposition for Mn, Al, Fe, and the rare earth elements (La, Ce, Sm). These were several though not all of the trace elements that have been found to be associated with Sahara sand events. Cd wasn't high for any of the sites; V and Pb were high at ENP and OKB and As was high at MIA. Other trace elements were also high for several of these sites including Ba and Ti. However, all of the metals were not necessarily higher for these sites, Cd, Cu, S, and Zn had lower than average percent deposition.

This is a different pattern of trace element deposition than that seen for T9 which is the other time frame during which the Southern sites seemed to be impacted by Sahara dust events. During T9, only KYB and DVE had some trace elements and ionic species that were greatly above expected values. Very few of the elements that we expected to see elevated were higher at these sites. There was also very little precipitation at most of the southern region sites during this turf period. Also, unlike T5 where the sites were impacted for several days, during this period, the effected day, July 30, 2009 was a single day at the end of the turf period potentially being less influential on dry deposition.

The associations between the metals in wet deposition during T5 were investigated. Na^+, Cl^-, Mg, Pb, Mn, V and Ba were highest correlated with other trace elements and ionic species.

These include several of the metals thought to be associated with Sahara sand events. The most highly correlated trace elements were associated with at least 10 other trace elements ($R^2 > 0.9$) these included Mg, Cr, Ba, Ce, Al, Mn, Fe, Co, K, and Pb. Hg was highly correlated with Na^+, Cl^-, NO_2, Mo, Pb, S, Ni, and Cu.

Although there was strong evidence that southern sites in particular were impacted by the Sahara sand event as indicated in wet and dry deposition during the T5 period, there was less evidence that this was associated with the high Hg wet deposition observed. Additionally, T9 did not seem to have higher Hg wet or dry deposition but also didn't have elevated deposition of other trace elements.

Conclusions

There were measurable amounts of both wet and dry deposition for most of the trace elements and ionic species that were investigated in this study. There was both spatial and temporal variability across the sites often at higher amounts than measured for Hg. Although some of the trace elements and ionic species were highly correlated, many of them followed different geographic trends from each other largely seemingly driven by the local emission sources.

Whereas in paper two we observed that the ratio of wet to dry deposition was variable depending on the site with wet deposition always being greater, from this study we see an even greater variation in this ratio where wet deposition varied from being a small portion of the total deposition to comprising most of the total deposition. This variation frequently occurred between sites even within the same trace element or ionic species. There was some evidence to

suggest that for some trace elements and ionic species, this ratio of wet to dry deposition was associated with the impact of local emission sources.

An examination of trace element and ionic species in wet and dry deposition at the Florida sites confirms the possibilities of using these to determine emission source impacts at a site. Correlation coefficients were helpful in identifying specific sources based off of factor profiles and also determining if these sources also seemed to be associated with enhanced Hg deposition. The enrichment factors provided additional information, particularly in areas like MIA where there were several different source types that mixed and negated some of the correlation coefficient signals.

One of the greatest strengths of this data set lies in its breadth, allowing spatial coverage across the state of Florida. However, the valuable insight that this spatial variability provided which was that even within a given region or part of a region, there was still high spatial variability that disadvantaged the combining of sites and limited the number of samples available for analysis. The total duration of the study periods were not conducive to rigorous multivariate analyses for a more statistically robust investigation of source profiles or determination of the amount of Hg attributed to a given emission source type. For future work, it would be interesting to extend the duration of the study to collect enough samples to conduct PMF analysis. This would be particularly interesting for the dry deposition data which has historically been much more limited than wet deposition. Additionally, collecting data during different seasons would provide an interesting contrast as there is usually less wet deposition the rest of the year as well less impact of Sahara sands.

References

Dong, Z., Bank, M.S., Spengler, J.D., 2015. Assessing metal exposures in a community near a cement plant in the northeast U.S. Int. J. Environ. Res. Public Health 12, 952–969. https://doi.org/10.3390/ijerph120100952

Dvonch, J.T., Keeler, G.J., Marsik, F.J., 2005. The influence of meteorological conditions on the wet deposition of mercury in southern Florida. J. Appl. Meteorol. 44, 1421–1435. https://doi.org/10.1175/jam2272.1

Dvonch, J.T., Graney, J.R., Marsik, F.J., Keeler, G.J., Stevens, R.K., 1998. An investigation of source receptor relationships for mercury in south Florida using event precipitation data. Sci. Total Environ. 213, 95–108. https://doi.org/10.1016/S0048-9697(98)00144-2

Graney, J.R., Dvonch, J.T., Keeler, G.J., 2004. Use of multi-element tracers to source apportion mercury in south Florida aerosols. Atmos. Environ. 38, 1715–1726. https://doi.org/10.1016/j.atmosenv.2003.12.018

Graney, J.R., Dvonch, J.T., Keeler, G.J., 2004. Use of multi-element tracers to source apportion mercury in south Florida aerosols. Atmos. Environ. 38, 1715–1726. https://doi.org/10.1016/j.atmosenv.2003.12.018

Gratz, L.E., Keeler, G.J., 2011. Sources of mercury in precipitation to Underhill, VT. Atmos. Environ. 45, 5440–5449. https://doi.org/10.1016/j.atmosenv.2011.07.001

Gratz, L.E., Keeler, G.J., Morishita, M., Barres, J.A., Dvonch, J.T., 2013. Assessing the emission sources of atmospheric mercury in wet deposition across Illinois. Sci. Total Environ. 448, 120–131. https://doi.org/10.1016/j.scitotenv.2012.11.011

Hall, N.L., Dvonch, J.T., Marsik, F.J., Barres, J.A., Landis, M.S., 2017. An artificial turf-based surrogate surface collector for the direct measurement of atmospheric mercury dry deposition. Int. J. Environ. Res. Public Health 14. https://doi.org/10.3390/ijerph14020173

Hoyer, M., Burke, J., Keeler, G., 1995. Atmospheric sources, transport and deposition of mercury in Michigan: Two years of event precipitation. Water, Air, Soil Pollut. 80, 199–208. https://doi.org/10.1007/BF01189668

Lenes, J.M., Prospero, J.M., Landing, W.M., Virmani, J.I., Walsh, J.J., 2012. A model of Saharan dust deposition to the eastern Gulf of Mexico. Mar. Chem. 134–135, 1–9. https://doi.org/10.1016/j.marchem.2012.02.007

Lynam, M., Dvonch, J.T., Barres, J., Percy, K., 2017. Atmospheric wet deposition of mercury to the Athabasca Oil Sands Region, Alberta, Canada. Air Qual. Atmos. Heal. 83–93. https://doi.org/10.1007/s11869-017-0524-6

Lynam, M.M., Dvonch, J.T., Hall, N.L., Morishita, M., Barres, J.A., 2014. Trace elements and major ions in atmospheric wet and dry deposition across central Illinois, USA. Air Qual. Atmos. Heal. 8, 135–147. https://doi.org/10.1007/s11869-014-0274-7

Lynam, M.M., Dvonch, J.T., Hall, N.L., Morishita, M., Barres, J.A., 2014. Spatial patterns in wet and dry deposition of atmospheric mercury and trace elements in central Illinois, USA. Environ. Sci. Pollut. Res. 21, 4032–4043. https://doi.org/10.1007/s11356-013-2011-4

Ma, L.Q., Tan, F., Harris, W.G., 1997. Concentrations and Distributions of Eleven Metals in Florida Soils. J. Environ. Qual. 26, 769. https://doi.org/10.2134/jeq1997.00472425002600030025x

Malcolm, E.G., Ford, A.C., Redding, T.A., Richardson, M.C., Strain, B.M., Tetzner, S.W., 2009. Experimental investigation of the scavenging of gaseous mercury by sea salt aerosol. J. Atmos. Chem. 63, 221–234. https://doi.org/10.1007/s10874-010-9165-y

Mason 1917-2009, B. (Brian H., Moore, C.B., n.d. Principles of geochemistry / Brian Mason, Carleton B. Moore. Wiley.

Michael, R., Stuart, A.L., Trotz, M.A., Akiwumi, F., 2016. Source apportionment of wet-deposited atmospheric mercury in Tampa, Florida. Atmos. Res. 170, 168–175. https://doi.org/10.1016/j.atmosres.2015.11.017

National Atmospheric Deposition Program (NRSP-3). 2017. NADP Program Office, Wisconsin State Laboratory of Hygiene, 465 Henry Mall, Madison, WI 53706.

Pancras, J.P., Vedantham, R., Landis, M.S., Norris, G.A., Ondov, J.M., 2011. Application of EPA unmix and nonparametric wind regression on high time resolution trace elements and speciated mercury in Tampa, Florida Aerosol. Environ. Sci. Technol. 45, 3511–3518. https://doi.org/10.1021/es103400h

Perry, K.D., Cahill, T.A., Eldred, R.A., Dutcher, D.D., Gill, T.E., 1997. Long-range transport of North African dust to the eastern United States 102, 11225–11238.

Prospero, J.M., 1999. Long-range transport of mineral dust in the global atmosphere: Impact of African dust on the environment of the southeastern United States. Proc. Natl. Acad. Sci. 96, 3396–3403. https://doi.org/10.1073/pnas.96.7.3396

Prospero, J.M., Landing, W.M., Schulz, M., 2010. African dust deposition to Florida: Temporal and spatial variability and comparisons to models. J. Geophys. Res. Atmos. 115, 1–20. https://doi.org/10.1029/2009JD012773

Prospero, J.M., Olmez, I., Ames, M., 2001. Al and Fe in PM 2.5 and PM 10 suspended particles in South-Central Florida: The impact of the long range transport of African mineral dust. Water. Air. Soil Pollut. 125, 291–317. https://doi.org/10.1023/A:1005277214288

Seinfeld, J.H., Pandis, S.N., 2016. Atmospheric Chemistry and Physics : From Air Pollution to Climate Change. John Wiley & Sons, Incorporated, New York, UNITED STATES.

Sherman, L.S., Blum, J.D., Keeler, G.J., Demers, J.D., Dvonch, J.T., 2012. Investigation of Local Mercury Deposition from a Coal-Fired Power Plant Using Mercury Isotopes 382–390. https://doi.org/10.1021/es202793c

UNEP, 2015. Global Mercury Assessment 2013. UNEP Chem. Branch, Geneva, Switz. 36.

U.S. Environmental Protection Agency (U.S. EPA). National Emissions Inventory (NEI) Data and Documentation. http://www.epa.gov/ttnchie1/net/2008inventory.html 2008. [Site visited: October-11-2012; Site updated: 28-August-2012].

Table 4.1: Description of Florida measurement campaign sites

Site Code	Site Name	Region	Latitude	Longitude	Coastal
MBI	Mobile Bay, AL	West	30.6715	-87.9360	Near
BLG	Big Lagoon State Park	West	30.3166	-87.4038	
OLF	Pensacola Supersite	West	30.5500	-87.3751	
UWF	University of West Florida	West	30.5455	-87.2114	
BWR	Blackwater River State Park	West	30.7111	-86.8764	
JKS	Jacksonville Supersite	East	30.2475	-81.9512	Far
GBP	Goldhead Branch State Park	East	29.8235	-81.9434	Far
CSF	Carey State Forest	East	30.3966	-81.9170	
NJK	Pumpkin Patch Site	East	30.4657	-81.5182	
OCS	Seahorse Ranch, Amelia Island	East	30.5227	-81.4415	Near
LTI	Little Talbot Island	East	30.4296	-81.4106	Near
CRS	Crystal River	Central	29.0250	-82.6165	
UCF	University of Central Florida	Central	28.5920	-81.1901	
HSB	Hillsborough County Park	Central	28.1440	-82.2281	
PCT	Plant City	Central	28.0325	-82.1002	
SDK	Sand Key State Park	Central	27.9599	-82.8245	Near
TPA	Tampa Supersite	Central	27.9134	-82.3751	
DSO	Fort Desoto State Park	Central	27.6227	-82.7137	Near
MKA	Myakka River State Park	Central	27.2224	-82.2971	
OKB	Okeechobee Lake	South	26.6981	-80.8076	Far
DVE	Davie Supersite	South	26.0843	-80.2407	
EHP	Everglades Holiday Park	South	26.0580	-80.4517	
FKE	Fakahatchee Strand	South	25.9513	-81.3603	
MIA	Miami	South	25.8993	-80.3827	
KYB	Bill Baggs Cape State Park	South	25.6719	-80.1574	Near
ENP	Everglades National Park	South	25.3896	-80.6800	

Table 4.2: Summary of the method detection limit (MDL), average sample field blank value as analyzed by turf, throughfall and precipitation concentration as well as the number of blanks below the MDL for each species. Ionic species, SO_4^{2-}, NO_3^-, Cl^-, NH_4^+ and Na^+ are measured in mg/L. Remaining trace elements are measured in μg/L.

	MDL	Field Blank			Samples less than MDL		
		Turf	Throughfall	Precip	Turf	Throughfall	Precip
Rb	0.003	0.005	0.005	0.004	43	46	49
Sr	0.055	0.205	0.189	0.115	1	17	63
Cd	0.002	0.003	0.002	0.002	54	59	68
La	0.004	0.004	0.003	0.003	63	76	72
Ce	0.003	0.007	0.003	0.003	29	75	72
Sm	0.001	0.001	0.001	0.001	76	76	74
Pb	0.019	0.026	0.015	0.024	63	66	63
Mg	1.247	11.672	4.765	2.610	0	25	53
Al	0.553	9.963	1.593	1.150	0	35	33
P	0.862	2.951	1.172	2.729	10	42	30
S	17.025	26.925	18.150	22.228	36	50	47
Ti	0.094	0.311	0.060	0.055	14	76	72
V	0.016	0.012	0.011	0.015	70	75	72
Cr	0.006	0.042	0.043	0.030	1	19	17
Mn	0.022	0.134	0.052	0.060	0	47	49
Fe	0.630	2.153	1.069	0.679	10	68	68
Co	0.002	0.003	0.008	0.005	64	36	37
Ni	0.018	1.048	0.202	0.236	7	14	17
Cu	0.026	0.215	0.199	0.384	22	9	16
Zn	0.046	1.667	1.853	1.135	1	4	21
As	0.011	0.006	0.006	0.008	75	75	74
Se	0.070	0.035	0.035	0.036	77	77	74
SO_4^{2-}	0.030	0.071	0.060	0.056	49	71	60
NO_3^-	0.043	0.373	0.067	0.029	0	59	74
Cl^-	0.023	0.165	0.079	0.083	0	6	12
NH_4^+	0.024	0.030	0.040	0.042	48	73	67
Na^+	0.001	0.087	0.060	0.063	0	0	11
Ca	2.883	117.677	49.642	39.687	0	3	23
Ba	0.034	0.268	0.067	0.112	2	49	47

Table 4.3: ATSS sampler precision calculated as percent difference of the mean dry deposition for the TPA, ENP, and JKS sites where collocated samplers were deployed.

	DVE	JKS	TPA
N	10	9	8
Hg	-30.4%	-14.4%	14.5%
Rb	15.9%	-10.9%	-74.0%
Sr	74.5%	-32.0%	40.4%
Cd	-12.0%	-10.0%	14.1%
La	-8.3%	2.8%	1.3%
Ce	0.5%	-21.6%	-86.7%
Sm	2.3%	-17.0%	100.0%
Pb	45.6%	4.5%	-94.6%
Mg	-2.3%	-84.9%	73.0%
Al	32.5%	21.7%	-34.7%
P	-18.0%	12.0%	-12.2%
S	16.9%	-2.9%	-23.1%
Ti	-2.2%	7.9%	-21.2%
V	-104.3%	-73.4%	41.3%
Cr	-45.5%	-41.7%	-20.8%
Mn	11.6%	13.3%	10.3%
Fe	1.8%	-1.5%	-20.2%
Co	-0.1%	8.1%	-23.2%
Ni	4.2%	19.4%	-31.3%
Cu	12.7%	-11.3%	-23.0%
Zn	-1.3%	19.4%	-24.7%
As	-17.9%	-43.9%	16.2%
Se	12.9%	14.0%	1.9%
SO_4^{2-}	-1.1%	0.3%	-25.9%
NO_3^-	-23.3%	-41.9%	19.3%
Cl^-	3.5%	11.2%	-0.6%
NH_4^+	-3.3%	20.6%	-19.3%
Na^+	-1.2%	10.7%	3.3%
Ca	30.6%	-158.5%	12.8%
Ba	13.1%	48.8%	27.2%

Table 4.4: Monthly total of dry deposition by species. Sites are ordered from North to South. Hg is reported in ng/m^2, trace elements are reported in µg/m^2, ionic species are reported in mg/m^2.

	MBI	BLG	OLF	UWF	BWR	JKS	GBP	CSF	NJK	OCS	LTI
Hg	1814.3	1989.0	2691.6	2407.3	2330.9	3576.2	2409.3	3850.3	2448.8	2010.3	1457.8
Rb	8.2	7.5	9.8	105.1	29.1	12.0	9.7	55.9	5.3	5.3	4.4
Sr	48.6	82.9	48.6	58.2	55.2	37.6	41.9	51.9	73.7	52.3	93.6
Cd	0.4	0.4	0.3	0.5	0.4	0.3	0.3	0.6	0.4	0.2	0.4
La	4.4	5.3	5.1	3.4	6.5	4.1	4.0	5.3	2.8	2.1	1.7
Ce	9.2	7.4	6.8	5.2	9.8	8.9	8.6	10.5	4.9	3.9	3.1
Sm	0.7	0.5	0.6	0.4	0.8	0.7	0.8	0.8	0.3	0.3	0.3
Pb	9.0	5.3	2.9	9.7	21.2	8.2	2.1	27.2	15.1	8.5	2.6
Mg	5269	14739	5259	10147	6935	4393	3662	10353	5202	8208	9578
Al	3096	3268	3391	2572	4425	4448	4890	5426	2711	2614	1581
P	1372	735	1243	8472	1522	3978	4356	16818	1238	1713	5432
S	36703	56285	75957	83139	73190	65475	30955	77518	59255	49591	54229
Ti	56.6	50.2	60.6	51.9	71.7	72.0	71.7	88.7	49.8	48.4	23.4
V	29.7	34.5	43.0	41.2	43.0	38.6	27.6	38.8	62.8	36.8	34.2
Cr	8.2	8.4	10.8	7.4	8.1	10.1	7.6	13.4	9.6	6.7	4.9
Mn	149.9	121.3	146.9	190.8	455.9	135.2	113.9	244.5	100.0	78.0	206.7
Fe	3130	2503	2475	2144	3058	3035	2905	4017	2500	1807	1314
Co	1.9	1.8	2.0	2.1	2.0	2.4	2.1	2.8	2.6	1.2	1.1
Ni	223.2	23.4	33.4	28.9	32.0	25.2	15.3	69.2	58.0	32.0	23.1
Cu	39.5	36.2	74.7	105.5	49.1	95.4	50.6	122.3	58.5	38.5	45.2
Zn	490.5	204.0	668.6	643.4	271.8	438.4	309.2	2118.8	373.3	312.7	256.0
As	4.9	6.7	14.2	15.1	10.2	12.0	4.7	11.9	6.7	6.2	5.5
Se	9.5	15.8	20.6	31.6	27.9	21.0	7.2	19.2	21.6	10.9	23.9
SO_4^{2-}	89.3	140.5	190.5	188.4	183.7	146.8	76.5	169.0	157.0	114.2	130.8
NO_3^-	83.9	133.7	163.8	263.0	141.5	130.7	94.1	167.1	112.9	97.6	80.0
Cl^-	54.3	191.6	58.6	86.0	65.7	50.1	32.6	38.2	61.3	100.7	101.1
NH_4^+	21.5	24.2	40.9	68.1	36.6	42.4	37.1	89.6	21.9	27.8	35.5
Na^+	36.5	120.7	40.5	57.5	45.3	22.1	20.1	38.0	37.3	68.3	67.5
Ca	21698	12714	13646	14195	16251	12089	13973	20040	22563	11260	18410
Ba	76.4	79.8	113.0	52.3	73.3	55.4	51.1	85.5	73.0	50.9	34.7

	CRS	UCF	HSB	PCT	SDK	TPA	DSO	MKA	OKB	DVE	EHP	FKE	MIA	KYB	ENP
Hg	2133.3	2522.0	3360.7	2436.1	2053.6	2868.7	1784.4	3595.3	1843.1	6863.9	4900.1	2930.5	6676.9	1616.4	5544.4
Rb	10.2	14.2	22.0	27.8	11.5	20.3	16.3	45.7	63.4	57.2	112.3	107.4	64.5	14.9	69.4
Sr	44.9	136.1	160.9	125.6	149.5	159.0	175.9	237.5	297.9	760.7	595.0	343.4	1724.8	237.0	505.2
Cd	0.8	2.3	1.0	1.3	0.6	1.2	0.6	1.8	0.5	1.7	0.9	0.7	1.8	0.4	1.2
La	4.5	8.3	15.3	13.2	6.7	14.6	10.7	24.5	22.0	43.1	56.7	20.9	63.8	8.9	49.0
Ce	10.3	18.6	33.7	22.2	16.0	33.6	25.4	59.3	53.8	98.3	127.7	50.5	149.0	21.4	116.2
Sm	0.9	1.6	3.2	2.0	1.5	3.0	2.3	5.4	5.0	9.2	11.7	4.7	12.7	1.9	10.9
Pb	7.0	42.7	38.2	31.9	9.7	31.4	15.6	24.0	19.6	109.6	56.2	23.2	151.9	9.8	42.4
Mg	6687	7732	12443	8665	20202	12381	25802	17805	16931	30558	34900	33787	34021	19785	25495
Al	5232	9143	15371	10407	6911	15561	11918	26392	21869	39987	56155	23981	47520	10581	51171
P	4487	1001	3992	11971	2337	1679	776	10319	25340	1317	6602	26387	4236	658	1233
S	47220	45603	51413	46012	29177	43504	63689	35715	28203	84867	50858	52228	56921	33663	41723
Ti	82.7	135.5	186.7	139.5	98.5	207.5	160.0	330.5	279.0	613.2	870.3	294.3	706.1	133.4	647.7
V	28.2	38.9	71.6	56.7	27.8	63.3	82.0	70.8	53.3	183.1	147.7	81.1	212.6	54.6	122.4
Cr	10.7	16.8	31.6	20.0	15.0	26.0	45.3	34.3	25.8	64.4	78.6	41.6	82.2	19.1	56.0
Mn	120.3	280.9	400.9	233.8	196.7	395.0	236.1	667.2	652.7	1118.1	1428.2	1023.0	1572.1	249.2	1253.9
Fe	3557	6439	10806	7306	4993	11541	8202	18184	15850	31632	40659	16823	37847	7284	36228
Co	3.2	10.1	10.0	7.2	4.6	10.8	6.1	14.8	13.3	28.5	31.5	13.0	32.4	6.1	28.6
Ni	8.4	30.7	47.7	38.3	15.0	33.6	210.8	39.2	35.5	123.8	84.1	45.8	109.9	23.4	71.9
Cu	22.2	186.1	116.1	98.2	40.2	66.1	55.1	116.0	120.4	288.5	122.0	145.3	389.5	29.4	123.5
Zn	257.9	1283.9	5544.4	576.6	368.1	456.2	761.3	680.5	580.1	847.4	487.1	1337.5	1848.3	3352.4	715.7
As	4.0	9.3	9.5	10.4	2.8	8.6	5.3	6.6	5.7	10.2	7.4	6.9	15.8	3.7	6.7
Se	25.4	6.1	8.2	6.6	4.2	8.5	20.0	6.6	3.3	19.1	5.2	8.4	8.2	4.2	9.2
SO_4^{2-}	125.7	130.6	696.9	160.5	66.1	126.4	67.0	83.3	60.5	198.7	123.0	80.2	154.3	88.1	113.9
NO_3^-	67.6	166.3	153.9	140.6	75.7	81.2	58.6	116.1	68.6	261.0	145.4	105.3	268.6	68.0	102.8
Cl^-	67.5	73.4	110.6	56.1	231.2	85.0	155.4	80.1	48.4	300.8	99.7	96.6	126.6	227.7	99.7
NH_4^+	39.6	32.7	158.2	105.3	21.7	27.9	6.3	92.0	66.3	58.6	25.3	18.4	44.6	8.3	12.8
Na^+	44.5	38.9	326.0	52.8	146.2	63.2	127.4	62.5	39.3	133.5	71.2	110.1	100.0	145.6	64.7
Ca	7896	28901	36356	30881	27867	31080	34735	33617	37831	128232	113653	176483	513489	28616	62760
Ba	12.0	187.3	147.2	91.2	59.0	167.4	106.1	297.1	263.8	825.2	667.0	249.6	903.9	70.5	738.6

Table 4.5: Monthly total of dry deposition by species. Sites are ordered from North to South. Hg is reported in ng/m^2, trace elements are reported in µg/m^2, ionic species are reported in mg/m^2.

	MBI	BLG	OLF	UWF	BWR	JKS	GBP	CSF	NJK	OCS	LTI
Hg	1.4	1.1	0.6	1.6	0.9	1.2	0.9	1.2	1.0	1.0	1.3
Rb	380.9	5.9	8.8	2129.7	21.3	7.5	4.6	15.4	8.2	5.0	17.1
Sr	2086.6	213.1	69.5	887.2	50.0	78.6	60.4	100.6	171.2	169.9	979.6
Cd	1.2	0.8	0.4	22.5	0.5	0.8	0.5	2.0	1.0	0.5	2.0
La	8.7	4.1	4.3	8.4	3.1	3.0	2.6	3.8	4.5	2.7	6.7
Ce	17.2	6.8	8.7	23.6	5.2	5.3	4.7	6.5	7.0	4.6	12.4
Sm	1.4	0.6	0.6	1.3	0.4	0.5	0.4	0.6	0.6	0.4	1.2
Pb	28.3	32.3	19.8	56.9	12.7	38.7	7.5	17.7	29.8	14.2	23.3
Mg	140078	19942	5414	122647	3451	5210	2419	4723	13924	16559	125333
Al	4064	2231	3764	14991	2829	2905	2607	4447	3488	1850	4867
P	128543	850	1091	259844	2293	3701	1050	9973	981	2525	2050
S	61683	29186	19214	126073	14343	16061	9680	16774	29681	31383	131704
Ti	100.6	74.0	71.6	175.5	61.1	88.6	50.3	153.6	129.8	56.7	116.2
V	28.8	19.5	14.0	33.7	11.6	23.2	14.1	24.1	88.3	41.3	101.7
Cr	8.5	4.4	4.4	41.7	2.2	8.9	16.0	5.8	6.3	5.1	9.2
Mn	2000.0	167.2	140.8	4329.6	332.1	261.1	83.1	143.2	98.8	87.6	173.4
Fe	6181.9	2129.0	1750.0	7470.0	1362.9	2368.0	1778.3	2139.9	2564.1	1600.0	5103.4
Co	5.3	1.5	1.2	4.4	0.6	1.3	2.4	1.3	2.7	0.8	3.1
Ni	1628.2	434.3	232.3	77.8	26.0	4.2	20.5	25.1	339.5	6.3	416.0
Cu	458.4	110.9	94.3	2302.7	21.1	121.8	301.0	75.9	74.0	48.0	204.9
Zn	1330.2	348.0	118.5	9771.1	354.8	1092.9	99.9	308.4	738.8	178.2	107.6
As	7.3	5.2	9.0	57.9	3.6	5.6	3.9	6.3	4.9	5.6	8.1
Se	7.5	10.0	6.6	13.5	8.6	8.0	5.2	14.4	13.6	8.8	10.9
SO_4^{2-}	187.6	77.1	47.4	229.6	33.1	39.8	25.7	40.3	67.3	81.5	355.0
NO_3^-	30.9	50.0	30.0	18.8	27.3	34.0	33.2	28.1	30.9	53.6	129.3
Cl^-	126.0	216.9	49.9	94.7	8.7	26.0	31.2	36.8	162.6	189.9	1980.9
NH_4^+	84.9	20.8	21.5	627.8	17.2	36.6	18.0	19.7	19.0	18.2	19.6
Na^+	48.0	140.6	34.9	53.6	7.0	19.3	15.1	22.6	106.4	131.3	1188.0
Ca	291078	26142	18678	301269	14534	20463	22686	23421	36716	24352	75874
Ba	427.6	82.5	89.6	473.9	47.4	82.1	64.4	92.8	83.3	62.8	97.3

	CRS	UCF	HSB	PCT	SDK	TPA	DSO	MKA	OKB	DVE	EHP	FKE	MIA	KYB	ENP
Hg	1.9	1.3	0.8	1.7	0.9	1.2	1.1	1.3	0.9	1.5	0.8	0.8	1.4	0.6	1.1
Rb	11.0	19.5	30.4	383.9	8.0	24.7	6.2	36.0	33.3	25.8	258.8	104.7	154.3	15.4	26.3
Sr	166.9	155.5	191.9	398.5	317.0	348.1	225.6	635.7	407.3	540.6	3688.4	242.1	6586.7	997.2	224.8
Cd	2.6	7.2	0.6	5.3	0.4	6.1	0.4	1.4	0.6	1.2	2.6	1.5	6.2	1.3	0.4
La	4.7	6.5	6.8	9.2	5.7	12.0	4.7	17.2	11.5	18.5	25.3	8.5	42.0	9.7	19.4
Ce	9.2	12.7	12.8	14.7	11.0	23.3	8.9	39.2	25.9	40.8	54.1	18.8	66.9	22.1	40.9
Sm	1.0	1.2	1.2	1.4	1.1	2.3	0.9	3.7	2.4	3.7	5.3	1.9	7.2	2.1	3.7
Pb	20.0	23.4	22.9	41.8	15.6	133.4	13.9	22.5	56.6	60.5	62.9	24.6	305.7	47.9	42.8
Mg	12456	6441	8465	47765	17157	12284	15226	18004	11232	16519	62251	20779	41128	20183	12190
Al	3561	6370	5051	6768	5040	11620	4512	22226	12590	23332	29702	10856	35729	11528	21320
P	6176	6245	4838	94006	1455	8670	986	3841	8979	1206	122659	5999	10783	1713	1254
S	54162	28913	26640	59994	17375	42482	19672	18442	22277	22455	112153	15804	32755	21158	15209
Ti	145.2	209.5	184.3	209.5	113.7	407.2	94.9	338.1	233.6	395.9	765.8	168.4	728.5	195.0	404.8
V	18.2	46.1	30.2	28.5	19.8	66.6	28.9	50.0	31.7	65.0	68.4	27.8	164.5	36.6	47.5
Cr	7.7	16.9	22.1	19.9	8.7	42.0	5.9	21.1	17.1	30.8	48.0	13.9	125.7	17.9	31.7
Mn	128.9	148.5	215.7	827.5	149.4	369.7	114.4	756.1	276.4	405.1	800.1	271.7	747.0	234.5	387.5
Fe	2229.3	3984.1	3739.8	5184.2	3375.4	11845.9	2764.2	13060.5	6859.3	14555.1	18232.4	6176.4	35635.7	7068.3	12590.6
Co	3.6	3.8	4.6	3.5	2.6	6.6	2.2	16.7	5.3	9.3	11.1	4.7	18.4	5.3	9.1
Ni	179.8	51.4	33.7	52.5	5.9	65.5	13.3	78.2	25.2	120.7	60.1	23.4	225.4	43.2	40.7
Cu	93.6	312.8	146.9	607.2	42.2	249.2	28.0	248.5	199.9	437.2	819.5	162.7	584.5	92.6	43.8
Zn	216.4	1014.5	342.3	1566.1	73.5	1879.7	130.8	1207.5	475.9	645.3	2327.9	397.1	5665.8	3019.9	113.6
As	3.3	4.0	5.0	12.5	3.9	22.9	2.5	6.0	9.2	7.6	11.8	3.7	29.6	5.4	3.3
Se	25.1	5.0	8.6	5.4	6.0	7.7	7.2	5.5	5.2	5.0	8.1	5.2	8.9	5.3	7.0
SO_4^{2-}	94.9	33.6	166.5	101.6	34.9	92.7	167.0	54.9	41.0	71.3	270.0	40.8	66.7	56.7	39.0
NO_3^-	29.5	35.7	88.2	11.0	37.6	44.8	30.9	48.5	43.5	100.4	63.2	34.4	62.4	21.7	22.4
Cl^-	39.5	15.8	35.0	25.0	209.9	69.4	205.6	60.5	54.7	100.3	236.1	61.3	88.4	229.9	83.9
NH_4^+	35.9	46.0	79.6	266.8	7.1	41.9	83.4	26.9	39.0	42.3	246.9	74.6	27.2	6.0	21.4
Na^+	45.1	20.6	101.5	33.0	115.6	55.0	159.7	48.8	31.4	82.0	130.3	38.1	31.3	137.8	65.0
Ca	43662	39863	43410	123061	82809	90704	33510	78658	77021	105627	641353	144811	2420526	105173	33234
Ba	105.1	176.9	187.4	248.7	85.0	316.9	69.8	481.5	249.8	569.7	536.5	170.3	1255.7	108.3	183.2

Table 4.6: Site rankings for the highest and lowest species' dry deposition, wet deposition and volume-weighted mean concentration [VWM].

Highest	**1**	**2**	**3**
Dry Dep	EHP	MIA	UWF
Wet Dep	MIA	EHP	ENP
[VWM]	MIA	EHP	OKB

Lowest	**26**	**25**	**24**
Dry Dep	BWR	GBP	OCS
Wet Dep	GBP	OCS	CRS
[VWM]	OLF	JKS	UWF

Table 4.7: The sites with the highest, second highest and third highest minimum values by trace element or ionic species for dry deposition and precipitation concentration.

	Dry Deposition			Precipitation Concentration		
	1	2	3	1	2	3
Hg	CRS	DVE	MBI	MIA	EHP	ENP
Rb	MIA	TPA	LTI	MKA	OKB	HSB
Sr	MIA	KYB	LTI	MIA	DVE	KYB
Cd	MIA	TPA	PCT	UCF	PCT	MBI
La	MIA	TPA	LTI	MIA	HSB	MKA
Ce	MIA	TPA	UCF	MIA	MKA	HSB
Sm	MIA	TPA	UCF	MKA	HSB	SDK
Pb	MIA	TPA	EHP	MIA	DVE	CSF
Mg	LTI	MIA	UWF	SDK	MIA	DVE
Al	MIA	TPA	UCF	MKA	MIA	HSB
P	UWF	TPA	PCT	OKB	MKA	HSB
S	LTI	UWF	MIA	LTI	KYB	NJK
Ti	MIA	TPA	UWF	MIA	DVE	MKA
V	MIA	LTI	TPA	KYB	MIA	EHP
Cr	MIA	EHP	TPA	MIA	HSB	DVE
Mn	MIA	TPA	TPA	MIA	MKA	DVE
Fe	MIA	TPA	MBI	MIA	MKA	DVE
Co	MIA	EHP	TPA	DVE	MIA	UCF
Ni	MIA	EHP	TPA	MIA	OCS	DVE
Cu	MIA	DVE	TPA	MIA	DVE	OKB
Zn	MIA	TPA	OKB	MIA	OKB	KYB
As	MIA	UWF	DVE	OKB	MIA	JKS
Se	UWF	MIA	BLG	LTI	MBI	MBI
SO_4^{2-}	LTI	UWF	MIA	LTI	KYB	NJK
NO_3^-	LTI	DVE	EHP	OKB	KYB	LTI
Cl^-	LTI	OCS	KYB	LTI	SDK	KYB
NH_4^+	JKS	HSB	CSF	LTI	NJK	UCF
Na^+	LTI	OCS	DVE	LTI	SDK	KYB
Ca	MIA	EHP	KYB	MIA	DVE	EHP
Ba	MIA	TPA	MBI	MIA	DVE	UCF

Table 4.8: Relative standard deviation for dry deposition, wet deposition and concentration as a percent.

	Dry Deposition	Wet Deposition	[VWM]
Hg	62.3	92.8	34.3
Rb	108.3	130.8	99.7
Sr	77.5	95.4	125.5
Cd	128.0	118.4	62.5
La	66.6	116.3	105.7
Ce	81.4	119.2	111.3
Sm	76.5	121.3	113.3
Pb	91.3	109.9	102.4
Mg	86.6	98.1	69.5
Al	90.0	116.7	103.0
P	124.0	126.8	165.4
S	74.9	82.5	24.2
Ti	79.2	116.4	102.9
V	66.6	97.7	60.2
Cr	94.7	103.0	80.6
Mn	86.9	120.0	92.6
Fe	77.2	116.5	103.5
Co	95.9	114.9	99.9
Ni	149.9	103.5	113.6
Cu	125.9	102.6	70.8
Zn	123.2	120.2	142.6
As	72.2	93.8	27.3
Se	58.2	92.3	67.2
SO_4^{2-}	86.1	87.0	71.9
NO_3^-	90.3	78.1	27.4
Cl^-	87.2	84.9	84.4
NH_4^+	141.6	110.5	78.0
Na^+	90.4	93.1	85.9
Ca	73.7	95.3	155.9
Ba	93.1	114.9	109.0

Table 4.9: Ratio of wet to dry deposition by site for trace elements and ionic species.

	MBI	BLG	OLF	UWF	BWR	JKS	GBP	CSF	NJK	OCS	LTI
Hg	1.3	1.7	4.9	1.5	2.5	3.1	2.7	3.2	2.5	1.9	1.2
Rb	0.0	1.3	1.1	0.0	1.4	1.6	2.1	3.6	0.6	1.1	0.3
Sr	0.0	0.4	0.7	0.1	1.1	0.5	0.7	0.5	0.4	0.3	0.1
Cd	0.3	0.5	0.6	0.0	0.9	0.3	0.7	0.3	0.4	0.4	0.2
La	0.5	1.3	1.2	0.4	2.1	1.4	1.5	1.4	0.6	0.8	0.2
Ce	0.5	1.1	0.8	0.2	1.9	1.7	1.8	1.6	0.7	0.9	0.2
Sm	0.5	0.9	0.9	0.3	2.2	1.4	1.9	1.3	0.6	0.8	0.3
Pb	0.3	0.2	0.1	0.2	1.7	0.2	0.3	1.5	0.5	0.6	0.1
Mg	0.0	0.7	1.0	0.1	2.0	0.8	1.5	2.2	0.4	0.5	0.1
Al	0.8	1.5	0.9	0.2	1.6	1.5	1.9	1.2	0.8	1.4	0.3
P	0.0	0.9	1.1	0.0	0.7	1.1	4.1	1.7	1.3	0.7	2.7
S	0.6	1.9	4.0	0.7	5.1	4.1	3.2	4.6	2.0	1.6	0.4
Ti	0.6	0.7	0.8	0.3	1.2	0.8	1.4	0.6	0.4	0.9	0.2
V	1.0	1.8	3.1	1.2	3.7	1.7	2.0	1.6	0.7	0.9	0.3
Cr	1.0	1.9	2.5	0.2	3.6	1.1	0.5	2.3	1.5	1.3	0.5
Mn	0.1	0.7	1.0	0.0	1.4	0.5	1.4	1.7	1.0	0.9	1.2
Fe	0.5	1.2	1.4	0.3	2.2	1.3	1.6	1.9	1.0	1.1	0.3
Co	0.4	1.2	1.7	0.5	3.6	1.9	0.9	2.2	1.0	1.5	0.4
Ni	0.1	0.1	0.1	0.4	1.2	6.0	0.7	2.8	0.2	5.1	0.1
Cu	0.1	0.3	0.8	0.0	2.3	0.8	0.2	1.6	0.8	0.8	0.2
Zn	0.4	0.6	5.6	0.1	0.8	0.4	3.1	**6.9**	0.5	1.8	2.4
As	0.7	1.3	1.6	0.3	2.8	2.1	1.2	1.9	1.4	1.1	0.7
Se	1.3	1.6	3.1	2.3	3.2	2.6	1.4	1.3	1.6	1.2	2.2
SO_4^{2-}	0.5	1.8	4.0	0.8	5.6	3.7	3.0	4.2	2.3	1.4	0.4
NO_3^-	2.7	2.7	5.5	**14.0**	5.2	3.8	2.8	5.9	3.6	1.8	0.6
Cl^-	0.4	0.9	1.2	0.9	**7.6**	1.9	1.0	1.0	0.4	0.5	0.1
NH_4^+	0.3	1.2	1.9	0.1	2.1	1.2	2.1	4.5	1.2	1.5	1.8
Na^+	0.8	0.9	1.2	1.1	**6.4**	1.1	1.3	1.7	0.4	0.5	0.1
Ca	0.1	0.5	0.7	0.0	1.1	0.6	0.6	0.9	0.6	0.5	0.2
Ba	0.2	1.0	1.3	0.1	1.5	0.7	0.8	0.9	0.9	0.8	0.4

	CRS	UCF	HSB	PCT	SDK	TPA	DSO	MKA	OKB	DVE	EHP	FKE	MIA	KYB	ENP
Hg	1.1	2.0	4.2	1.5	2.3	2.4	1.7	2.8	2.0	4.7	**6.3**	3.6	4.9	2.9	4.8
Rb	0.9	0.7	0.7	0.1	1.4	0.8	2.6	1.3	1.9	2.2	0.4	1.0	0.4	1.0	2.6
Sr	0.3	0.9	0.8	0.3	0.5	0.5	0.8	0.4	0.7	1.4	0.2	1.4	0.3	0.2	2.2
Cd	0.3	0.3	1.8	0.2	1.6	0.2	1.5	1.3	0.9	1.4	0.3	0.4	0.3	0.3	2.6
La	0.9	1.3	2.2	1.4	1.2	1.2	2.3	1.4	1.9	2.3	2.2	2.5	1.5	0.9	2.5
Ce	1.1	1.5	2.6	1.5	1.5	1.4	2.9	1.5	2.1	2.4	2.4	2.7	2.2	1.0	2.8
Sm	0.9	1.4	2.7	1.4	1.3	1.3	2.7	1.5	2.1	2.5	2.2	2.5	1.8	0.9	2.9
Pb	0.4	1.8	1.7	0.8	0.6	0.2	1.1	1.1	0.3	1.8	0.9	0.9	0.5	0.2	1.0
Mg	0.5	1.2	1.5	0.2	1.2	1.0	1.7	1.0	1.5	1.8	0.6	1.6	0.8	1.0	2.1
Al	1.5	1.4	3.0	1.5	1.4	1.3	2.6	1.2	1.7	1.7	1.9	2.2	1.3	0.9	2.4
P	0.7	0.2	0.8	0.1	1.6	0.2	0.8	2.7	2.8	1.1	0.1	4.4	0.4	0.4	1.0
S	0.9	1.6	1.9	0.8	1.7	1.0	3.2	1.9	1.3	3.8	0.5	3.3	1.7	1.6	2.7
Ti	0.6	0.6	1.0	0.7	0.9	0.5	1.7	1.0	1.2	1.5	1.1	1.7	1.0	0.7	1.6
V	1.6	0.8	2.4	2.0	1.4	0.9	2.8	1.4	1.7	2.8	2.2	2.9	1.3	1.5	2.6
Cr	1.4	1.0	1.4	1.0	1.7	0.6	**7.6**	1.6	1.5	2.1	1.6	3.0	0.7	1.1	1.8
Mn	0.9	1.9	1.9	0.3	1.3	1.1	2.1	0.9	2.4	2.8	1.8	3.8	2.1	1.1	3.2
Fe	1.6	1.6	2.9	1.4	1.5	1.0	3.0	1.4	2.3	2.2	2.2	2.7	1.1	1.0	2.9
Co	0.9	2.7	2.2	2.0	1.8	1.6	2.8	0.9	2.5	3.1	2.8	2.8	1.8	1.1	3.2
Ni	0.0	0.6	1.4	0.7	2.5	0.5	**15.8**	0.5	1.4	1.0	1.4	2.0	0.5	0.5	1.8
Cu	0.2	0.6	0.8	0.2	1.0	0.3	2.0	0.5	0.6	0.7	0.1	0.9	0.7	0.3	2.8
Zn	1.2	1.3	**16.2**	0.4	5.0	0.2	5.8	0.6	1.2	1.3	0.2	3.4	0.3	1.1	**6.3**
As	1.2	2.3	1.9	0.8	0.7	0.4	2.1	1.1	0.6	1.3	0.6	1.9	0.5	0.7	2.0
Se	1.0	1.2	1.0	1.2	0.7	1.1	2.8	1.2	0.6	3.8	0.6	1.6	0.9	0.8	1.3
SO_4^{2-}	1.3	3.9	4.2	1.6	1.9	1.4	0.4	1.5	1.5	2.8	0.5	2.0	2.3	1.6	2.9
NO_3^-	2.3	4.7	1.7	**12.8**	2.0	1.8	1.9	2.4	1.6	2.6	2.3	3.1	4.3	3.1	4.6
Cl^-	1.7	4.7	3.2	2.2	1.1	1.2	0.8	1.3	0.9	3.0	0.4	1.6	1.4	1.0	1.2
NH_4^+	1.1	0.7	2.0	0.4	3.0	0.7	0.1	3.4	1.7	1.4	0.1	0.2	1.6	1.4	0.6
Na^+	1.0	1.9	3.2	1.6	1.3	1.1	0.8	1.3	1.3	1.6	0.5	2.9	3.2	1.1	1.0
Ca	0.2	0.7	0.8	0.3	0.3	0.3	1.0	0.4	0.5	1.2	0.2	1.2	0.2	0.3	1.9
Ba	0.1	1.1	0.8	0.4	0.7	0.5	1.5	0.6	1.1	1.4	1.2	1.5	0.7	0.7	4.0

Table 4.10: Correlation coefficients of dry deposition for trace elements and ionic species by region.

East	Hg	Rb	Sr	Cd	La	Ce	Sm	Pb	Mg	Al	P	S	Ti	V	Cr	Mn	Fe	Co	Ni	Cu	Zn	As	Se	SO_4^{2-}	NO_3^-	Cl^-	NH_4^+	Na^+	Ca	Ba
Hg	1.00	0.01	0.19	0.08	-0.02	0.03	0.02	0.03	0.15	-0.04	0.00	0.18	-0.01	0.04	-0.01	0.04	0.04	0.03	-0.11	0.05	0.09	0.19	0.12	0.17	0.26	0.14	0.30	0.14	0.12	0.20
Rb	0.01	1.00	0.33	0.19	0.60	0.58	0.55	0.18	0.32	0.83	0.91	0.39	0.85	0.18	0.12	0.50	0.41	0.13	0.09	0.18	0.16	0.25	0.06	0.37	0.26	0.30	-0.03	0.30	0.41	0.45
Sr	0.19	0.33	1.00	0.03	0.60	0.62	0.68	0.00	0.95	0.28	-0.01	0.97	0.14	0.47	0.06	0.13	0.65	0.25	0.14	0.04	-0.11	0.36	0.19	0.97	0.73	0.94	-0.04	0.95	0.88	0.12
Cd	0.08	0.19	0.03	1.00	0.06	0.02	0.06	0.18	-0.01	0.07	0.19	0.06	0.15	0.21	-0.02	0.29	-0.03	0.05	0.09	0.01	0.17	0.16	0.11	0.03	0.21	-0.04	0.24	-0.04	0.19	0.30
La	-0.02	0.60	0.60	0.06	1.00	0.94	0.91	0.25	0.53	0.76	0.38	0.62	0.67	0.68	0.16	0.37	0.84	0.40	0.26	0.16	0.07	0.49	0.31	0.63	0.55	0.51	0.00	0.52	0.69	0.55
Ce	0.03	0.58	0.62	0.02	0.94	1.00	0.97	0.28	0.57	0.77	0.35	0.64	0.65	0.52	0.22	0.40	0.88	0.37	0.16	0.14	0.07	0.47	0.25	0.66	0.55	0.55	0.01	0.56	0.67	0.58
Sm	0.02	0.55	0.68	0.06	0.91	0.97	1.00	0.22	0.62	0.73	0.30	0.67	0.59	0.55	0.16	0.36	0.90	0.35	0.19	0.13	-0.01	0.44	0.18	0.69	0.60	0.60	-0.02	0.61	0.70	0.55
Pb	0.03	0.18	0.00	0.18	0.25	0.28	0.22	1.00	-0.06	0.20	0.20	0.05	0.29	0.18	0.21	0.67	0.34	0.17	0.17	0.11	0.76	0.22	0.14	0.02	0.10	-0.08	0.24	-0.07	0.22	0.36
Mg	0.15	0.32	0.95	-0.01	0.53	0.57	0.62	-0.06	1.00	0.22	-0.03	0.94	0.06	0.42	0.04	0.12	0.56	0.21	0.14	0.04	-0.13	0.29	0.13	0.97	0.69	1.00	-0.14	1.00	0.82	0.02
Al	-0.04	0.83	0.28	0.07	0.76	0.77	0.73	0.20	0.22	1.00	0.72	0.33	0.87	0.35	0.17	0.55	0.67	0.30	0.05	0.14	0.13	0.34	0.24	0.32	0.30	0.20	-0.03	0.20	0.39	0.65
P	0.00	0.91	-0.01	0.19	0.38	0.35	0.30	0.20	-0.03	0.72	1.00	0.07	0.86	0.00	0.12	0.44	0.15	-0.01	-0.04	0.19	0.23	0.20	0.00	0.04	0.02	-0.05	0.15	-0.05	0.10	0.39
S	0.18	0.39	0.97	0.06	0.62	0.64	0.67	0.05	0.94	0.33	0.07	1.00	0.18	0.52	0.07	0.18	0.64	0.27	0.13	0.04	-0.05	0.44	0.28	0.99	0.78	0.93	-0.02	0.94	0.89	0.16
Ti	-0.01	0.85	0.14	0.15	0.67	0.65	0.59	0.29	0.06	0.87	0.86	0.18	1.00	0.27	0.12	0.45	0.46	0.15	0.01	0.17	0.23	0.29	0.15	0.16	0.11	0.04	0.16	0.04	0.26	0.57
V	0.04	0.18	0.47	0.21	0.68	0.52	0.55	0.18	0.42	0.35	0.00	0.52	0.27	1.00	0.03	0.21	0.57	0.38	0.22	0.00	0.02	0.36	0.37	0.51	0.58	0.39	-0.01	0.40	0.57	0.34
Cr	-0.01	0.12	0.06	-0.02	0.16	0.22	0.16	0.21	0.04	0.17	0.12	0.07	0.12	0.03	1.00	0.25	0.20	0.15	0.04	0.04	0.14	0.18	0.01	0.08	0.16	0.04	0.06	0.04	0.22	0.32
Mn	0.04	0.50	0.13	0.29	0.37	0.40	0.36	0.67	0.12	0.55	0.44	0.18	0.45	0.21	0.25	1.00	0.45	0.19	0.02	0.11	0.51	0.33	0.11	0.17	0.27	0.09	0.11	0.10	0.30	0.44
Fe	0.04	0.41	0.65	-0.03	0.84	0.88	0.90	0.34	0.56	0.67	0.15	0.64	0.46	0.57	0.20	0.45	1.00	0.46	0.25	0.16	0.13	0.44	0.22	0.64	0.63	0.55	-0.05	0.55	0.71	0.56
Co	0.03	0.13	0.25	0.05	0.40	0.37	0.35	0.17	0.21	0.30	-0.01	0.27	0.15	0.38	0.15	0.19	0.46	1.00	0.26	0.70	0.12	0.34	0.37	0.28	0.42	0.21	-0.02	0.21	0.42	0.35
Ni	-0.11	0.09	0.14	0.09	0.26	0.16	0.19	0.17	0.14	0.05	-0.04	0.13	0.01	0.22	0.04	0.02	0.25	0.26	1.00	0.23	0.34	0.04	-0.05	0.14	0.24	0.14	-0.19	0.15	0.30	0.14
Cu	0.05	0.18	0.04	0.01	0.16	0.14	0.13	0.11	0.04	0.14	0.19	0.04	0.17	0.00	0.04	0.11	0.16	0.70	0.23	1.00	0.22	0.18	-0.07	0.06	0.17	0.04	0.14	0.04	0.11	0.10
Zn	0.09	0.16	-0.11	0.17	0.07	0.07	-0.01	0.76	-0.13	0.13	0.23	-0.05	0.23	0.02	0.14	0.51	0.13	0.12	0.34	0.22	1.00	0.18	0.10	-0.09	-0.03	-0.14	0.41	-0.14	0.12	0.33
As	0.19	0.25	0.36	0.16	0.49	0.47	0.44	0.22	0.29	0.34	0.20	0.44	0.29	0.36	0.18	0.33	0.44	0.34	0.04	0.18	0.18	1.00	0.66	0.41	0.46	0.26	0.29	0.27	0.49	0.53
Se	0.12	0.06	0.19	0.11	0.31	0.25	0.18	0.14	0.13	0.24	0.00	0.28	0.15	0.37	0.01	0.11	0.22	0.37	-0.05	-0.07	0.10	0.66	1.00	0.25	0.22	0.11	0.12	0.12	0.29	0.40
SO_4^{2-}	0.17	0.37	0.97	0.03	0.63	0.66	0.69	0.02	0.97	0.32	0.04	0.99	0.16	0.51	0.08	0.17	0.64	0.28	0.14	0.06	-0.09	0.41	0.25	1.00	0.78	0.96	-0.05	0.96	0.87	0.15
NO_3^-	0.26	0.26	0.73	0.21	0.55	0.55	0.60	0.10	0.69	0.30	0.02	0.78	0.11	0.58	0.16	0.27	0.63	0.42	0.24	0.17	-0.03	0.46	0.22	0.78	1.00	0.65	0.05	0.67	0.75	0.29
Cl^-	0.14	0.30	0.94	-0.04	0.51	0.55	0.60	-0.08	1.00	0.20	-0.05	0.93	0.04	0.39	0.04	0.09	0.55	0.21	0.14	0.04	-0.14	0.26	0.11	0.96	0.65	1.00	-0.15	1.00	0.80	-0.02
NH_4^+	0.30	-0.03	-0.04	0.24	0.00	0.01	-0.02	0.24	-0.14	-0.03	0.15	-0.02	0.16	-0.01	0.06	0.11	-0.05	-0.02	-0.19	0.14	0.41	0.29	0.12	-0.05	0.05	-0.15	1.00	-0.15	-0.03	0.14
Na^+	0.14	0.30	0.95	-0.04	0.52	0.56	0.61	-0.07	1.00	0.20	-0.05	0.94	0.04	0.40	0.04	0.10	0.55	0.21	0.15	0.04	-0.14	0.27	0.12	0.96	0.67	1.00	-0.15	1.00	0.81	-0.01
Ca	0.12	0.41	0.88	0.19	0.69	0.67	0.70	0.22	0.82	0.39	0.10	0.89	0.26	0.57	0.22	0.30	0.71	0.42	0.30	0.11	0.12	0.49	0.29	0.87	0.75	0.80	-0.03	0.81	1.00	0.37
Ba	0.20	0.45	0.12	0.30	0.55	0.58	0.55	0.36	0.02	0.65	0.39	0.16	0.57	0.34	0.32	0.44	0.56	0.35	0.14	0.10	0.33	0.53	0.40	0.15	0.29	-0.02	0.14	-0.01	0.37	1.00

Central	Hg	Rb	Sr	Cd	La	Ce	Sm	Pb	Mg	Al	P	S	Ti	V	Cr	Mn	Fe	Co	Ni	Cu	Zn	As	Se	SO_4^{2-}	NO_3^-	Cl^-	NH_4^+	Na^+	Ca	Ba
Hg	1.00	0.09	0.12	0.03	0.07	0.06	0.07	0.11	0.09	0.05	0.13	0.17	-0.01	0.04	0.07	0.09	0.07	0.07	0.05	0.09	0.01	0.19	0.26	0.06	-0.06	0.00	0.13	0.00	0.17	0.16
Rb	0.09	1.00	0.27	0.15	0.13	0.08	0.08	0.09	0.65	0.07	0.97	0.50	0.01	0.04	0.22	0.68	0.14	0.07	0.01	0.78	0.53	0.14	-0.06	0.08	-0.08	-0.04	0.60	-0.03	0.70	0.15
Sr	0.12	0.27	1.00	-0.02	0.76	0.74	0.75	0.21	0.72	0.75	0.25	0.57	0.58	0.50	0.38	0.74	0.75	0.75	0.16	0.32	0.53	0.21	0.00	0.43	0.34	0.56	0.22	0.56	0.79	0.74
Cd	0.03	0.15	-0.02	1.00	0.03	-0.01	-0.01	0.15	0.05	-0.01	0.20	0.33	0.06	0.65	0.16	0.11	0.04	-0.02	0.10	0.34	0.54	0.27	0.00	-0.04	-0.04	-0.06	0.14	-0.06	0.13	0.06
La	0.07	0.13	0.76	0.03	1.00	0.99	0.99	0.37	0.24	0.98	0.12	0.20	0.80	0.63	0.47	0.77	0.97	0.93	0.20	0.31	0.60	0.28	-0.02	0.16	0.28	0.01	0.17	0.03	0.58	0.89
Ce	0.06	0.08	0.74	-0.01	0.99	1.00	1.00	0.34	0.20	0.99	0.06	0.15	0.80	0.61	0.45	0.74	0.97	0.94	0.22	0.25	0.54	0.24	-0.02	0.14	0.29	0.01	0.12	0.03	0.53	0.88
Sm	0.07	0.08	0.75	-0.01	0.99	1.00	1.00	0.35	0.20	0.99	0.06	0.16	0.79	0.60	0.46	0.73	0.97	0.94	0.21	0.24	0.54	0.26	-0.01	0.13	0.29	0.01	0.14	0.03	0.54	0.88
Pb	0.11	0.09	0.21	0.15	0.37	0.34	0.35	1.00	0.02	0.32	0.11	0.14	0.48	0.41	0.47	0.27	0.47	0.26	0.04	0.20	0.45	0.38	0.03	0.09	0.04	-0.12	0.11	-0.11	0.32	0.40
Mg	0.09	0.65	0.72	0.05	0.24	0.20	0.20	0.02	1.00	0.19	0.64	0.80	0.11	0.14	0.21	0.57	0.24	0.19	0.03	0.50	0.41	0.13	-0.02	0.46	0.15	0.70	0.41	0.68	0.78	0.22
Al	0.05	0.07	0.75	-0.01	0.98	0.99	0.99	0.32	0.19	1.00	0.04	0.13	0.80	0.61	0.44	0.74	0.97	0.96	0.21	0.23	0.55	0.23	-0.02	0.14	0.28	0.00	0.09	0.03	0.53	0.90
P	0.13	0.97	0.25	0.20	0.12	0.06	0.06	0.11	0.64	0.04	1.00	0.53	0.00	0.03	0.20	0.65	0.11	0.03	0.00	0.80	0.53	0.16	-0.05	0.09	-0.11	-0.03	0.72	-0.03	0.69	0.12
S	0.17	0.50	0.57	0.33	0.20	0.15	0.16	0.14	0.80	0.13	0.53	1.00	0.19	0.33	0.22	0.43	0.19	0.13	0.04	0.47	0.45	0.21	0.36	0.50	0.11	0.56	0.40	0.56	0.67	0.18
Ti	-0.01	0.01	0.58	0.06	0.80	0.80	0.79	0.48	0.11	0.80	0.00	0.19	1.00	0.54	0.52	0.54	0.85	0.74	0.11	0.26	0.53	0.25	0.07	0.18	0.20	0.01	0.12	0.04	0.40	0.78
V	0.04	0.04	0.50	0.65	0.63	0.61	0.60	0.41	0.14	0.61	0.03	0.33	0.54	1.00	0.38	0.48	0.65	0.59	0.18	0.24	0.69	0.25	0.07	0.16	0.21	0.04	0.06	0.08	0.42	0.62
Cr	0.07	0.22	0.38	0.16	0.47	0.45	0.46	0.47	0.21	0.44	0.20	0.22	0.52	0.38	1.00	0.44	0.54	0.38	0.05	0.35	0.47	0.81	-0.01	0.09	0.38	0.04	0.13	0.05	0.44	0.46
Mn	0.09	0.68	0.74	0.11	0.77	0.74	0.73	0.27	0.57	0.74	0.65	0.43	0.54	0.48	0.44	1.00	0.76	0.75	0.16	0.68	0.77	0.24	-0.04	0.14	0.18	-0.01	0.41	0.00	0.86	0.76
Fe	0.07	0.14	0.75	0.04	0.97	0.97	0.97	0.47	0.24	0.97	0.11	0.19	0.85	0.65	0.54	0.76	1.00	0.92	0.19	0.29	0.63	0.32	-0.03	0.16	0.27	0.01	0.12	0.04	0.58	0.91
Co	0.07	0.07	0.75	-0.02	0.93	0.94	0.94	0.26	0.19	0.96	0.03	0.13	0.74	0.59	0.38	0.75	0.92	1.00	0.23	0.21	0.55	0.17	0.01	0.08	0.29	0.00	0.02	0.01	0.52	0.91
Ni	0.05	0.01	0.16	0.10	0.20	0.22	0.21	0.04	0.03	0.21	0.00	0.04	0.11	0.18	0.05	0.16	0.19	0.23	1.00	0.02	0.16	-0.01	0.00	0.02	0.04	0.01	-0.01	0.02	0.05	0.21
Cu	0.09	0.78	0.32	0.34	0.31	0.25	0.24	0.20	0.50	0.23	0.80	0.47	0.26	0.24	0.35	0.68	0.29	0.21	0.02	1.00	0.66	0.24	-0.08	0.04	-0.06	-0.08	0.50	-0.08	0.65	0.35
Zn	0.01	0.53	0.53	0.54	0.60	0.54	0.54	0.45	0.41	0.55	0.53	0.45	0.53	0.69	0.47	0.77	0.63	0.55	0.16	0.66	1.00	0.33	-0.08	0.04	-0.09	-0.06	0.31	-0.06	0.71	0.60
As	0.19	0.14	0.21	0.27	0.28	0.24	0.26	0.38	0.13	0.23	0.16	0.21	0.25	0.25	0.81	0.24	0.32	0.17	-0.01	0.24	0.33	1.00	0.01	0.05	0.22	0.01	0.10	0.01	0.29	0.25
Se	0.26	-0.06	0.00	0.00	-0.02	-0.02	-0.01	0.03	-0.02	0.02	-0.05	0.36	0.07	0.07	0.01	0.04	0.03	0.01	0.00	0.08	0.08	0.01	1.00	0.30	0.05	0.00	0.01	0.05	0.02	0.01
SO_4^{2-}	0.06	0.08	0.43	-0.04	0.16	0.14	0.13	0.09	0.46	0.14	0.09	0.50	0.18	0.16	0.09	0.14	0.16	0.08	0.02	0.04	0.04	0.05	0.30	1.00	0.20	0.54	0.33	0.69	0.27	0.14
NO_3^-	-0.06	-0.08	0.34	-0.04	0.28	0.29	0.29	0.04	0.15	0.28	-0.11	0.11	0.20	0.21	0.38	0.18	0.27	0.29	0.04	-0.06	0.09	0.22	-0.05	0.20	1.00	0.22	-0.03	0.23	0.20	0.28
Cl^-	0.00	-0.04	0.56	-0.06	0.01	0.01	0.01	-0.12	0.70	0.00	-0.03	0.56	0.01	0.04	0.04	-0.01	0.01	0.00	0.01	-0.08	-0.06	0.01	0.00	0.54	0.22	1.00	0.01	0.97	0.28	-0.03
NH_4^+	0.13	0.60	0.22	0.14	0.17	0.12	0.14	0.11	0.41	0.09	0.72	0.40	0.12	0.06	0.13	0.41	0.12	0.02	-0.01	0.50	0.31	0.10	0.01	0.33	0.03	0.01	1.00	0.07	0.43	0.12
Na^+	0.00	-0.03	0.56	-0.06	0.03	0.03	0.03	-0.11	0.68	0.03	-0.03	0.56	0.04	0.08	0.05	0.00	0.04	0.01	0.02	-0.08	-0.06	0.01	0.05	0.69	0.23	0.97	0.07	1.00	0.28	0.00
Ca	0.17	0.70	0.79	0.13	0.58	0.53	0.54	0.32	0.78	0.53	0.69	0.67	0.40	0.42	0.44	0.86	0.58	0.52	0.05	0.65	0.71	0.29	0.02	0.27	0.20	0.28	0.43	0.28	1.00	0.56
Ba	0.16	0.15	0.74	0.06	0.89	0.88	0.88	0.40	0.22	0.90	0.12	0.18	0.78	0.62	0.46	0.76	0.91	0.91	0.21	0.35	0.60	0.25	0.01	0.14	0.28	-0.03	0.12	0.00	0.56	1.00

South	Hg	Rb	Sr	Cd	La	Ce	Sm	Pb	Mg	Al	P	S	Ti	V	Cr	Mn	Fe	Co	Ni	Cu	Zn	As	Se	SO42-	NO3-	Cl-	NH4+	Na+	Ca	Ba
Hg	1.00	0.07	0.03	0.17	0.51	0.54	0.52	0.18	0.09	0.60	0.04	0.04	0.46	0.44	0.48	0.45	0.58	0.58	0.23	0.13	0.01	0.21	0.19	0.06	0.16	-0.23	0.02	-0.23	0.06	0.32
Rb	0.07	1.00	0.52	0.51	0.22	0.23	0.25	0.09	0.91	0.25	0.71	0.47	0.36	0.19	0.32	0.57	0.25	0.26	0.08	0.49	0.29	0.39	0.38	0.40	-0.07	0.43	0.21	0.19	0.33	0.30
Sr	0.03	0.52	1.00	0.75	0.51	0.34	0.41	0.65	0.63	0.20	0.40	0.33	0.47	0.67	0.67	0.47	0.39	0.34	0.43	0.43	0.58	0.82	0.34	0.27	0.07	0.35	0.01	0.14	0.94	0.56
Cd	0.17	0.51	0.75	1.00	0.47	0.32	0.38	0.74	0.53	0.23	0.41	0.38	0.42	0.66	0.65	0.51	0.44	0.39	0.36	0.59	0.71	0.75	0.40	0.34	0.12	0.20	0.26	0.01	0.79	0.62
La	0.51	0.22	0.51	0.47	1.00	0.97	0.98	0.43	0.31	0.87	0.28	0.39	0.93	0.84	0.88	0.83	0.93	0.95	0.49	0.35	0.37	0.64	0.47	0.38	0.12	0.11	-0.04	-0.02	0.50	0.66
Ce	0.54	0.23	0.34	0.32	0.97	1.00	0.99	0.23	0.31	0.94	0.30	0.41	0.94	0.71	0.79	0.85	0.93	0.97	0.39	0.31	0.26	0.49	0.45	0.40	0.10	0.14	-0.06	0.04	0.28	0.58
Sm	0.52	0.25	0.41	0.38	0.98	0.99	1.00	0.30	0.33	0.92	0.30	0.41	0.94	0.76	0.84	0.85	0.94	0.97	0.42	0.32	0.29	0.55	0.47	0.40	0.10	0.14	-0.06	0.03	0.37	0.61
Pb	0.18	0.09	0.65	0.74	0.43	0.23	0.30	1.00	0.15	0.11	0.04	0.09	0.27	0.70	0.62	0.27	0.35	0.31	0.38	0.34	0.60	0.73	0.26	0.04	0.09	-0.09	0.07	-0.22	0.79	0.54
Mg	0.09	0.91	0.63	0.53	0.31	0.31	0.33	0.15	1.00	0.31	0.76	0.52	0.45	0.29	0.38	0.65	0.32	0.32	0.17	0.53	0.41	0.46	0.42	0.44	-0.01	0.62	0.12	0.36	0.41	0.36
Al	0.60	0.25	0.20	0.23	0.87	0.94	0.92	0.11	0.31	1.00	0.29	0.38	0.85	0.62	0.75	0.82	0.95	0.96	0.35	0.27	0.16	0.43	0.39	0.37	0.12	0.12	-0.03	0.02	0.13	0.52
P	0.04	0.71	0.40	0.41	0.28	0.30	0.30	0.04	0.76	0.29	1.00	0.89	0.51	0.17	0.22	0.66	0.26	0.27	0.03	0.80	0.34	0.32	0.59	0.84	0.03	0.48	0.37	0.22	0.17	0.33
S	0.04	0.47	0.33	0.38	0.39	0.41	0.41	0.09	0.52	0.38	0.89	1.00	0.61	0.28	0.29	0.63	0.35	0.36	0.05	0.83	0.34	0.34	0.62	0.97	0.15	0.44	0.35	0.25	0.15	0.43
Ti	0.46	0.36	0.47	0.42	0.93	0.94	0.94	0.27	0.45	0.85	0.51	0.61	1.00	0.70	0.75	0.87	0.85	0.89	0.35	0.50	0.35	0.55	0.58	0.59	0.10	0.24	-0.01	0.09	0.36	0.62
V	0.44	0.19	0.67	0.66	0.84	0.71	0.76	0.70	0.29	0.62	0.17	0.28	0.70	1.00	0.90	0.64	0.80	0.76	0.66	0.35	0.51	0.81	0.39	0.26	0.34	0.05	-0.05	-0.09	0.74	0.68
Cr	0.48	0.32	0.67	0.65	0.88	0.79	0.84	0.62	0.38	0.75	0.22	0.29	0.75	0.90	1.00	0.73	0.90	0.86	0.52	0.34	0.46	0.83	0.44	0.26	0.16	0.08	-0.06	-0.08	0.70	0.72
Mn	0.45	0.57	0.47	0.51	0.83	0.85	0.85	0.27	0.65	0.82	0.66	0.63	0.87	0.64	0.73	1.00	0.82	0.85	0.35	0.59	0.36	0.56	0.52	0.58	0.06	0.30	0.27	0.07	0.36	0.60
Fe	0.58	0.25	0.39	0.44	0.93	0.93	0.94	0.35	0.32	0.95	0.26	0.35	0.85	0.80	0.90	0.82	1.00	0.98	0.47	0.32	0.32	0.63	0.43	0.34	0.16	0.09	-0.04	-0.04	0.39	0.65
Co	0.58	0.26	0.34	0.39	0.95	0.97	0.97	0.31	0.32	0.96	0.27	0.36	0.89	0.76	0.86	0.85	0.98	1.00	0.43	0.30	0.29	0.56	0.45	0.35	0.12	0.10	-0.05	-0.02	0.33	0.62
Ni	0.23	0.08	0.43	0.36	0.49	0.39	0.42	0.38	0.17	0.35	0.03	0.05	0.35	0.66	0.52	0.35	0.47	0.43	1.00	0.16	0.23	0.51	0.17	0.03	0.38	0.02	-0.05	-0.04	0.49	0.34
Cu	0.13	0.49	0.43	0.59	0.35	0.31	0.32	0.34	0.53	0.27	0.80	0.83	0.50	0.35	0.34	0.59	0.32	0.30	0.16	1.00	0.43	0.43	0.55	0.80	0.18	0.27	0.44	0.04	0.32	0.65
Zn	0.01	0.29	0.58	0.71	0.37	0.26	0.29	0.60	0.41	0.16	0.34	0.34	0.35	0.51	0.46	0.36	0.32	0.29	0.23	0.43	1.00	0.51	0.30	0.31	0.03	0.37	0.07	0.21	0.58	0.46
As	0.21	0.39	0.82	0.75	0.64	0.49	0.55	0.73	0.46	0.43	0.32	0.34	0.55	0.81	0.83	0.56	0.63	0.56	0.51	0.43	0.51	1.00	0.38	0.28	0.20	0.12	0.03	-0.09	0.84	0.64
Se	0.19	0.38	0.34	0.40	0.47	0.45	0.47	0.26	0.42	0.39	0.59	0.62	0.58	0.39	0.44	0.52	0.43	0.45	0.17	0.55	0.30	0.38	1.00	0.60	-0.02	0.25	-0.05	0.07	0.27	0.46
SO_4^{2-}	0.06	0.40	0.27	0.34	0.38	0.40	0.40	0.04	0.44	0.37	0.84	0.97	0.59	0.26	0.26	0.58	0.34	0.35	0.03	0.80	0.31	0.28	0.60	1.00	0.24	0.44	0.32	0.29	0.10	0.40
NO_3^-	0.16	-0.07	0.07	0.12	0.12	0.10	0.10	0.09	-0.01	0.12	0.03	0.15	0.10	0.34	0.16	0.06	0.16	0.12	0.38	0.18	0.03	0.20	-0.02	0.24	1.00	0.06	0.00	0.12	0.07	0.14
Cl^-	-0.23	0.43	0.35	0.20	0.11	0.14	0.14	-0.09	0.62	0.12	0.48	0.44	0.24	0.05	0.08	0.30	0.09	0.10	0.02	0.27	0.37	0.12	0.25	0.44	0.06	1.00	0.01	0.90	0.12	0.08
NH_4^+	0.02	0.21	0.01	0.26	-0.04	-0.06	-0.06	0.07	0.12	-0.03	0.37	0.35	-0.01	-0.05	-0.06	0.27	-0.04	-0.05	-0.05	0.44	0.07	0.03	-0.05	0.32	0.00	0.01	1.00	-0.02	-0.02	-0.05
Na^+	-0.23	0.19	0.14	0.01	-0.02	0.04	0.03	-0.22	0.36	0.02	0.22	0.25	0.09	-0.09	-0.08	0.07	-0.04	-0.02	-0.04	0.04	0.21	-0.09	-0.07	0.29	0.12	0.90	-0.02	1.00	-0.06	-0.10
Ca	0.06	0.33	0.94	0.79	0.50	0.28	0.37	0.79	0.41	0.13	0.17	0.15	0.36	0.74	0.70	0.36	0.39	0.33	0.49	0.32	0.58	0.84	0.27	0.10	0.07	0.12	-0.02	-0.06	1.00	0.57
Ba	0.32	0.30	0.56	0.62	0.66	0.58	0.61	0.54	0.36	0.52	0.33	0.43	0.62	0.68	0.72	0.60	0.65	0.62	0.34	0.65	0.46	0.64	0.46	0.40	0.14	0.08	-0.05	-0.10	0.57	1.00

West	Hg	Rb	Sr	Cd	La	Ce	Sm	Pb	Mg	Al	P	S	Ti	V	Cr	Mn	Fe	Co	Ni	Cu	Zn	As	Se	SO42-	NO3-	Cl-	NH4+	Na+	Ca	Ba
Hg	1.00	0.04	0.08	-0.02	0.06	0.02	0.05	0.18	0.07	0.00	0.06	0.03	0.14	0.17	0.00	0.00	0.12	0.06	0.12	0.00	-0.01	0.02	0.11	0.13	-0.04	-0.10	-0.06	-0.13	0.04	0.07
Rb	0.04	1.00	0.37	0.78	0.62	0.73	0.61	0.63	0.70	0.87	0.90	0.85	0.52	0.59	0.70	0.86	0.77	0.69	0.01	0.92	0.85	0.31	0.50	0.52	-0.22	0.11	0.63	0.09	0.67	0.67
Sr	0.08	0.37	1.00	0.24	0.62	0.52	0.66	0.27	0.90	0.32	0.65	0.50	0.32	0.31	0.33	0.53	0.67	0.72	0.50	0.40	0.32	0.08	0.02	0.44	-0.29	0.28	0.24	0.09	0.90	0.86
Cd	-0.02	0.78	0.24	1.00	0.67	0.84	0.66	0.75	0.55	0.95	0.81	0.91	0.31	0.71	0.67	0.91	0.75	0.61	-0.04	0.89	0.95	0.34	0.57	0.64	-0.08	0.15	0.95	0.17	0.54	0.58
La	0.06	0.62	0.62	0.67	1.00	0.95	0.98	0.68	0.78	0.78	0.78	0.76	0.67	0.67	0.57	0.80	0.94	0.86	0.32	0.68	0.68	0.20	0.36	0.46	-0.13	0.17	0.64	0.13	0.71	0.81
Ce	0.02	0.73	0.52	0.84	0.95	1.00	0.95	0.73	0.76	0.92	0.85	0.87	0.57	0.71	0.64	0.90	0.94	0.84	0.20	0.80	0.82	0.24	0.44	0.56	-0.14	0.18	0.79	0.16	0.69	0.78
Sm	0.05	0.61	0.66	0.66	0.98	0.95	1.00	0.63	0.79	0.78	0.78	0.75	0.62	0.63	0.57	0.80	0.94	0.85	0.32	0.66	0.67	0.18	0.33	0.46	-0.17	0.21	0.62	0.16	0.74	0.82
Pb	0.18	0.63	0.27	0.75	0.68	0.73	0.63	1.00	0.51	0.74	0.66	0.77	0.43	0.72	0.68	0.75	0.72	0.62	0.09	0.74	0.79	0.30	0.55	0.52	0.07	0.11	0.72	0.13	0.51	0.62
Mg	0.07	0.70	0.90	0.55	0.78	0.76	0.79	0.51	1.00	0.64	0.89	0.79	0.48	0.54	0.54	0.81	0.87	0.90	0.44	0.70	0.63	0.22	0.28	0.62	-0.26	0.32	0.52	0.17	0.94	0.92
Al	0.00	0.87	0.32	0.95	0.78	0.92	0.78	0.74	0.64	1.00	0.88	0.91	0.48	0.71	0.68	0.93	0.85	0.72	0.00	0.91	0.92	0.31	0.54	0.58	-0.14	0.12	0.86	0.14	0.60	0.65
P	0.06	0.90	0.65	0.81	0.78	0.85	0.78	0.66	0.89	0.88	1.00	0.95	0.54	0.66	0.70	0.96	0.90	0.83	0.17	0.91	0.87	0.36	0.46	0.69	-0.25	0.20	0.75	0.11	0.86	0.86
S	0.03	0.85	0.50	0.91	0.76	0.87	0.75	0.77	0.79	0.91	0.95	1.00	0.50	0.76	0.70	0.96	0.86	0.80	0.14	0.92	0.92	0.40	0.60	0.74	-0.08	0.27	0.89	0.22	0.75	0.78
Ti	0.14	0.52	0.32	0.31	0.67	0.57	0.62	0.43	0.48	0.48	0.54	0.50	1.00	0.50	0.34	0.45	0.63	0.53	0.10	0.45	0.37	0.51	0.31	0.18	0.05	0.12	0.31	0.13	0.43	0.53
V	0.17	0.59	0.31	0.71	0.67	0.71	0.63	0.72	0.54	0.71	0.66	0.76	0.50	1.00	0.48	0.71	0.74	0.62	0.14	0.67	0.67	0.40	0.63	0.48	0.26	0.21	0.68	0.26	0.49	0.56
Cr	0.00	0.70	0.33	0.67	0.57	0.64	0.57	0.68	0.54	0.68	0.70	0.70	0.34	0.48	1.00	0.73	0.63	0.56	0.04	0.76	0.85	0.25	0.42	0.44	-0.21	0.14	0.61	0.11	0.59	0.70
Mn	0.00	0.86	0.53	0.91	0.80	0.90	0.80	0.75	0.81	0.93	0.96	0.96	0.45	0.71	0.73	1.00	0.89	0.81	0.15	0.93	0.94	0.33	0.53	0.70	-0.19	0.19	0.86	0.14	0.78	0.81
Fe	0.12	0.77	0.67	0.75	0.94	0.94	0.94	0.72	0.87	0.85	0.90	0.86	0.63	0.74	0.63	0.89	1.00	0.90	0.36	0.82	0.77	0.28	0.42	0.54	-0.16	0.18	0.68	0.12	0.82	0.87
Co	0.06	0.69	0.72	0.61	0.86	0.84	0.85	0.62	0.90	0.72	0.83	0.80	0.53	0.62	0.56	0.81	0.90	1.00	0.56	0.72	0.66	0.19	0.35	0.49	-0.23	0.19	0.57	0.11	0.81	0.84
Ni	0.12	0.01	0.50	-0.04	0.32	0.20	0.32	0.09	0.44	0.00	0.17	0.14	0.10	0.14	0.04	0.15	0.36	0.56	1.00	0.08	-0.01	0.11	0.10	0.02	-0.07	0.10	-0.01	0.02	0.34	0.33
Cu	0.00	0.92	0.40	0.89	0.68	0.80	0.66	0.74	0.70	0.91	0.91	0.92	0.45	0.67	0.76	0.93	0.82	0.72	0.08	1.00	0.93	0.44	0.53	0.59	-0.20	0.12	0.79	0.10	0.73	0.73
Zn	-0.01	0.85	0.32	0.95	0.68	0.82	0.67	0.79	0.63	0.92	0.87	0.92	0.37	0.67	0.85	0.94	0.77	0.66	-0.01	0.93	1.00	0.35	0.58	0.64	-0.14	0.14	0.89	0.14	0.63	0.70
As	0.02	0.31	0.08	0.34	0.20	0.24	0.18	0.30	0.22	0.31	0.36	0.40	0.51	0.40	0.25	0.33	0.28	0.19	-0.11	0.44	0.35	1.00	0.28	0.29	-0.05	0.06	0.40	0.06	0.30	0.28
Se	0.11	0.50	0.02	0.57	0.36	0.44	0.33	0.55	0.28	0.54	0.46	0.60	0.31	0.63	0.42	0.53	0.42	0.35	-0.10	0.53	0.58	0.28	1.00	0.35	0.30	0.30	0.56	0.38	0.23	0.30
SO_4^{2-}	0.13	0.52	0.44	0.64	0.46	0.56	0.46	0.52	0.62	0.58	0.69	0.74	0.18	0.48	0.44	0.70	0.54	0.49	0.02	0.59	0.64	0.29	0.35	1.00	-0.04	0.45	0.67	0.28	0.56	0.55
NO_3^-	-0.04	-0.22	-0.29	-0.08	-0.13	-0.14	-0.17	-0.07	-0.26	-0.14	-0.25	-0.08	-0.05	-0.26	-0.21	-0.19	-0.16	-0.23	-0.07	-0.20	-0.14	-0.05	-0.30	-0.04	1.00	0.44	-0.03	0.56	-0.34	-0.29
Cl^-	-0.10	-0.11	-0.28	-0.15	-0.17	-0.18	-0.21	-0.11	-0.32	-0.12	-0.20	-0.27	-0.12	-0.21	-0.14	-0.19	-0.18	-0.19	-0.10	-0.12	-0.14	-0.06	-0.30	-0.45	-0.44	1.00	-0.17	0.95	-0.22	-0.20
NH_4^+	-0.06	0.63	0.24	0.95	0.64	0.79	0.62	0.72	0.52	0.86	0.75	0.89	0.31	0.68	0.61	0.86	0.68	0.57	-0.01	0.79	0.89	0.40	0.56	0.67	-0.03	0.17	1.00	0.17	0.49	0.56
Na^+	-0.13	0.09	0.09	0.17	0.13	0.16	0.16	0.13	0.17	0.14	0.11	0.22	0.13	0.26	0.11	0.14	0.12	0.11	0.02	0.10	0.14	0.06	0.38	0.28	0.56	0.95	0.17	1.00	0.08	0.06
Ca	0.04	0.67	0.90	0.54	0.71	0.69	0.74	0.51	0.94	0.60	0.86	0.75	0.43	0.49	0.59	0.78	0.82	0.81	0.34	0.73	0.63	0.30	0.23	0.56	-0.34	0.22	0.49	0.08	1.00	0.95
Ba	0.07	0.67	0.86	0.58	0.81	0.78	0.82	0.62	0.92	0.65	0.86	0.78	0.53	0.56	0.70	0.81	0.87	0.84	0.33	0.73	0.70	0.28	0.30	0.55	-0.29	0.20	0.56	0.06	0.95	1.00

Table 4.11: Correlation coefficients for Hg wet deposition for trace elements and ionic species by region

East	Hg	Rb	Sr	Cd	La	Ce	Sm	Pb	Mg	Al	P	S	Ti	V	Cr	Mn	Fe	Co	Ni	Cu	Zn	As	Se	SO4	NO3	Cl	NH4	Na_ion	Ca	Ba
Hg	1.00	0.08	0.50	0.64	0.80	0.72	0.67	0.73	0.42	0.59	0.19	0.88	0.66	0.72	0.81	0.50	0.70	0.76	0.81	0.71	0.49	0.92	0.82	0.87	0.95	0.55	0.48	0.56	0.76	0.82
Rb	0.08	1.00	0.19	0.38	0.14	0.15	0.14	0.10	0.68	0.16	0.92	0.14	0.14	0.06	0.15	0.56	0.15	0.16	0.09	0.51	0.72	0.08	0.05	0.08	0.07	0.07	0.83	0.09	0.16	0.23
Sr	0.50	0.19	1.00	0.68	0.60	0.55	0.57	0.42	0.77	0.57	0.38	0.69	0.59	0.73	0.65	0.81	0.66	0.66	0.56	0.53	0.32	0.52	0.71	0.70	0.54	0.77	0.52	0.79	0.88	0.69
Cd	0.64	0.38	0.68	1.00	0.63	0.56	0.52	0.70	0.63	0.49	0.54	0.72	0.50	0.66	0.71	0.84	0.61	0.65	0.72	0.69	0.64	0.66	0.69	0.69	0.65	0.47	0.67	0.53	0.81	0.72
La	0.80	0.14	0.60	0.63	1.00	0.98	0.96	0.68	0.48	0.92	0.29	0.77	0.95	0.69	0.92	0.63	0.96	0.91	0.73	0.71	0.49	0.80	0.66	0.76	0.79	0.44	0.50	0.52	0.75	0.88
Ce	0.72	0.15	0.55	0.56	0.98	1.00	0.99	0.58	0.43	0.93	0.28	0.69	0.97	0.59	0.84	0.61	0.93	0.86	0.64	0.67	0.48	0.73	0.58	0.67	0.71	0.37	0.49	0.43	0.65	0.81
Sm	0.67	0.14	0.57	0.52	0.96	0.99	1.00	0.49	0.46	0.95	0.28	0.64	0.97	0.56	0.80	0.61	0.92	0.84	0.56	0.63	0.42	0.67	0.55	0.63	0.66	0.40	0.47	0.46	0.62	0.78
Pb	0.73	0.10	0.42	0.70	0.68	0.58	0.49	1.00	0.31	0.45	0.18	0.76	0.56	0.67	0.76	0.46	0.62	0.60	0.88	0.60	0.61	0.79	0.60	0.74	0.75	0.29	0.40	0.39	0.71	0.75
Mg	0.42	0.68	0.77	0.63	0.48	0.43	0.46	0.31	1.00	0.48	0.77	0.57	0.47	0.54	0.54	0.83	0.53	0.52	0.43	0.63	0.59	0.42	0.53	0.54	0.43	0.72	0.80	0.76	0.66	0.60
Al	0.59	0.16	0.57	0.49	0.92	0.93	0.95	0.45	0.48	1.00	0.30	0.56	0.97	0.57	0.84	0.59	0.97	0.88	0.54	0.54	0.34	0.55	0.45	0.54	0.55	0.38	0.42	0.46	0.60	0.77
P	0.19	0.92	0.38	0.54	0.29	0.28	0.28	0.18	0.77	0.30	1.00	0.29	0.26	0.14	0.32	0.75	0.31	0.31	0.19	0.66	0.71	0.21	0.20	0.23	0.19	0.18	0.87	0.25	0.34	0.33
S	0.88	0.14	0.69	0.72	0.77	0.69	0.64	0.76	0.57	0.56	0.29	1.00	0.64	0.72	0.81	0.65	0.70	0.75	0.87	0.76	0.56	0.94	0.91	0.99	0.94	0.65	0.59	0.70	0.85	0.86
Ti	0.66	0.14	0.59	0.50	0.95	0.97	0.97	0.56	0.47	0.97	0.26	0.64	1.00	0.64	0.85	0.59	0.97	0.88	0.62	0.60	0.42	0.64	0.52	0.63	0.64	0.40	0.44	0.46	0.65	0.83
V	0.72	0.06	0.73	0.66	0.69	0.59	0.56	0.67	0.54	0.57	0.14	0.72	0.64	1.00	0.78	0.55	0.71	0.74	0.70	0.57	0.27	0.67	0.74	0.75	0.68	0.68	0.35	0.66	0.86	0.79
Cr	0.81	0.15	0.65	0.71	0.92	0.84	0.80	0.76	0.54	0.84	0.32	0.81	0.85	0.78	1.00	0.65	0.94	0.93	0.80	0.71	0.44	0.78	0.67	0.79	0.78	0.51	0.47	0.62	0.84	0.91
Mn	0.50	0.56	0.81	0.84	0.63	0.61	0.61	0.46	0.83	0.59	0.75	0.65	0.59	0.55	0.65	1.00	0.65	0.65	0.52	0.73	0.64	0.54	0.62	0.61	0.52	0.51	0.80	0.57	0.76	0.66
Fe	0.70	0.15	0.66	0.61	0.96	0.93	0.92	0.62	0.53	0.97	0.31	0.70	0.97	0.71	0.94	0.65	1.00	0.94	0.68	0.64	0.41	0.67	0.58	0.68	0.67	0.45	0.46	0.55	0.75	0.87
Co	0.76	0.16	0.66	0.65	0.91	0.86	0.84	0.60	0.52	0.88	0.31	0.75	0.88	0.74	0.93	0.65	0.94	1.00	0.73	0.66	0.41	0.70	0.69	0.74	0.73	0.48	0.48	0.55	0.80	0.92
Ni	0.81	0.09	0.56	0.72	0.73	0.64	0.56	0.88	0.43	0.54	0.19	0.87	0.62	0.70	0.80	0.52	0.68	0.73	1.00	0.59	0.61	0.82	0.75	0.86	0.86	0.49	0.46	0.57	0.80	0.84
Cu	0.71	0.51	0.53	0.69	0.71	0.67	0.63	0.60	0.63	0.54	0.66	0.76	0.60	0.57	0.71	0.73	0.64	0.66	0.59	1.00	0.68	0.76	0.66	0.71	0.72	0.39	0.76	0.44	0.68	0.68
Zn	0.49	0.72	0.32	0.64	0.49	0.48	0.42	0.61	0.59	0.34	0.71	0.56	0.42	0.27	0.44	0.64	0.41	0.41	0.61	0.68	1.00	0.54	0.41	0.51	0.53	0.16	0.85	0.22	0.46	0.56
As	0.92	0.08	0.52	0.66	0.80	0.73	0.67	0.79	0.42	0.55	0.21	0.94	0.64	0.67	0.78	0.54	0.67	0.70	0.82	0.76	0.54	1.00	0.84	0.92	0.96	0.54	0.53	0.55	0.74	0.80
Se	0.82	0.05	0.71	0.69	0.66	0.58	0.55	0.60	0.53	0.45	0.20	0.91	0.52	0.74	0.67	0.62	0.58	0.69	0.75	0.66	0.41	0.84	1.00	0.93	0.86	0.72	0.49	0.69	0.81	0.77
SO4	0.87	0.08	0.70	0.69	0.76	0.67	0.63	0.74	0.54	0.54	0.23	0.99	0.63	0.75	0.79	0.61	0.68	0.74	0.86	0.71	0.51	0.92	0.93	1.00	0.94	0.67	0.54	0.71	0.86	0.85
NO3	0.95	0.07	0.54	0.65	0.79	0.71	0.66	0.75	0.43	0.55	0.19	0.94	0.64	0.68	0.78	0.52	0.67	0.73	0.86	0.72	0.53	0.96	0.86	0.94	1.00	0.58	0.52	0.60	0.77	0.84
Cl	0.55	0.07	0.77	0.47	0.44	0.37	0.40	0.29	0.72	0.38	0.18	0.65	0.40	0.68	0.51	0.51	0.45	0.48	0.49	0.39	0.16	0.54	0.72	0.67	0.58	1.00	0.38	0.93	0.67	0.57
NH4	0.48	0.83	0.52	0.67	0.50	0.49	0.47	0.40	0.80	0.42	0.87	0.59	0.44	0.35	0.47	0.80	0.46	0.48	0.46	0.76	0.85	0.53	0.49	0.54	0.52	0.38	1.00	0.38	0.54	0.57
Na_ion	0.56	0.09	0.79	0.53	0.52	0.43	0.46	0.39	0.76	0.46	0.25	0.70	0.46	0.66	0.62	0.57	0.55	0.55	0.57	0.44	0.22	0.55	0.69	0.71	0.60	0.93	0.38	1.00	0.72	0.64
Ca	0.76	0.16	0.88	0.81	0.75	0.65	0.62	0.71	0.66	0.60	0.34	0.85	0.65	0.86	0.84	0.76	0.75	0.80	0.80	0.68	0.46	0.74	0.81	0.86	0.77	0.67	0.54	0.72	1.00	0.86
Ba	0.82	0.23	0.69	0.72	0.88	0.81	0.78	0.75	0.60	0.77	0.33	0.86	0.83	0.79	0.91	0.66	0.87	0.92	0.84	0.68	0.56	0.80	0.77	0.85	0.84	0.57	0.57	0.64	0.86	1.00

Central	Hg	Rb	Sr	Cd	La	Ce	Sm	Pb	Mg	Al	P	S	Ti	V	Cr	Mn	Fe	Co	Ni	Cu	Zn	As	Se	SO42-	NO3-	Cl-	NH4+	Na+	Ca	Ba
Hg	1.00	0.58	0.73	0.60	0.62	0.61	0.61	0.71	0.61	0.63	0.36	0.74	0.62	0.71	0.52	0.65	0.62	0.71	0.28	0.51	0.11	0.72	0.56	0.33	0.79	0.56	0.39	0.39	0.73	0.55
Rb	0.58	1.00	0.71	0.58	0.73	0.74	0.74	0.55	0.63	0.75	0.77	0.55	0.72	0.65	0.51	0.77	0.75	0.74	0.28	0.58	0.24	0.52	0.38	0.13	0.55	0.39	0.56	0.19	0.61	0.71
Sr	0.73	0.71	1.00	0.47	0.91	0.91	0.92	0.83	0.88	0.92	0.25	0.80	0.90	0.93	0.74	0.92	0.91	0.93	0.52	0.54	0.22	0.75	0.57	0.18	0.69	0.68	0.22	0.33	0.93	0.87
Cd	0.60	0.58	0.47	1.00	0.34	0.34	0.34	0.50	0.39	0.37	0.66	0.51	0.31	0.42	0.31	0.41	0.35	0.46	0.15	0.63	0.08	0.55	0.33	0.24	0.57	0.32	0.50	0.25	0.45	0.35
La	0.62	0.73	0.91	0.34	1.00	0.99	0.99	0.79	0.70	0.99	0.23	0.66	0.98	0.84	0.72	0.97	0.99	0.95	0.32	0.48	0.26	0.68	0.46	0.16	0.64	0.46	0.23	0.24	0.82	0.95
Ce	0.61	0.74	0.91	0.34	0.99	1.00	1.00	0.76	0.71	1.00	0.23	0.64	0.99	0.84	0.72	0.98	1.00	0.95	0.33	0.47	0.27	0.65	0.47	0.15	0.61	0.47	0.22	0.24	0.80	0.96
Sm	0.61	0.74	0.92	0.34	0.99	1.00	1.00	0.77	0.71	0.99	0.24	0.65	0.98	0.84	0.72	0.98	0.99	0.95	0.33	0.47	0.28	0.65	0.47	0.15	0.61	0.48	0.22	0.24	0.81	0.96
Pb	0.71	0.55	0.83	0.50	0.79	0.76	0.77	1.00	0.57	0.77	0.19	0.72	0.74	0.79	0.67	0.78	0.77	0.86	0.24	0.64	0.29	0.86	0.45	0.26	0.81	0.47	0.24	0.28	0.88	0.76
Mg	0.61	0.63	0.88	0.39	0.70	0.71	0.71	0.57	1.00	0.73	0.25	0.85	0.72	0.89	0.71	0.69	0.72	0.70	0.73	0.43	0.16	0.56	0.68	0.13	0.47	0.81	0.18	0.37	0.81	0.63
Al	0.63	0.75	0.92	0.37	0.99	1.00	0.99	0.77	0.73	1.00	0.24	0.66	0.99	0.85	0.68	0.99	1.00	0.96	0.39	0.48	0.28	0.65	0.47	0.16	0.63	0.47	0.23	0.24	0.80	0.96
P	0.36	0.77	0.25	0.66	0.23	0.23	0.24	0.19	0.25	0.24	1.00	0.23	0.19	0.19	0.13	0.28	0.23	0.25	0.04	0.46	0.05	0.23	0.14	0.18	0.31	0.13	0.71	0.16	0.20	0.19
S	0.74	0.55	0.80	0.51	0.66	0.64	0.65	0.72	0.85	0.66	0.23	1.00	0.65	0.91	0.77	0.62	0.66	0.68	0.59	0.53	0.20	0.76	0.87	0.24	0.64	0.70	0.23	0.38	0.85	0.56
Ti	0.62	0.72	0.90	0.31	0.98	0.99	0.98	0.74	0.72	0.99	0.19	0.65	1.00	0.84	0.67	0.97	0.99	0.95	0.41	0.44	0.28	0.64	0.46	0.15	0.61	0.46	0.20	0.23	0.77	0.96
V	0.71	0.65	0.93	0.42	0.84	0.84	0.84	0.79	0.89	0.85	0.19	0.91	0.84	1.00	0.81	0.82	0.85	0.84	0.63	0.52	0.26	0.75	0.72	0.19	0.64	0.64	0.20	0.34	0.91	0.76
Cr	0.52	0.51	0.74	0.31	0.72	0.72	0.72	0.67	0.71	0.68	0.13	0.77	0.67	0.81	1.00	0.63	0.69	0.64	0.25	0.42	0.18	0.69	0.74	0.13	0.38	0.65	0.10	0.31	0.85	0.60
Mn	0.65	0.77	0.92	0.41	0.97	0.98	0.98	0.78	0.69	0.99	0.28	0.62	0.97	0.82	0.63	1.00	0.99	0.98	0.33	0.50	0.27	0.65	0.41	0.18	0.68	0.45	0.27	0.24	0.79	0.97
Fe	0.62	0.75	0.91	0.35	0.99	1.00	0.99	0.77	0.72	1.00	0.23	0.66	0.99	0.85	0.69	0.99	1.00	0.96	0.37	0.47	0.28	0.65	0.47	0.16	0.63	0.47	0.23	0.24	0.80	0.96
Co	0.71	0.74	0.93	0.46	0.95	0.95	0.95	0.86	0.70	0.96	0.25	0.68	0.95	0.84	0.64	0.98	0.96	1.00	0.36	0.54	0.27	0.72	0.43	0.19	0.74	0.48	0.27	0.25	0.83	0.96
Ni	0.28	0.28	0.52	0.15	0.32	0.33	0.33	0.24	0.73	0.39	0.04	0.59	0.41	0.63	0.25	0.33	0.37	0.36	1.00	0.21	0.13	0.24	0.44	0.05	0.18	0.33	0.03	0.20	0.39	0.32
Cu	0.51	0.58	0.54	0.63	0.48	0.47	0.47	0.64	0.43	0.48	0.46	0.53	0.44	0.52	0.42	0.50	0.47	0.54	0.21	1.00	0.42	0.58	0.32	0.17	0.58	0.31	0.38	0.19	0.56	0.47
Zn	0.11	0.24	0.22	0.08	0.26	0.27	0.28	0.29	0.16	0.28	0.05	0.20	0.28	0.26	0.18	0.27	0.28	0.27	0.13	0.42	1.00	0.29	0.10	0.04	0.21	0.06	0.06	0.03	0.16	0.24
As	0.72	0.52	0.75	0.55	0.68	0.65	0.65	0.86	0.56	0.65	0.23	0.76	0.64	0.75	0.69	0.65	0.65	0.72	0.24	0.58	0.29	1.00	0.53	0.28	0.74	0.49	0.27	0.31	0.82	0.63
Se	0.56	0.38	0.57	0.33	0.46	0.47	0.47	0.45	0.68	0.47	0.14	0.87	0.46	0.72	0.74	0.41	0.47	0.43	0.44	0.32	0.10	0.53	1.00	0.14	0.31	0.59	0.09	0.28	0.65	0.33
SO4	0.33	0.13	0.18	0.24	0.16	0.15	0.15	0.26	0.13	0.16	0.18	0.24	0.15	0.19	0.13	0.18	0.16	0.19	0.05	0.17	0.04	0.28	0.14	1.00	0.33	0.23	0.79	0.94	0.22	0.13
NO3	0.79	0.55	0.69	0.57	0.64	0.61	0.61	0.81	0.47	0.63	0.31	0.64	0.61	0.64	0.38	0.68	0.63	0.74	0.18	0.58	0.21	0.74	0.31	0.33	1.00	0.44	0.39	0.31	0.70	0.62
Cl	0.56	0.39	0.68	0.32	0.46	0.47	0.48	0.47	0.81	0.47	0.13	0.70	0.46	0.64	0.65	0.45	0.47	0.48	0.33	0.31	0.06	0.49	0.59	0.23	0.44	1.00	0.18	0.51	0.70	0.37
NH4	0.39	0.56	0.22	0.50	0.23	0.22	0.22	0.24	0.18	0.23	0.71	0.23	0.20	0.20	0.10	0.27	0.23	0.27	0.03	0.38	0.06	0.27	0.09	0.79	0.39	0.18	1.00	0.73	0.21	0.20
Na_ion	0.39	0.19	0.33	0.25	0.24	0.24	0.24	0.28	0.37	0.24	0.16	0.38	0.23	0.34	0.31	0.24	0.24	0.25	0.20	0.19	0.03	0.31	0.28	0.94	0.31	0.51	0.73	1.00	0.37	0.18
Ca	0.73	0.61	0.93	0.45	0.82	0.80	0.81	0.88	0.81	0.80	0.20	0.85	0.77	0.91	0.85	0.79	0.80	0.83	0.39	0.56	0.16	0.82	0.65	0.22	0.70	0.70	0.21	0.37	1.00	0.74
Ba	0.55	0.71	0.87	0.35	0.95	0.96	0.96	0.76	0.63	0.96	0.19	0.56	0.96	0.76	0.60	0.97	0.96	0.96	0.32	0.47	0.24	0.63	0.33	0.13	0.62	0.37	0.20	0.18	0.74	1.00

South	Hg	Rb	Sr	Cd	La	Ce	Sm	Pb	Mg	Al	P	S	Ti	V	Cr	Mn	Fe	Co	Ni	Cu	Zn	As	Se	SO42-	NO3-	Cl-	NH4+	Na+	Ca	Ba
Hg	1.00	0.58	0.79	0.59	0.81	0.80	0.81	0.83	0.73	0.79	0.03	0.83	0.80	0.86	0.83	0.79	0.81	0.83	0.91	0.68	0.31	0.82	0.79	0.88	0.66	0.46	0.37	0.59	0.57	0.86
Rb	0.58	1.00	0.66	0.36	0.73	0.72	0.73	0.52	0.93	0.73	0.44	0.56	0.72	0.64	0.73	0.75	0.73	0.74	0.65	0.51	0.13	0.62	0.39	0.54	0.25	0.29	0.19	0.49	0.61	0.72
Sr	0.79	0.66	1.00	0.66	0.81	0.81	0.80	0.91	0.79	0.75	0.09	0.67	0.75	0.82	0.81	0.79	0.78	0.81	0.82	0.76	0.25	0.89	0.54	0.73	0.64	0.42	0.32	0.55	0.88	0.85
Cd	0.59	0.36	0.66	1.00	0.35	0.33	0.34	0.79	0.42	0.33	0.19	0.70	0.34	0.60	0.42	0.38	0.36	0.40	0.62	0.80	0.30	0.63	0.59	0.65	0.75	0.28	0.50	0.35	0.61	0.46
La	0.81	0.73	0.81	0.35	1.00	1.00	1.00	0.72	0.84	0.97	0.03	0.60	0.97	0.83	0.97	0.97	0.98	0.99	0.85	0.44	0.11	0.83	0.50	0.68	0.40	0.38	0.20	0.51	0.56	0.98
Ce	0.80	0.72	0.81	0.33	1.00	1.00	1.00	0.72	0.84	0.97	0.03	0.59	0.96	0.82	0.96	0.97	0.98	0.99	0.84	0.43	0.11	0.83	0.50	0.67	0.39	0.37	0.20	0.51	0.55	0.98
Sm	0.81	0.73	0.80	0.34	1.00	1.00	1.00	0.71	0.84	0.98	0.04	0.59	0.97	0.82	0.97	0.97	0.98	0.99	0.85	0.43	0.10	0.82	0.51	0.68	0.39	0.38	0.21	0.51	0.54	0.98
Pb	0.83	0.52	0.91	0.79	0.72	0.72	0.71	1.00	0.66	0.68	0.00	0.75	0.70	0.83	0.76	0.70	0.71	0.75	0.86	0.85	0.24	0.86	0.69	0.80	0.79	0.41	0.43	0.51	0.74	0.81
Mg	0.73	0.93	0.79	0.42	0.84	0.84	0.84	0.66	1.00	0.84	0.29	0.70	0.84	0.79	0.85	0.85	0.85	0.85	0.79	0.59	0.28	0.76	0.55	0.72	0.43	0.52	0.26	0.73	0.66	0.84
Al	0.79	0.73	0.75	0.33	0.97	0.97	0.98	0.68	0.84	1.00	0.03	0.62	0.99	0.84	0.99	0.95	1.00	0.99	0.86	0.41	0.10	0.78	0.54	0.69	0.43	0.40	0.22	0.53	0.47	0.97
P	0.03	0.44	0.09	0.19	0.03	0.03	0.04	0.00	0.29	0.03	1.00	0.29	0.02	0.01	0.06	0.23	0.03	0.03	0.01	0.22	0.23	0.11	0.08	0.01	-0.06	-0.05	0.24	0.10	0.34	0.01
S	0.83	0.56	0.67	0.70	0.60	0.59	0.59	0.75	0.70	0.62	0.29	1.00	0.64	0.83	0.70	0.67	0.63	0.65	0.83	0.68	0.49	0.74	0.86	0.93	0.76	0.60	0.46	0.72	0.53	0.67
Ti	0.80	0.72	0.75	0.34	0.97	0.96	0.97	0.70	0.84	0.99	0.02	0.64	1.00	0.85	0.99	0.94	0.99	0.98	0.87	0.43	0.11	0.77	0.54	0.71	0.45	0.41	0.22	0.53	0.48	0.96
V	0.86	0.64	0.82	0.60	0.83	0.82	0.82	0.83	0.79	0.84	0.01	0.83	0.85	1.00	0.88	0.81	0.85	0.86	0.96	0.68	0.27	0.83	0.71	0.90	0.74	0.48	0.39	0.62	0.58	0.87
Cr	0.83	0.73	0.81	0.42	0.97	0.96	0.97	0.76	0.85	0.99	0.06	0.70	0.99	0.88	1.00	0.96	0.99	0.99	0.90	0.50	0.17	0.83	0.60	0.76	0.53	0.43	0.26	0.58	0.55	0.97
Mn	0.79	0.75	0.79	0.38	0.97	0.97	0.97	0.70	0.85	0.95	0.23	0.67	0.94	0.81	0.96	1.00	0.96	0.96	0.83	0.44	0.19	0.82	0.54	0.67	0.39	0.37	0.22	0.53	0.60	0.95
Fe	0.81	0.73	0.78	0.36	0.98	0.98	0.98	0.71	0.85	1.00	0.03	0.63	0.99	0.85	0.99	0.96	1.00	0.99	0.88	0.45	0.11	0.79	0.55	0.71	0.45	0.41	0.23	0.54	0.50	0.98
Co	0.83	0.74	0.81	0.40	0.99	0.99	0.99	0.75	0.85	0.99	0.03	0.65	0.98	0.86	0.99	0.96	0.99	1.00	0.88	0.48	0.12	0.84	0.56	0.73	0.47	0.41	0.25	0.54	0.54	0.99
Ni	0.91	0.65	0.82	0.62	0.85	0.84	0.85	0.86	0.79	0.86	0.01	0.83	0.87	0.96	0.90	0.83	0.88	0.88	1.00	0.68	0.19	0.83	0.77	0.90	0.70	0.47	0.40	0.60	0.56	0.91
Cu	0.68	0.51	0.76	0.80	0.44	0.43	0.43	0.85	0.59	0.41	0.22	0.68	0.43	0.68	0.50	0.44	0.45	0.48	0.68	1.00	0.26	0.67	0.60	0.68	0.76	0.34	0.53	0.44	0.74	0.56
Zn	0.31	0.13	0.25	0.30	0.11	0.11	0.10	0.24	0.28	0.10	0.23	0.49	0.11	0.27	0.17	0.19	0.11	0.12	0.19	0.26	1.00	0.28	0.30	0.44	0.33	0.47	0.15	0.59	0.29	0.11
As	0.82	0.62	0.89	0.63	0.83	0.83	0.82	0.86	0.76	0.78	0.11	0.74	0.77	0.83	0.83	0.82	0.79	0.84	0.83	0.67	0.28	1.00	0.64	0.78	0.66	0.43	0.39	0.58	0.72	0.84
Se	0.79	0.39	0.54	0.59	0.50	0.50	0.51	0.69	0.55	0.54	0.08	0.86	0.54	0.71	0.60	0.54	0.55	0.56	0.77	0.60	0.30	0.64	1.00	0.82	0.72	0.58	0.46	0.66	0.34	0.61
SO4	0.88	0.54	0.73	0.65	0.68	0.67	0.68	0.80	0.72	0.69	0.01	0.93	0.71	0.90	0.76	0.67	0.71	0.73	0.90	0.68	0.44	0.78	0.82	1.00	0.80	0.58	0.44	0.75	0.49	0.74
NO3	0.66	0.25	0.64	0.75	0.40	0.39	0.39	0.79	0.43	0.43	-0.06	0.76	0.45	0.74	0.53	0.39	0.45	0.47	0.70	0.76	0.33	0.66	0.72	0.80	1.00	0.41	0.47	0.54	0.48	0.52
Cl	0.46	0.29	0.42	0.28	0.38	0.37	0.38	0.41	0.52	0.40	-0.05	0.60	0.41	0.48	0.43	0.37	0.41	0.41	0.47	0.34	0.47	0.43	0.58	0.58	0.41	1.00	0.25	0.83	0.24	0.41
NH4	0.37	0.19	0.32	0.50	0.20	0.20	0.21	0.43	0.26	0.22	0.24	0.46	0.22	0.39	0.26	0.22	0.23	0.25	0.40	0.53	0.15	0.39	0.46	0.44	0.47	0.25	1.00	0.23	0.23	0.28
Na_ion	0.59	0.49	0.55	0.35	0.51	0.51	0.51	0.51	0.73	0.53	0.10	0.72	0.53	0.62	0.58	0.53	0.54	0.54	0.60	0.44	0.59	0.58	0.66	0.75	0.54	0.83	0.23	1.00	0.41	0.53
Ca	0.57	0.61	0.88	0.61	0.56	0.55	0.54	0.74	0.66	0.47	0.34	0.53	0.48	0.58	0.55	0.60	0.50	0.54	0.56	0.74	0.29	0.72	0.34	0.49	0.48	0.24	0.23	0.41	1.00	0.59
Ba	0.86	0.72	0.85	0.46	0.98	0.98	0.98	0.81	0.84	0.97	0.01	0.67	0.96	0.87	0.97	0.95	0.98	0.99	0.91	0.56	0.11	0.84	0.61	0.74	0.52	0.41	0.28	0.53	0.59	1.00

West	Hg	Rb	Sr	Cd	La	Ce	Sm	Pb	Mg	Al	P	S	Ti	V	Cr	Mn	Fe	Co	Ni	Cu	Zn	As	Se	SO42-	NO3-	Cl-	NH4+	Na+	Ca	Ba
Hg	1.00	0.22	0.72	0.65	0.72	0.57	0.55	0.57	0.59	0.65	0.43	0.83	0.69	0.87	0.80	0.52	0.65	0.77	0.29	0.74	0.69	0.78	0.75	0.84	0.77	0.54	0.77	0.56	0.74	0.85
Rb	0.22	1.00	0.28	0.61	0.06	0.11	0.12	0.46	0.51	0.17	0.88	0.17	0.20	0.33	0.16	0.37	0.14	0.22	0.04	0.68	0.24	0.12	0.17	0.14	0.02	0.25	0.29	0.26	0.19	0.04
Sr	0.72	0.28	1.00	0.67	0.66	0.58	0.54	0.52	0.87	0.72	0.35	0.69	0.69	0.72	0.79	0.47	0.66	0.77	0.22	0.61	0.55	0.60	0.59	0.70	0.55	0.82	0.60	0.84	0.81	0.75
Cd	0.65	0.61	0.67	1.00	0.59	0.52	0.49	0.70	0.66	0.60	0.65	0.66	0.62	0.75	0.69	0.38	0.59	0.67	0.21	0.80	0.60	0.57	0.63	0.65	0.50	0.50	0.65	0.52	0.64	0.60
La	0.72	0.06	0.66	0.59	1.00	0.87	0.86	0.64	0.45	0.86	0.23	0.71	0.89	0.77	0.86	0.39	0.89	0.87	0.50	0.56	0.63	0.63	0.70	0.74	0.64	0.40	0.59	0.41	0.62	0.81
Ce	0.57	0.11	0.58	0.52	0.87	1.00	0.99	0.59	0.36	0.93	0.24	0.46	0.92	0.52	0.78	0.44	0.99	0.89	0.71	0.43	0.50	0.46	0.45	0.47	0.43	0.25	0.39	0.27	0.57	0.66
Sm	0.55	0.12	0.54	0.49	0.86	0.99	1.00	0.59	0.32	0.93	0.24	0.43	0.92	0.51	0.77	0.43	0.97	0.87	0.69	0.44	0.48	0.43	0.44	0.44	0.39	0.20	0.37	0.22	0.53	0.64
Pb	0.57	0.46	0.52	0.70	0.64	0.59	0.59	1.00	0.44	0.63	0.51	0.52	0.64	0.67	0.53	0.53	0.62	0.62	0.33	0.58	0.41	0.40	0.58	0.52	0.38	0.27	0.50	0.30	0.62	0.48
Mg	0.59	0.51	0.87	0.66	0.45	0.36	0.32	0.44	1.00	0.48	0.51	0.54	0.46	0.62	0.58	0.40	0.44	0.53	0.12	0.63	0.40	0.40	0.45	0.54	0.40	0.95	0.48	0.95	0.60	0.49
Al	0.65	0.17	0.72	0.60	0.86	0.93	0.93	0.63	0.48	1.00	0.27	0.58	0.98	0.64	0.88	0.50	0.95	0.92	0.46	0.54	0.58	0.57	0.57	0.59	0.52	0.37	0.52	0.39	0.67	0.75
P	0.43	0.88	0.35	0.65	0.23	0.24	0.24	0.51	0.51	0.27	1.00	0.40	0.35	0.49	0.31	0.33	0.30	0.41	0.15	0.83	0.46	0.39	0.44	0.37	0.36	0.27	0.60	0.29	0.31	0.21
S	0.83	0.17	0.69	0.66	0.71	0.46	0.43	0.52	0.54	0.58	0.40	1.00	0.66	0.87	0.78	0.32	0.56	0.74	0.07	0.78	0.77	0.91	0.94	1.00	0.87	0.49	0.90	0.51	0.66	0.80
Ti	0.69	0.20	0.69	0.62	0.89	0.92	0.92	0.64	0.46	0.98	0.35	0.66	1.00	0.71	0.91	0.45	0.95	0.94	0.45	0.63	0.68	0.65	0.66	0.66	0.60	0.34	0.63	0.35	0.69	0.78
V	0.87	0.33	0.72	0.75	0.77	0.52	0.51	0.67	0.62	0.64	0.49	0.87	0.71	1.00	0.82	0.41	0.61	0.73	0.13	0.82	0.78	0.73	0.83	0.88	0.76	0.53	0.83	0.55	0.78	0.80
Cr	0.80	0.16	0.79	0.69	0.86	0.78	0.77	0.53	0.58	0.88	0.31	0.78	0.91	0.82	1.00	0.38	0.85	0.90	0.33	0.71	0.81	0.74	0.70	0.79	0.70	0.51	0.70	0.53	0.77	0.88
Mn	0.52	0.37	0.47	0.38	0.39	0.44	0.43	0.53	0.40	0.50	0.33	0.32	0.45	0.41	0.38	1.00	0.45	0.51	0.29	0.39	0.29	0.29	0.34	0.32	0.22	0.26	0.26	0.27	0.47	0.34
Fe	0.65	0.14	0.66	0.59	0.89	0.99	0.97	0.62	0.44	0.95	0.30	0.56	0.95	0.61	0.85	0.45	1.00	0.94	0.68	0.53	0.60	0.55	0.54	0.57	0.52	0.33	0.50	0.35	0.67	0.74
Co	0.77	0.22	0.77	0.67	0.87	0.89	0.87	0.62	0.53	0.92	0.41	0.74	0.94	0.73	0.90	0.51	0.94	1.00	0.53	0.69	0.74	0.72	0.70	0.74	0.68	0.41	0.68	0.43	0.75	0.82
Ni	0.29	0.04	0.22	0.21	0.50	0.71	0.69	0.33	0.12	0.46	0.15	0.07	0.45	0.13	0.33	0.29	0.68	0.53	1.00	0.14	0.24	0.09	0.03	0.07	0.07	0.07	0.02	0.07	0.32	0.28
Cu	0.74	0.68	0.61	0.80	0.56	0.43	0.44	0.58	0.63	0.54	0.83	0.78	0.63	0.82	0.71	0.39	0.53	0.69	0.14	1.00	0.81	0.71	0.74	0.76	0.65	0.44	0.83	0.46	0.59	0.62
Zn	0.69	0.24	0.55	0.60	0.63	0.50	0.48	0.41	0.40	0.58	0.46	0.77	0.68	0.78	0.81	0.29	0.60	0.74	0.24	0.81	1.00	0.70	0.71	0.76	0.72	0.31	0.78	0.33	0.71	0.65
As	0.78	0.12	0.60	0.57	0.63	0.46	0.43	0.40	0.40	0.57	0.39	0.91	0.65	0.73	0.74	0.29	0.55	0.72	0.09	0.71	0.70	1.00	0.88	0.91	0.88	0.34	0.89	0.37	0.55	0.78
Se	0.75	0.17	0.59	0.63	0.70	0.45	0.44	0.58	0.45	0.57	0.44	0.94	0.66	0.83	0.70	0.34	0.54	0.70	0.03	0.74	0.71	0.88	1.00	0.94	0.88	0.38	0.91	0.41	0.57	0.70
SO4	0.84	0.14	0.70	0.65	0.74	0.47	0.44	0.52	0.54	0.59	0.37	1.00	0.66	0.88	0.79	0.32	0.57	0.74	0.07	0.76	0.76	0.91	0.94	1.00	0.87	0.50	0.90	0.53	0.67	0.83
NO3	0.77	0.02	0.55	0.50	0.64	0.43	0.39	0.38	0.40	0.52	0.36	0.87	0.60	0.76	0.70	0.22	0.52	0.68	0.07	0.65	0.72	0.88	0.88	0.87	1.00	0.38	0.88	0.40	0.55	0.67
Cl	0.54	0.25	0.82	0.50	0.40	0.25	0.20	0.27	0.95	0.37	0.27	0.49	0.34	0.53	0.51	0.26	0.33	0.41	0.07	0.44	0.31	0.34	0.38	0.50	0.38	1.00	0.39	1.00	0.53	0.46
NH4	0.77	0.29	0.60	0.65	0.59	0.39	0.37	0.50	0.48	0.52	0.60	0.90	0.63	0.83	0.70	0.26	0.50	0.68	0.02	0.83	0.78	0.89	0.91	0.90	0.88	0.39	1.00	0.42	0.63	0.69
Na_ion	0.56	0.26	0.84	0.52	0.41	0.27	0.22	0.30	0.95	0.39	0.29	0.51	0.35	0.55	0.53	0.27	0.35	0.43	0.07	0.46	0.33	0.37	0.41	0.53	0.40	1.00	0.42	1.00	0.55	0.49
Ca	0.74	0.19	0.81	0.64	0.62	0.57	0.53	0.62	0.60	0.67	0.31	0.66	0.69	0.78	0.77	0.47	0.67	0.75	0.32	0.59	0.71	0.55	0.57	0.67	0.55	0.53	0.63	0.55	1.00	0.72
Ba	0.85	0.04	0.75	0.60	0.81	0.66	0.64	0.48	0.49	0.75	0.21	0.80	0.78	0.80	0.88	0.34	0.74	0.82	0.28	0.62	0.65	0.78	0.70	0.83	0.67	0.46	0.69	0.49	0.72	1.00

Table 4.12: Median enrichment factors calculated with Al as a reference element for the precipitation concentration of trace elements by site. Factors greater than 500 are bolded to indicate probable anthropogenic impact, while those less than 10 is assumed to be naturally occurring.

	Hg	Rb	Sr	Cd	La	Ce	Sm	Pb	Mg	Al	P	S	Ti	V	Cr	Mn	Fe	Co	Ni	Cu	Zn	As	Se
MBI	**803.6**	2.4	3.6	40.4	4.3	3.0	1.7	16.3	6.4	1.0	41.5	**3907.7**	0.3	7.9	2.5	3.8	1.5	1.6	15.3	38.9	134.1	101.0	**6512.9**
BLG	**843.2**	2.4	4.3	46.9	4.1	3.1	1.8	8.4	10.2	1.0	21.9	**6028.5**	0.3	6.5	2.1	3.5	1.2	1.8	10.8	20.3	111.5	108.1	**9175.6**
OLF	**1114.3**	2.5	2.8	36.7	3.7	2.5	2.2	6.8	5.2	1.0	40.9	**8093.2**	0.4	10.0	2.8	3.5	1.1	1.9	12.5	35.9	289.6	176.9	**9877.8**
UWF	**1091.2**	4.2	3.2	47.5	2.9	2.5	1.7	23.7	8.9	1.0	172.6	**10821.2**	0.4	10.3	2.3	4.3	1.2	2.7	11.5	39.8	321.4	337.1	**15833.0**
BWR	**803.9**	4.2	3.9	46.5	3.2	2.9	2.5	39.5	7.8	1.0	43.1	**8177.7**	0.3	6.4	1.8	7.4	1.1	1.4	7.4	19.4	99.9	136.9	**12528.3**
JKS	**863.2**	2.0	2.0	21.4	2.8	2.5	2.1	12.0	3.6	1.0	32.6	**5399.5**	0.3	6.0	2.2	2.9	1.1	1.8	6.5	23.3	89.9	127.7	**8542.6**
GBP	**1088.3**	2.6	2.1	42.8	2.8	2.4	2.6	3.9	3.9	1.0	122.0	**4131.1**	0.2	3.0	1.9	3.3	1.1	1.6	5.6	27.5	140.1	91.9	**4989.0**
CSF	**622.7**	2.0	2.1	42.1	2.5	2.2	1.7	34.6	3.4	1.0	36.1	**4111.9**	0.3	4.7	1.9	2.8	1.1	1.4	12.5	22.2	105.7	96.0	**4894.6**
NJK	**683.1**	1.9	6.0	61.9	2.9	2.4	1.6	11.9	8.7	1.0	23.1	**4963.1**	0.3	13.1	2.8	3.2	1.4	1.8	24.4	35.2	203.1	109.2	**6658.2**
OCS	**624.6**	1.8	6.1	35.2	2.2	2.1	1.8	4.2	16.8	1.0	31.4	**8179.7**	0.3	11.3	2.3	3.0	1.2	1.6	12.8	37.0	165.6	150.5	**9039.2**
LTI	**671.0**	2.4	11.7	75.4	2.8	2.6	2.3	8.1	23.8	1.0	118.2	**11036.8**	0.3	14.9	3.3	5.8	1.3	2.3	17.1	28.5	150.4	148.2	**23692.2**
CRS	494.0	1.7	2.1	48.4	2.4	2.7	2.4	9.5	4.7	1.0	29.8	**2541.9**	0.2	2.9	2.1	1.8	1.1	2.1	2.0	3.4	76.8	41.7	**6645.8**
UCF	412.6	1.5	3.9	144.8	2.5	2.7	2.2	43.7	3.2	1.0	13.8	**1849.9**	0.3	2.7	1.6	2.8	1.1	3.7	4.5	30.1	63.7	57.8	**1077.0**
HSB	358.6	1.4	2.0	28.4	2.6	3.0	2.7	16.9	4.0	1.0	21.7	**1357.9**	0.2	3.9	2.1	2.2	1.1	2.0	4.3	14.1	86.6	32.8	**889.2**
PCT	317.9	1.1	2.4	53.3	2.9	2.9	2.4	15.2	3.2	1.0	18.3	**1288.8**	0.3	3.2	1.7	1.8	1.2	2.7	4.8	12.9	57.4	40.2	**1024.6**
SDK	299.6	1.6	5.5	9.3	2.4	3.0	2.7	9.0	13.9	1.0	9.9	**1857.9**	0.3	2.8	1.7	2.5	1.2	2.1	2.8	7.8	74.5	21.7	**1329.1**
TPA	326.0	1.2	2.5	29.7	2.5	2.8	2.5	18.3	4.8	1.0	9.2	**1294.1**	0.3	3.2	1.2	2.2	1.2	2.1	2.6	7.1	62.3	28.0	**1240.7**
DSO	280.6	1.3	3.6	23.7	2.6	3.1	2.8	5.0	7.5	1.0	6.6	**1728.1**	0.3	4.5	1.2	1.7	1.1	1.7	3.8	6.3	57.4	23.3	**2702.0**
MKA	194.2	1.3	2.1	6.2	2.3	2.9	2.7	6.0	3.0	1.0	9.4	**537.1**	0.2	2.3	1.1	2.2	1.1	1.8	2.0	3.9	29.4	13.7	**705.0**
OKB	138.8	2.5	4.1	27.9	2.3	2.8	2.5	7.9	5.1	1.0	149.5	**1061.2**	0.2	2.3	1.2	2.7	1.4	2.3	3.1	17.0	82.6	24.9	**598.8**
DVE	109.4	1.3	3.4	10.4	2.9	3.3	3.0	10.5	3.1	1.0	2.7	**566.2**	0.3	2.4	1.2	2.5	1.2	2.2	2.6	8.3	13.7	11.9	**756.2**
EHP	229.9	1.3	2.5	4.2	2.5	2.9	2.7	6.2	2.8	1.0	18.2	**616.4**	0.3	2.0	1.2	2.1	1.2	1.8	2.6	6.2	22.1	12.4	428.2
FKE	433.1	1.5	1.9	15.7	2.5	2.9	2.6	5.3	3.9	1.0	19.7	**1327.3**	0.3	3.3	2.4	1.9	1.2	2.0	2.3	13.7	35.1	19.8	**1245.5**
MIA	182.6	1.1	28.0	40.5	3.6	3.6	3.0	54.8	4.9	1.0	15.7	**808.1**	0.4	4.9	2.4	3.0	1.6	2.3	4.8	26.7	159.2	32.8	**528.5**
KYB	295.0	1.5	7.8	12.6	2.3	2.6	2.2	6.7	6.7	1.0	7.6	**2639.2**	0.2	6.0	2.9	2.0	1.1	1.9	3.7	2.8	152.8	27.6	**1815.2**
ENP	230.2	1.3	3.6	12.9	2.4	2.9	2.8	5.6	2.5	1.0	2.1	**792.0**	0.2	2.8	0.9	2.2	1.1	2.2	3.2	5.9	11.4	9.6	**535.0**

Table 4.13: Median enrichment factors calculated with Al as a reference element for the dry deposition of trace elements by site. Factors greater than 500 are bolded to indicate probable anthropogenic impact, while those less than 10 is assumed to be naturally occurring.

	Hg	Rb	Sr	Cd	La	Ce	Sm	Pb	Mg	Al	P	S	Ti	V	Cr	Mn	Fe	Co	Ni	Cu	Zn	As	Se
MBI	434.0	44.0	61.8	92.4	5.6	4.9	4.1	44.8	83.2	1.0	**1274.5**	**5287.9**	0.5	3.9	1.4	24.7	2.5	3.5	324.3	117.1	276.5	87.6	**2759.6**
BLG	478.9	2.4	17.8	164.2	5.0	4.0	3.4	80.1	25.3	1.0	21.2	**4190.9**	0.6	5.0	0.9	5.8	1.3	2.0	0.0	7.8	82.8	105.1	**6398.8**
OLF	149.5	2.3	6.0	29.7	3.2	3.0	2.3	31.6	5.8	1.0	23.2	**1570.9**	0.4	2.4	0.4	3.2	0.7	0.8	32.4	20.0	25.0	91.2	**2989.0**
UWF	209.8	155.7	13.1	310.8	3.0	2.2	1.5	33.8	49.3	1.0	**1596.5**	**3907.1**	0.8	2.6	1.5	22.9	1.2	1.1	6.8	185.4	**738.8**	286.2	**4304.4**
BWR	275.9	5.1	4.1	55.6	2.6	2.6	1.6	30.0	3.9	1.0	36.2	**1759.0**	0.4	2.3	0.3	8.9	0.8	0.8	9.6	6.2	56.7	72.2	**3811.8**
JKS	403.7	2.7	5.6	66.1	3.9	3.6	3.1	55.5	7.2	1.0	86.8	**1503.5**	0.5	5.7	2.2	5.8	1.4	1.3	0.4	43.0	184.2	78.8	**4573.9**
GBP	445.2	2.1	5.4	45.1	2.9	2.2	2.3	20.7	3.0	1.0	40.1	**1540.9**	0.3	3.8	1.5	2.8	0.9	0.9	7.0	21.3	0.3	71.4	**4933.8**
CSF	482.7	1.2	4.2	31.6	3.5	2.5	2.4	45.2	4.6	1.0	19.9	**921.2**	0.7	3.8	1.1	2.6	1.1	1.0	0.0	14.4	91.8	54.9	**3845.0**
NJK	318.6	2.2	9.8	92.7	3.7	2.7	2.3	56.4	13.8	1.0	21.5	**2328.3**	0.7	13.1	1.4	2.4	1.2	1.9	4.7	20.1	176.4	60.6	**5762.0**
OCS	**528.0**	2.2	21.5	72.7	4.8	3.7	3.9	36.9	43.3	1.0	35.1	**6067.3**	0.6	10.2	1.2	3.9	1.3	1.5	0.0	32.4	6.7	94.6	**6954.2**
LTI	235.4	3.9	50.3	42.5	4.2	3.9	3.8	37.2	85.2	1.0	20.5	**9555.7**	0.5	12.5	1.6	3.1	1.8	2.1	2.1	41.7	28.8	78.1	**3697.1**
CRS	**560.8**	2.1	11.3	146.0	4.1	3.8	4.0	28.2	18.5	1.0	36.8	**3766.5**	0.7	3.0	1.5	3.5	1.1	3.3	11.5	35.7	29.3	35.0	**9620.2**
UCF	144.4	2.0	4.8	83.2	2.8	2.7	2.4	19.2	3.2	1.0	35.3	**938.9**	0.5	1.7	1.6	1.6	1.0	1.2	3.4	22.5	105.0	20.4	**1413.9**
HSB	155.7	3.5	8.7	12.2	4.0	3.5	3.4	19.8	5.8	1.0	73.4	**2246.9**	0.7	3.0	2.8	3.7	1.3	2.1	4.9	47.2	90.5	53.9	**3098.6**
PCT	108.6	5.3	10.4	201.6	3.5	3.0	2.9	32.9	8.7	1.0	331.9	**2084.8**	0.4	2.6	1.7	4.4	1.2	1.4	6.7	62.2	79.6	73.0	**1121.3**
SDK	323.6	1.2	13.5	37.4	3.2	3.0	3.0	16.1	11.4	1.0	21.8	**1064.6**	0.4	3.0	1.6	2.3	1.1	1.2	0.6	11.7	13.5	32.7	**2476.0**
TPA	145.1	2.0	6.7	135.8	3.1	2.9	2.9	71.3	4.1	1.0	56.5	**1264.5**	0.6	3.8	2.3	2.6	1.9	2.1	4.2	31.9	207.5	40.7	**1087.8**
DSO	293.6	1.2	12.8	24.5	2.6	2.7	2.7	10.0	15.3	1.0	18.5	**1363.6**	0.3	4.3	1.2	2.4	1.0	1.5	1.0	6.9	8.3	27.9	**2886.8**
MKA	132.8	1.1	5.4	3.9	2.2	2.6	2.4	5.7	2.7	1.0	14.1	284.4	0.3	1.3	0.9	1.9	0.9	1.6	1.9	6.4	29.9	12.9	**620.8**
OKB	73.3	2.3	10.6	13.9	3.2	3.1	3.1	26.9	8.4	1.0	94.4	**1489.7**	0.4	2.6	1.5	3.3	1.2	2.3	3.0	29.2	97.5	49.2	**1420.1**
DVE	89.4	1.1	5.1	25.7	2.3	2.5	2.4	25.9	3.3	1.0	4.3	408.8	0.3	1.7	1.1	1.6	1.1	1.4	3.9	21.6	44.9	17.8	462.8
EHP	38.5	2.2	37.0	35.5	2.7	2.5	2.5	14.1	6.2	1.0	73.1	**1122.7**	0.4	1.6	1.7	2.3	1.1	1.7	3.1	27.2	75.8	30.6	**651.6**
FKE	95.1	1.5	5.6	21.4	2.4	2.7	2.6	10.0	5.4	1.0	19.2	407.8	0.2	1.3	1.1	2.1	1.0	1.5	2.0	5.0	11.0	15.0	**1039.1**
MIA	45.5	1.2	78.0	127.5	5.2	3.8	4.2	97.3	6.8	1.0	28.1	467.2	0.6	4.9	4.8	2.7	2.3	2.3	4.8	41.4	347.4	63.3	**680.7**
KYB	55.3	1.2	24.9	48.8	2.5	2.7	2.4	8.4	6.9	1.0	8.7	**507.0**	0.3	2.3	1.3	1.9	1.0	1.5	2.2	7.1	112.8	30.5	**1047.3**
ENP	79.1	1.3	3.0	5.8	3.1	2.7	2.4	9.2	3.9	1.0	5.0	489.6	0.3	2.2	1.0	1.8	1.0	1.5	2.5	1.5	3.0	11.6	**720.0**

Table 4.14: Median enrichment factors calculated with Ti as a reference element for the precipitation concentration of trace elements by site. Factors greater than 500 are bolded to indicate probable anthropogenic impact, while those less than 10 is assumed to be naturally occurring.

	Hg	Rb	Sr	Cd	La	Ce	Sm	Pb	Mg	Al	P	S	Ti	V	Cr	Mn	Fe	Co	Ni	Cu	Zn	As	Se
MBI	**2155**	7.7	9.8	106.6	12.1	11.0	5.3	45.1	15.8	3.1	81.0	**14938**	1.0	32.7	7.1	10.5	4.2	5.1	32.5	80.6	399.8	223.0	**18256**
BLG	**2582**	8.3	18.5	178.6	11.8	11.4	7.5	29.0	46.6	3.6	90.0	**20048**	1.0	21.4	7.1	13.3	4.3	5.8	28.5	71.8	406.0	286.9	**31932**
OLF	**3163**	7.8	7.9	103.1	13.2	8.4	6.2	18.1	14.9	2.8	114.7	**25288**	1.0	25.8	7.4	10.1	3.7	5.0	32.1	100.6	**815.9**	**613.8**	**26533**
UWF	**3042**	11.3	8.6	109.9	8.2	7.1	5.0	61.0	24.2	2.8	430.7	**28366**	1.0	26.4	6.3	12.2	3.6	7.0	27.4	112.6	**771.5**	**944.4**	**45099**
BWR	**2190**	12.7	13.1	142.8	12.2	9.9	7.5	134.0	27.6	3.6	121.1	**24160**	1.0	21.6	5.5	25.4	3.8	5.3	32.9	68.4	321.1	468.3	**37340**
JKS	**2503**	5.7	6.4	70.8	7.8	8.8	7.8	51.2	13.2	3.5	122.1	**14352**	1.0	14.0	5.7	10.1	3.8	5.7	16.3	50.8	250.4	386.3	**21860**
GBP	**3236**	11.3	8.7	176.0	12.5	10.4	9.3	15.9	14.5	4.1	436.1	**17683**	1.0	13.0	7.1	11.8	4.4	5.9	18.8	108.1	433.0	279.0	**20533**
CSF	**2200**	5.7	6.1	118.4	8.6	8.5	6.2	131.9	11.7	3.5	100.3	**17940**	1.0	11.9	6.0	8.1	3.8	4.3	43.4	72.0	302.2	335.3	**17371**
NJK	**2329**	4.5	17.0	166.5	8.6	6.9	4.3	66.7	23.0	2.9	55.3	**16967**	1.0	43.5	9.5	8.6	4.1	5.5	70.7	98.0	486.4	299.4	**30140**
OCS	**1599**	5.1	16.9	91.7	6.7	5.6	5.6	13.4	54.8	2.9	105.9	**21320**	1.0	26.9	6.3	7.8	3.6	4.5	31.6	82.3	**600.1**	414.1	**20883**
LTI	**1923**	8.6	36.2	270.0	10.0	9.0	8.1	42.6	66.0	3.4	352.7	**38585**	1.0	61.1	11.3	21.3	4.4	8.8	67.1	141.3	**568.9**	**585.5**	**91223**
CRS	**1655**	6.3	5.4	194.6	9.1	10.2	8.9	35.5	18.7	4.0	120.2	**11072**	1.0	11.5	6.3	6.6	4.2	7.4	7.9	15.6	244.8	205.9	**20907**
UCF	**1346**	5.6	13.0	**542.1**	9.0	9.0	7.1	130.9	11.9	3.4	54.7	**6314**	1.0	8.8	5.7	9.4	4.0	12.1	13.5	90.2	212.5	196.6	**4481**
HSB	**2084**	6.7	9.9	169.1	12.4	13.6	11.9	63.3	18.6	4.4	113.5	**6776**	1.0	17.8	8.8	10.0	5.2	9.0	19.9	64.1	384.8	177.6	**5435**
PCT	**1267**	4.7	10.5	245.8	11.2	11.2	9.1	55.1	13.9	3.9	76.0	**5258**	1.0	12.6	6.3	7.5	4.5	8.8	20.2	51.1	251.7	177.3	**4100**
SDK	**904**	5.5	21.9	35.9	10.3	12.0	10.7	32.1	57.8	3.5	36.1	**7272**	1.0	9.9	7.9	8.9	4.1	8.3	13.9	27.0	262.3	77.5	**5865**
TPA	**1166**	4.7	9.4	101.3	9.8	10.3	8.7	65.8	15.1	3.8	32.7	**3917**	1.0	9.8	4.7	8.1	4.5	8.4	9.4	28.1	204.1	90.5	**4688**
DSO	**1029**	5.1	12.6	85.6	9.7	11.2	10.2	19.4	27.5	3.7	24.1	**7365**	1.0	16.3	4.4	7.0	4.2	7.0	11.6	22.6	247.9	85.5	**9600**
MKA	**1245**	5.7	9.9	31.1	10.9	13.1	12.4	30.6	14.6	4.3	32.8	**2871**	1.0	10.7	5.6	9.8	5.4	8.2	10.4	28.7	156.6	83.8	**3085**
OKB	**612**	9.4	15.2	112.6	9.6	11.9	10.7	30.6	18.5	4.2	**597.7**	**3797**	1.0	9.0	4.3	10.8	5.2	9.0	12.7	60.9	292.0	104.2	**2630**
DVE	406	4.7	13.0	43.2	10.1	12.0	11.2	37.0	10.7	3.6	9.0	**2275**	1.0	8.5	4.7	8.4	4.6	8.0	10.1	31.4	51.6	42.5	**2862**
EHP	**804**	4.8	16.1	16.0	9.8	12.0	11.1	29.9	11.2	4.0	66.7	**2331**	1.0	9.1	5.2	7.6	4.7	7.2	9.7	26.6	92.8	42.9	**1599**
FKE	**1694**	5.7	7.4	62.3	10.2	11.1	9.9	21.2	13.8	3.9	96.3	**4756**	1.0	12.9	8.3	7.1	4.9	7.9	11.6	53.5	136.0	78.0	**4463**
MIA	**513**	3.6	76.6	114.4	9.7	9.9	8.5	141.2	13.1	2.9	39.0	**2548**	1.0	11.9	6.5	8.0	4.6	6.7	13.0	71.6	414.9	79.8	**1101**
KYB	**1215**	6.2	28.5	48.8	10.1	11.0	9.1	27.7	33.4	4.1	39.1	**8273**	1.0	24.8	9.1	7.5	4.7	8.1	13.3	10.9	**605.4**	113.8	**5690**
ENP	**948**	5.3	13.9	54.5	9.8	11.4	10.6	20.3	10.0	4.1	8.6	**3282**	1.0	10.9	3.4	8.8	4.5	8.8	13.0	23.2	43.7	40.4	**2301**

Table 4.15: Median enrichment factors calculated with Ti as a reference element for the dry deposition of trace elements by site. Factors greater than 500 are bolded to indicate probable anthropogenic impact, while those less than 10 is assumed to be naturally occurring.

	Hg	Rb	Sr	Cd	La	Ce	Sm	Pb	Mg	Al	P	S	Ti	V	Cr	Mn	Fe	Co	Ni	Cu	Zn	As	Se
MBI	**699**	8.1	31.7	109.7	11.2	11.9	8.0	105.3	60.6	1.8	204.0	**7908**	1.0	11.9	2.4	22.2	4.9	5.0	**743.4**	133.4	**581.8**	200.6	**7121**
BLG	**808**	3.7	32.7	220.2	8.3	6.5	4.3	112.1	48.6	1.7	37.2	**7297**	1.0	7.8	1.8	10.4	2.1	3.2	0.0	12.6	203.0	163.9	**11589**
OLF	430	5.4	9.4	82.8	7.7	6.8	5.5	76.0	12.5	2.3	81.3	**4570**	1.0	6.4	1.1	10.4	2.0	2.2	72.8	75.4	73.2	246.8	**10385**
UWF	401	422.3	53.7	**572.7**	5.5	3.9	3.1	78.1	117.2	1.3	**5174.6**	**9399**	1.0	5.7	5.0	81.5	3.1	3.3	10.4	**963.4**	**1915.0**	**559.3**	**5314**
BWR	**988**	12.4	8.1	158.8	7.6	7.2	4.4	55.9	9.8	2.8	79.2	**4162**	1.0	6.1	1.0	19.8	2.1	1.4	22.2	5.2	152.7	135.1	**8278**
JKS	**678**	4.7	9.5	89.6	8.1	5.5	5.6	131.4	16.9	1.9	158.3	**2387**	1.0	12.4	4.1	13.7	2.9	2.5	0.9	102.4	215.4	127.8	**9461**
GBP	**1180**	5.6	14.3	84.8	8.0	6.2	6.7	42.5	9.1	3.0	115.1	**4306**	1.0	8.9	2.7	7.5	2.6	2.5	21.2	69.9	1.1	199.4	**14045**
CSF	**935**	2.4	10.1	48.6	6.2	4.4	3.7	60.8	10.5	1.5	40.3	**2144**	1.0	8.3	2.2	5.1	1.8	1.8	0.0	38.6	204.4	123.6	**7933**
NJK	391	3.0	12.6	120.4	5.8	4.1	3.5	79.8	18.0	1.5	29.5	**3271**	1.0	20.7	2.2	3.6	1.6	3.0	7.1	25.3	234.1	91.0	**8505**
OCS	**993**	4.0	37.5	138.2	7.4	5.6	5.8	73.7	68.3	1.6	71.7	**9076**	1.0	18.2	2.4	7.7	2.3	2.0	0.0	87.3	11.7	227.6	**14742**
LTI	**542**	5.8	86.9	96.2	8.4	7.8	7.6	71.1	123.5	1.9	45.4	**16555**	1.0	26.2	2.9	7.7	4.1	5.2	7.2	73.2	68.6	178.3	**6632**
CRS	**878**	3.2	12.4	176.8	6.2	5.4	6.8	42.9	25.2	1.5	37.8	**5756**	1.0	4.6	2.7	5.8	1.8	4.9	22.5	31.8	30.2	39.6	**11709**
UCF	479	4.4	8.0	127.1	6.1	5.6	5.3	43.5	7.6	2.2	93.2	**1921**	1.0	3.0	3.0	2.9	2.1	2.4	5.8	76.6	206.2	31.2	**3299**
HSB	245	4.7	11.6	19.8	5.3	4.4	4.1	20.5	6.8	1.5	51.8	**2793**	1.0	4.9	3.8	5.8	1.8	2.5	6.3	60.2	119.3	66.0	**2952**
PCT	171	11.5	13.1	447.1	8.1	7.5	6.4	81.7	7.0	2.3	329.8	**2504**	1.0	5.5	2.9	7.8	2.2	2.4	14.4	117.7	174.3	124.9	**2334**
SDK	429	3.4	29.4	93.1	7.6	8.0	6.9	40.8	29.2	2.3	39.9	**2452**	1.0	5.2	3.7	5.4	2.7	2.7	1.6	25.5	23.9	79.3	**4758**
TPA	121	2.7	8.6	259.9	4.9	5.1	5.2	109.1	5.6	1.7	62.0	**1842**	1.0	4.7	3.2	3.7	2.7	2.9	7.2	41.1	346.0	52.9	**1292**
DSO	**964**	5.3	37.3	56.1	9.3	9.2	9.1	39.8	49.2	3.6	77.0	**5772**	1.0	18.1	2.9	8.0	3.4	5.8	4.0	31.2	24.0	92.4	**9135**
MKA	406	3.8	15.5	16.6	5.8	6.8	6.5	15.1	8.4	3.2	32.1	**814**	1.0	4.4	2.9	4.8	2.9	4.3	5.0	22.6	73.2	34.6	**1873**
OKB	192	5.5	23.5	34.6	7.2	7.4	6.8	49.8	11.4	2.3	147.6	**2143**	1.0	5.5	2.9	6.5	2.3	4.6	5.2	47.1	158.1	75.2	**2298**
DVE	315	3.3	15.4	75.7	6.8	7.6	7.2	70.9	8.2	3.2	15.8	**1677**	1.0	5.8	4.4	5.1	3.4	4.2	10.9	89.7	128.7	65.0	**1814**
EHP	85	4.3	81.2	61.5	6.1	5.7	5.9	27.6	10.0	2.3	104.2	**2069**	1.0	3.8	2.9	5.3	2.4	3.1	5.5	55.8	131.2	44.3	**1162**
FKE	202	7.1	12.0	66.4	7.9	9.3	9.1	20.2	16.7	4.1	82.3	**1373**	1.0	5.4	4.0	8.3	3.3	4.9	7.8	30.3	69.4	41.9	**2085**
MIA	93	2.1	118.8	218.8	8.1	5.8	6.4	149.5	11.0	1.6	43.6	**776**	1.0	8.0	7.9	4.4	3.9	4.4	9.3	69.5	**561.8**	105.3	**1115**
KYB	176	4.2	78.1	145.1	8.0	9.1	8.4	29.6	20.0	3.4	26.5	**1843**	1.0	5.4	4.2	6.2	3.5	4.9	6.3	21.6	330.6	68.1	**2180**
ENP	244	3.6	8.4	17.8	7.8	8.1	7.3	26.2	11.7	3.0	14.8	**1407**	1.0	6.5	2.7	5.5	2.8	4.4	6.9	3.9	8.2	39.5	**2358**

Chapter 5 : Conclusions

Hg dry deposition was measured across Florida using the novel ATSS sampling method developed as part of this dissertation. The ATSS sampler provided numerous advantages over previously existing sampling methods which had operational and physical limitations. Generally, the ATSS sampler was shown to be effective at measuring dry deposition for both Hg and many other trace elements and ionic species. We were able to use this method in Florida to conduct two large measurement campaigns covering much of state. This large spatial coverage enabled the comparison of Hg wet and dry deposition spatially both for sites less than 10 km apart and for sites across the state. The spatial variation in both wet and dry deposition was substantial adding to evidence that having good spatial coverage is important to understanding Hg deposition to a given area.

Suggestions for future work

As noted in Chapter 2 and 3, the ATSS method provides a good opportunity to conduct more extensive studies. Lengthening the duration of the intensives past 30 days or sampling during another season would allow analysis of Hg dry deposition trends during lower rainfall periods in Florida and capture a greater variety of meteorological events which were shown to be very influential on the month-long averages. Furthermore, although collecting samples on a finer temporal scale was beyond the resources for this study; the ATSS collection method is well

suited for this (particularly in areas with a high Hg deposition). Finer scale temporal data could reduce the variability in cofactors and might increase power in statistical models.

Statistical limitations do not allow the construction of a predictive model for dry deposition; however, there were a number of factors that were highlighted as potential variables to investigate for potential future modeling. We were able to independently test for coastal influence, antecedent dry period, rainfall duration as a percentage of sampling time, co-deposition of trace elements and ionic species, distance to source and category of the source. Independently, most of these variables did not seem to be significant, but dry deposition is controlled by a complicated series of factors and analyzed together, these may have been more indicative. Collecting additional data as well as having a finer temporal scale would probably be necessary to do this. Other factors that could contribute to developing a model could be the amount of moisture on the turf, the direction to sources combined with site specific meteorology, and $PM_{2.5}$ and PM_{10}.